Journal of the OPTICAL SOCIETY *of* AMERICA

VOLUME 38
No. 5

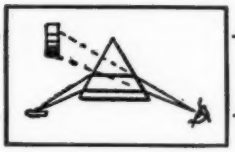

MAY
1948

Lenses of Extremely Wide Angle for Airplane Mapping . . . . . IRVINE C. GARDNER AND FRANCIS E. WASHER 421

Preparation of Aspherical Refracting Optical Surfaces by an Evaporation Technique . . . . . L. G. SCHULZ 432

Non-Adaptability of the ICI System to Some Near-Whites Which Show Absorption in the Far Blue Region of the Spectrum . . . . . A. E. JACOBSEN 442

Coefficients of Reflection of Magnesium Oxide and Magnesium Carbonate . . . . . FRANK BENFORD, GWEN P. LLOYD, AND SALLY SCHWARZ 445

New Contributions to the Optics of Intensely Light-Scattering Materials. Part I . . . . . PAUL KUBELKA 448

Illuminant in Textile Color Matching . . . . . DOROTHY NICKERSON 458

Method for Automatically Plotting Spectral Energy Distribution of Luminescent Materials . . . . . FRANK J. STUDER 467

Symposium on Electron and Light Microscopy 470

$CaSiO_3$: (Pb+Mn) Phosphor . . . . . JOHN B. MERRILL AND JAMES H. SCHULMAN 471

Erratum: Spectrochemical Determination of the Major Constituents of Minerals and Rocks . . . . . ASLAK KVALHEIM 479

Letters to the Edttor:

Emission Spectra of Zinc Cadmium Sulfides . . . . . FRANK J. STUDER AND D. A. LARSON 480
Lead Selenide Photo-Conductive Cells . . . . . J. STARKIEWICZ 481
Observations of Anticoronae on Mt. Washington . . . . . DAVID L. ARENBERG 481

Published monthly
at Prince and Lemon Sts., Lancaster, Pa.
by the
AMERICAN INSTITUTE OF PHYSICS
Incorporated
57 East 55 Street, New York 22, New York
FOR AND UNDER THE EDITORIAL SUPERVISION OF THE
OPTICAL SOCIETY OF AMERICA

THE OPTICAL SOCIETY OF AMERICA

Officers of the Society

RUDOLF KINGSLAKE, *President*
Eastman Kodak Company
Rochester, New York

WILLIAM F. MEGGERS, *Vice President*
National Bureau of Standards
Washington 25, D. C.

ARTHUR C. HARDY, *Secretary*
Massachusetts Institute of Technology
Cambridge 39, Massachusetts

W. W. GRAEPER, *Treasurer*
Bausch & Lomb Optical Company
Rochester 2, New York

The Board of Directors consists of the above officers; the Editor of the Journal; the Past President; and five directors-at-large.

G. R. HARRISON, *Editor and Past President*
Massachusetts Institute of Technology
Cambridge 39, Massachusetts

Directors-at-Large

FRANK BENFORD
General Electric Company
Schenectady, New York

F. M. BISHOP
Eastman Kodak Company
Rochester 4, New York

WALLACE R. BRODE
Ohio State University
Columbus 10, Ohio

A. H. BENNETT
American Optical Company
Buffalo 11, New York

E. H. LAND
Polaroid Corporation
Cambridge, Massachusetts

Local Sections

STANLEY S. BALLARD, *Secretary for Local Sections*

Rochester Section

ARTHUR F. TURNER, *President*
ROBERT N. WOLFE, *Vice President*
PAUL W. STEVENS, *Secretary*
HOMER C. IMES, *Treasurer*

Detroit Section

GERALD M. RASSWEILER, *Chairman*
JOHN SCHUCH, *Vice Chairman*
DANIEL L. HARMON, *Secretary*
HENRY TUTTLE, *Treasurer*

Niagara Frontier Section

ALLEN B. FUHR, *President*
GUY H. FETTERLEY, *Secretary*
HOYT G. THOMPSON, *Treasurer*

Patrons

AMERICAN OPTICAL COMPANY — BAUSCH & LOMB OPTICAL COMPANY
EASTMAN KODAK COMPANY

Corporation Members

ALLIED CHEMICAL AND DYE CORPORATION, NATIONAL ANILINE DIVISION, Buffalo, New York
AMERICAN CYSTOSCOPE MAKERS, INC., New York, New York
AMERICAN OPTICAL COMPANY, Southbridge, Massachusetts
ARGUS, INCORPORATED, Ann Arbor, Michigan
BAUSCH & LOMB OPTICAL COMPANY, Rochester, New York
BELL & HOWELL COMPANY, Chicago, Illinois
BELL TELEPHONE LABORATORIES, INC., New York, New York
CENTURY LIGHTING, INC., New York, New York
CORNING GLASS WORKS, Corning, New York
R. R. DONNELLEY & SONS COMPANY, Chicago, Illinois
E. I. DUPONT DE NEMOURS & COMPANY, INC., Chemical Department, Experimental Station, Wilmington, Delaware
EASTMAN KODAK COMPANY, Rochester, New York
EDMUND SALVAGE COMPANY, Oaklyn-Audubon, New Jersey
FAIRCHILD AVIATION CORPORATION, Jamaica, New York
FARRAND OPTICAL COMPANY, INC., New York, New York
FISH-SCHURMAN CORPORATION, New York, New York
GAERTNER SCIENTIFIC CORPORATION, Chicago, Illinois
W. & L. E. GURLEY, Troy, New York
INTERCHEMICAL CORPORATION, New York, New York
KEUFFEL & ESSER COMPANY, Hoboken, New Jersey
KOLLSMAN INSTRUMENT DIVISION OF SQUARE D COMPANY, Elmhurst, New York
NATIONAL CARBON COMPANY, Cleveland, Ohio
NATIONAL TECHNICAL LABORATORIES, South Pasadena, California
PERKIN-ELMER CORPORATION, Glenbrook, Connecticut
POLAROID CORPORATION, Cambridge, Massachusetts
PORTMAN MACHINE TOOL COMPANY, New Rochelle, New York
SIMPSON OPTICAL MANUFACTURING COMPANY, Chicago, Illinois
SOCONY-VACUUM LABORATORIES, Paulsboro, New Jersey
ARTHUR H. THOMAS COMPANY, Philadelphia, Pennsylvania
UNIVIS LENS COMPANY, Dayton, Ohio
ZENITH OPTICAL COMPANY, Huntington, West Virginia

THE OPTICAL SOCIETY OF AMERICA was organized in 1916 "*to increase and diffuse the knowledge of optics in all its branches, pure and applied, to promote the mutual interests of investigators of optical problems, of designers, manufacturers and users of optical instruments and apparatus of all kinds and to encourage cooperation among them.*" It aims to serve the interests of all who are engaged in any branch of optics from fundamental research to the manufacture of optical goods.

MEMBERSHIP

Regular Members: "Any person who has contributed materially to the advancement of optics is eligible for regular membership."

Associate Members: "Any person who is interested in optics is eligible for associate membership."

Corporate Members: "Any corporation desirous of encouraging the work of the Society is eligible for corporation membership."

Patrons: The payment, within any one year, of $1000 or more toward the expenses of the Society by any corporation or individual entitles such corporation or individual to the rank of patron.

The Society cordially invites to membership all who are interested in any branch of optics, either in research, in instruction, in optical or illuminating engineering, in the manufacture and distribution of optical goods of all kinds, or in physiological and medical optics.

ANNUAL DUES

Regular members, $8.50; Associate members, $6.00; Corporate members, $50.00. These dues include subscription to the Society's official journal, the *Journal of the Optical Society of America.*

CHANGES OF ADDRESS

All changes of address of members of the Optical Society of America should be communicated to the Secretary, Professor Arthur C. Hardy, Massachusetts Institute of Technology, Cambridge 39, Massachusetts.

Journal of the
OPTICAL SOCIETY
of AMERICA

VOLUME 38, NUMBER 5 MAY, 1948

Lenses of Extremely Wide Angle for Airplane Mapping

IRVINE C. GARDNER AND FRANCIS E. WASHER
Optical Instruments Section, National Bureau of Standards,
U. S. Department of Commerce, Washington 25, D. C.

(Received November 5, 1947)

If the illumination of the image produced by a wide-angle lens covering a field of 120° follows the cosine-fourth-power law, the illumination at the edge of the field will be one-sixteenth that at the center in the absence of vignetting. By introducing negative distortion, the illumination may be expected to be more uniform from the center to the edge of the field. In particular if there is no vignetting and if the diaphragm precedes the lens, there will be uniform illumination, even for a field as great as 180°, if the distortion is such that $r'=f\sin\beta$ where r' is the distance from center of the field to a given image point, β is the corresponding angular distance from the axis in the object space, and f is the focal length corresponding to the part of the image in the neighborhood of the axis.

During the war Zeiss developed a mapping lens with a large amount of negative distortion and a second rectifying system by which undistorted copies could be obtained from the distorted negative made with the camera lens. A German mapping lens and rectifying unit have been brought to this country, and detailed results of tests made at the National Bureau of Standards are given in the following paper. The lens, termed the Pleon, covers a field of 130°, and the distortion closely follows the law $r'=f\beta$, the distortion being somewhat less than that of the preceding formula. Measurements of the resolving power, of the effective size of the entrance pupil for different angular distances from the axis, and of the net distortion of the two systems are given. In the final print there is significant residual distortion resulting from the failure of the distortions of the two systems to exactly annul each other.

I. INTRODUCTION

IN general, a distortion-free photographic lens forms an image on a plane surface over which the illumination conforms, at least approximately, to the cosine-fourth-power law. According to this law, the illumination, E, of the image at any point in the field when there is no vignetting, is given by the equation

$$E=A_0\cos^4\beta, \tag{1}$$

where A_0 is the illumination at the axial point of the field and β is the angle, measured in the object space, between the axis and a chief ray passing through the object point conjugate to the image point under consideration. This law seriously restricts the extent of field that can be usefully covered by a wide-angle lens. To illustrate this, for a 90° field ($\beta=45°$) the ratio of the illumination at the edge of the field to that at the center is 0.25 in the absence of vignetting. Actually, with so large a field angle, vignetting is inevitable and the ratio is probably further reduced to the value 0.12 or possibly even less. If a useful field of 120° were achieved, the ratio would be 0.06 before vignetting is considered. This decrease in illumination from the center outward is a serious disadvantage when using black-and-white emulsion and makes the use of color film, because of its more limited latitude, quite impossible. The illumination over the field

can be made uniform by using a variable density filter a short distance in front of the lens and so designed that the illumination at the center of the field is reduced much more than that at the edge. Such a method is undesirable because it greatly reduces the effective speed of the lens and makes longer exposures necessary. Slusareff[1] has called attention to the approximate character of the cosine-fourth-power law and has cited a particular lens, designed by M. Russinoff, for which the illumination varies as the third power of the cosine. In this lens the image is free from distortion and the desirable departure from the cosine-fourth-power law arises because the entrance pupil, which is conjugate to a diaphragm within the lens, is larger for an oblique entering beam than for an axial entering beam.

II. WIDE ANGLE LENSES WITH NEGATIVE DISTORTION

It has been known for some time that a lens with a very large amount of negative distortion forms an image in which the illumination decreases much less rapidly from the center outward than is indicated by the cosine-fourth-power law. This is readily appreciated because, for the peripheral parts of the field, the luminous flux proceeding from a given small object area, for the lens with negative distortion, is concentrated on a region much smaller in area than for a distortion-free lens of the same equivalent focal length with consequent increase in the illumination. Gardner[2] describes a photogrammetric method in which photographs are taken from an airplane with a wide-angle lens by which large amounts of negative distortion are introduced. Subsequently, by the use of a copying or projection lens, a final print is made that is free from distortion. Merte[3] describes a wide-angle lens in which the first component is a negative meniscus. Distortion is not referred to in the patent, but computation shows that this lens does attain its wide coverage (180° is claimed) by introducing large amounts of distortion. Richter,[4] in the patent which evidently applies to the Pleon lens, describes two wide-angle systems, each of which consists of an achromatic negative meniscus system which introduces large amounts of distortion and a following positive system, relatively free from distortion, which forms a real image in the plane of the photographic emulsion. At present no information is available concerning United States or German patents assigned to the firm of Carl Zeiss and applying to the rectifying system used with the Pleon lens. In the patent literature that has just been discussed there are several statements concerning the more uniform illumination over the field of view resulting from the presence of large amounts of negative distortion. A quantitative statement of this effect has been given by Gardner,[5] and it is shown that if the diaphragm is in front of a photographic lens and if there is no vignetting, the field will be uniformly illuminated, even out to 180°, provided that the distortion is such that

$$r' = f \sin\beta, \tag{2}$$

where r' is the radial distance from the center of the field to a given object point, f is the equivalent focal length corresponding to the scale of imagery in the neighborhood of the axis of the lens, and β is as defined for Eq. (1). For a distortion-free lens,

$$r = f \tan\beta, \tag{3}$$

and it is evident that the linear distortion corresponding to the angle β in the true field is given by the equation

$$\text{Linear distortion} = f(\sin\beta - \tan\beta). \tag{4}$$

Applying this equation to a lens of 100-mm focal length, the distortions corresponding to values of β of 45° and 60° are 29 mm (1.14 in.) and 87 mm (3.4 in.), respectively. These values illustrate the extremely large values of distortion that are encountered when uniformity of image illumination is secured by this means.

The lenses of extremely wide angle that have been referred to have the diaphragm within the lens system and, consequently, Eq. (2) does not apply. However, the method by which Eq. (2) was derived can be applied to a lens system with

[1] G. Slusareff, J. Phys. U.S.S.R. **4**, 537 (1941); J. Opt. Soc. Am. **36**, 707 (1946).
[2] Irvine C. Gardner, U. S. Pat. No. 2,037,017 (April 14, 1936).
[3] W. Merte, U. S. Pat. No. 2,126,126 (August 9, 1938).
[4] R. Richter, U. S. Pat. No. 2,247,068 (June 24, 1941).
[5] Irvine C. Gardner, J. Research Nat. Bur. of Stand. (in press, 1947).

an internal diaphragm. For such a lens system the relation between distortion and uniformity of illumination must be determined by a computation applied to the design data of the lens under consideration, and no general statement can be made.

III. APPLICATIONS OF WIDE-ANGLE PHOTOGRAPHS WITH LARGE AMOUNTS OF DISTORTION

With the large amounts of distortion that have been considered it is evident that the scale of the photograph becomes rapidly smaller from the center outward, that straight lines not passing through the center become curved lines concave toward the center, and that the photographs cannot be assembled directly to form a mosaic. Such photographs may, however, be used in a variety of ways. In Germany the availability of photographs of this character led to the chance discovery that pilots of airplanes are not confused by such distortion if they are provided with photographs on which their location in flight is over the central portion of the picture. It was said that the outer, more distorted portion of the picture served as a "finder" and that the smaller scale with accompanying loss of detail at the edge of the picture suggests the loss of detail as the result of haze and increased distance when distant objects are viewed from a plane. The extremely wide-angle lenses, however, were not developed to produce photographs for the use of aviators, and it is not known how extensively the photographs were used for this purpose.

The large amount of radial distortion does not present any obstacle to the use of the photographs, in their original form, for mapping by means of slotted templates or other methods of radial triangulation, although the large negative distortion and the smaller scale to which peripheral points are recorded lessen the precision with which the radial angles can be constructed or the slots cut. With the extremely large coverage of each photograph it might be possible to orient a series of photographs with a minimum of ground control points, after which a sufficient number of additional points could be interpolated to serve as control for the use of narrower angle, distortion-free photographs from which a final map can be constructed. For such a procedure to succeed it would probably be necessary to have a particularly favorable array of very conspicuous landmarks, easily identified from the air and ground, to serve as control points.

In general, however, when a lens of the type under consideration (with large field and large negative distortion) has been developed, it has been the intention to develop an accompanying copy or enlarging lens with a large amount of positive distortion in order that the original distorted negative might be copied to produce an undistorted print. It has been mentioned that negative distortion tends to make the illumination more uniform from center to edge. By the same token positive distortion acts to increase the non-uniformity of illumination beyond that predicted by the cosine-fourth-power law, because the outer parts of the field, which in the natural course of events would be more faintly illuminated than the center, have the illumination further decreased as a consequence of the greater magnification. For the copying lens, however, this unevenness of illumination is not so detrimental as in the case of the airplane camera lens, because copying is a laboratory process with the source of illumination entirely under control, and the uniformity of illumination in the image can be compensated by illuminating the negative in an appropriate manner.

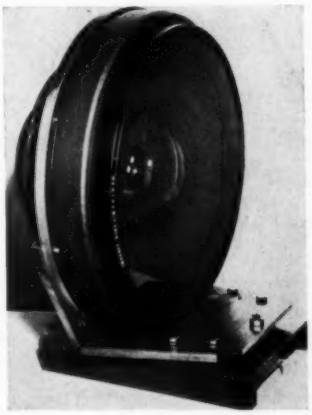

FIG. 1. The Pleon lens as mounted on a laboratory support for testing. The surface shown is the large first surface of the field compressor and is turned toward the object. The diameter of this surface is approximately one foot.

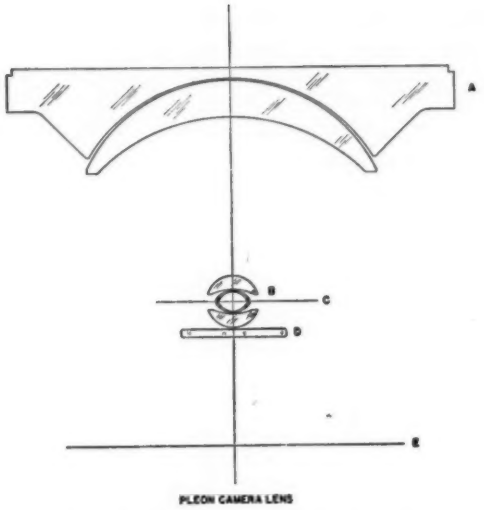

FIG. 2. The optical system of the Pleon lens.

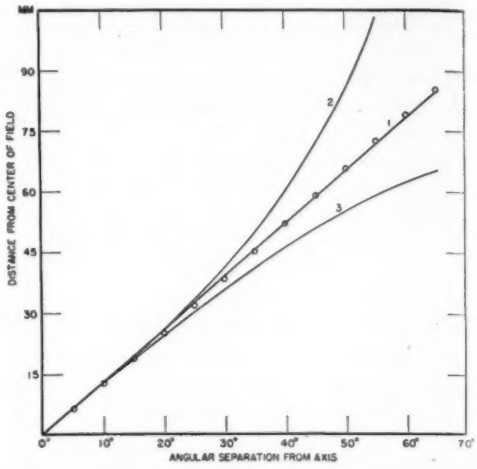

FIG. 3. Graph showing the relation between distance of image point from center of negative and angular displacement of corresponding object point from the axis for the Pleon lens. Curve 1 shows results of measurements made on Pleon lens and corresponds to equation $r'=f\theta$. Curves 2 and 3 correspond, respectively, to equation $r'=\tan\theta$ applying to a distortion-free lens, and to the equation $r'=f\sin\theta$.

One might envision the use of the copying lens of the preceding paragraph in a multiplex projector and the direct production of a contour map from the distorted photograph. The unevenness of illumination introduced by the projection lens, however, would introduce difficulties more serious for the multiplex operation than for the production of enlargements, and it appears that they might be insurmountable. On the other hand, the copying lens, instead of producing an enlargement, might be designed to produce a distortion-free diapositive of suitable scale to be used in a multiplex projector.

IV. THE PLEON LENS

During World War II, Richter, of Zeiss, designed a camera lens and a rectifying lens of the type under consideration. They were designated, respectively, the Pleon lens and the Pleon rectifier. Samples of the lenses and drawings of the optical system were obtained by the Intelligence groups working in Germany after the war. Figure 1 is a reproduction from a photograph of the Pleon lens tested. Figure 2 shows the optical system as specified (Fig. 2 and Table II) in U. S. Patent No. 2,247,068 (June 24, 1941). The first two elements form the member *A* which is an achromatized lens of the type sometimes referred to as a "field compressor." The lens is designed to cover a full field of 130°. The extreme chief rays entering the negative system and including this angle, after refraction, include an angle approximately 40.7°. (These values are based on ray tracing applied to the design data given in the patent.) This smaller field is then imaged by the second member of the system at *B*, which is similar to the Metrogon lens in design. The diaphragm is at *C*, and *D* represents a filter which is an integral part of the lens. The image plane is at *E*. To give an idea of the size of this lens it may be noted that for a nominal focal length of 72.5 mm the over-all diameter of the first negative component is 300 mm, and the distance from the plane surface of this component to the second surface of the filter *D* is 180 mm. In another method of considering this system, the negative member *A* and a portion of the positive power of the second member may be assumed to constitute a Galilean telescopic system used backward which produces an image at an infinite distance but much reduced in angular dimensions. The remaining power of the second member is utilized to form a real image on the photographic emulsion of this intermediate reduced image. The measured

equivalent focal length of the camera lens, corresponding to the center of the field, is 72.1 mm. The radius of the negative, corresponding to a half-angle of approximately 65°, is 85 mm and the linear distortion is −68.8 mm. In other words, in the absence of distortion, the radius of the negative corresponding to 65° and the given focal length would be 154 mm from Eq. (3). The distortion is such that

$$r' = f\beta, \tag{5}$$

where the notation is the same as for Eqs. (2) and (3). This relationship is illustrated by the graph of Fig. 3. Curves corresponding to the relations $r = f \tan\beta$ (see Eq. (3)) and $r' = f \sin\beta$ (see Eq. (2)) are also shown in Fig. 3. The distortion, therefore, is not so great as that of Eq. (2), but no direct deduction concerning the illumination can be made because the diaphragm is not in front of the lens system as was specified in the example of Part II. Experience shows that the illumination of the field is satisfactorily uniform. The resolving power is excellent, ranging from 82 lines per mm at the axis to 18 and 29 for tangential and radial lines, respectively, at 65°.

V. THE PLEON RECTIFIER

Two views of the Pleon rectifier are shown in Figs. 4 and 5. Figure 4 shows the instrument closed in position for making the rectified print. The film to be printed passes through the instrument near the center, the rolls of film resting in the metal pockets on either side. The paper is held flat near the bottom of the instrument by a vacuum back actuated by the small, motor-driven exhaust pump at the right. The over-all height of the instrument is approximately 4½ feet. Figure 5 shows the instrument open at the top to expose the glass pressure plate which holds the negative film flat and with the vacuum plate swung out to permit loading the instrument with a sheet of sensitive paper.

Figure 6 shows the optical system of the Pleon rectifier. The lamp, shown at A, was apparently a mercury arc of the pressure type, familiar in this country, with the mercury vapor contained in a capsule of fused quartz. The lamp of the rectifier received from Germany was broken and a duplicate was not obtainable. The rectifying system is not corrected chromatically, a filter, apparently of cobalt glass, forming a part of the system. The group of parts

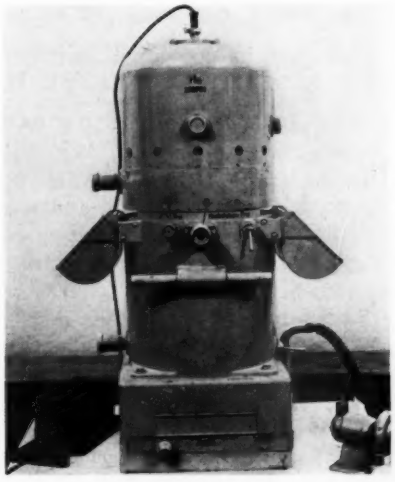

FIG. 4. The Pleon rectifier.—The film to be printed passes through the instrument near the center; the rolls of film rest in the metal pockets on either side. The paper is held flat near the bottom of the instrument by a vacuum back actuated by the small motor-driven exhaust pump at the right. The eyepice marked G is part of an auxiliary optical system for centering the negative. The knob, H, swings four prisms into position for viewing the collimator marks on the negative in order to center it.

FIG. 5. The Pleon rectifier.—The top of the instrument is swung to the left to expose the glass pressure plate by which the negative film is held flat during the operation of printing. The sensitive paper is held flat by the vacuum plate swung out of the instrument in position for loading. The two small doors near the bottom are for the insertion of paddles for dodging the print to compensate for differential illumination of the terrain at the time the exposure was made.

marked *B* comprises this filter and a condensing system. At *C* is the stage on which the negative to be copied is placed and also a variable density filter for compensating the otherwise uneven illumination of the image. This filter also failed to arrive from Germany and an approximate filter was produced by placing a photographic plate at *C* and exposing it by light transmitted backward through the optical system from *E*. The rectified image is produced in the plane at *E* by the projection system marked *D*. This part of the optical system contains one detail not clearly recognizable from Fig. 6. Lens *F* appears to be double convex. Actually, however, the surface nearer *E* is coated with black opaque paint except for an area on the axis not greater than 1 mm in diameter. This area, which is the limiting diaphragm of the system, is concave,

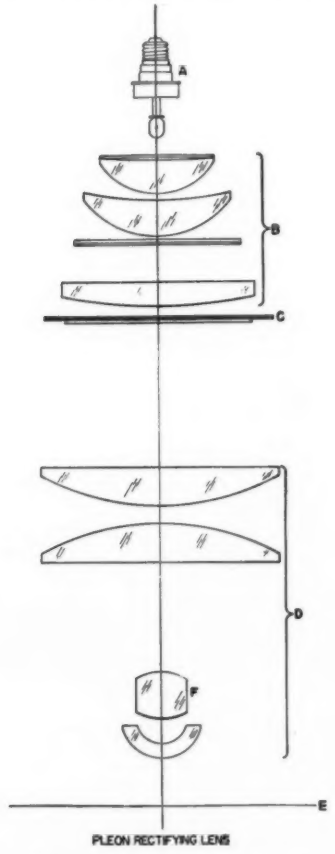

FIG. 6. The optical system of the Pleon rectifier.

the radius of curvature being approximately equal to that of the first surface of component *F*. The over-all length of the system, from the mercury capsule of the lamp to plane *E*, is approximately 110 cm. Figure 4 is a photograph of the complete rectifier. With the distortion changing so rapidly from the center outward, it is evident that the axial point of the negative must be carefully aligned with the axis of the rectifying system if the resulting print is to be distortion free or even radially symmetrical. To facilitate this adjustment an auxiliary optical system, not shown in Fig. 6, is provided. Immediately below the stage C there are four prisms by which the images, on the negative, of the four camera collimation markers can be simultaneously viewed and brought into coincidence with indexes in the rectifier. In Fig. 4, *G* is the eyepiece through which the markers are viewed and *H* is a knob for throwing the prisms out of the field after the adjustment has been completed. The vacuum plate which holds the paper flat is shown at *E*. Openings, covered by doors, shown on Fig. 5, are also provided for inserting a paddle over the printing paper for dodging to compensate for non-uniform illumination of the terrain at the time that the exposure was made.

VI. RESULTS OF MEASUREMENTS ON PLEON LENS AND RECTIFIER

The conjugate distances for the rectifying lens were so adjusted that there is a reduction on the axis of 1:0.82. Consequently, the scale of the rectified print corresponds to an equivalent focal length of 59.1 mm. The resulting circular print, for an angle of 65°, if accurately freed from distortion, would have a radius of 126.8 mm. For a point at the edge of the field ($\beta = 65°$) the magnification incidental to the rectification is 4.58 diameters. If the magnification on the axis were 1:1, the magnification at the edge would be 5.59 diameters. The resolving power of the camera lens was measured at 5° intervals. The over-all resolving power of the camera lens and the rectifying system was obtained by computation, the assumption being that the rectifying lens recorded faithfully all detail in the original negative. The final resolving power for any angle (measured in the object space), therefore, is equal to the resolving power of the Pleon lens

divided by the magnifying power of the rectifier for the same object ray. On the basis of such computation the resolving power on the final print is 100 lines per mm on the axis, and for 65° it is 4 and 6 lines, respectively, for tangential and radial lines.

In Fig. 7 the linear distortions are plotted for the camera lens, the rectifying unit, and the combination of the two systems. The values of the distortion for the camera lens have been multiplied by 0.82, corresponding to the axial reduction introduced by the rectifying system before being plotted on Fig. 7. This having been done, the distortion for the complete process corresponding to any angular distance from the axis is found by adding the ordinates corresponding to the lens and rectifier. It will be noticed that there is a net negative distortion of −4.34 mm at the edge of the resulting print after rectification. This is much too great for photogrammetric purposes. However, this result should be accepted with considerable caution because there is a possibility that camera lens and rectifier were designed to be selectively paired for use, and the two instruments received for test have not had the advantage of such pairing. Nevertheless, certain general considerations stand out. The camera lens has a negative distortion of −68.8 mm at the edge of the field. When the distortion is so large it is to be expected that not only third-order distortion but many higher orders of distortion are present. If the rectifier is to accomplish its purpose in a satisfactory manner, it must introduce the same orders of distortion in such magnitudes that each order of distortion in the negative is very closely compensated by a term of the same order in the rectifier. With camera lens and rectifier system so different in design it is hardly to be expected that complete compensation for all orders can be secured.

The camera lens tested was No. 2801326, nominal focal length 72.5 mm and maximum aperture ratio 1:8. It bore the Zeiss imprint and

TABLE I. Focal lengths of Pleon lens.

	Back focal length mm	Equivalent focal length mm
	74.78	72.13

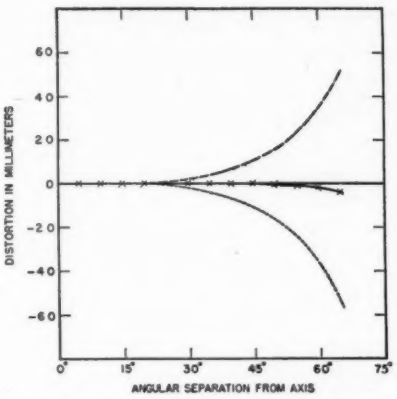

FIG. 7. Linear distortion of camera lens, rectifying system, and final rectified print. The dotted curve shows the linear distortion of the camera lens, multiplied by 0.82 to reduce the values to the scale of the rectified print. The dashed curve shows the linear distortion of the rectifying system. The full line curve, obtained by adding the corresponding ordinates of the first two curves, shows the residual distortion in the final print.

was definitely a Zeiss product. The rectifier was No. 200701 and bore the manufacturer's code designation "rln." Ordinarily, Zeiss products, during the war, were marked with the code "blc," but one of the German scientists now in this country affirms that the rectifier was manufactured by Zeiss, despite the code "rln."

The tables give the results of detailed tests made on these lenses.

A. Focal Lengths

The value of the equivalent focal length, given in Table I, is obtained from the approximate relation $f=d\cot 5°$, where f is the focal length and d is the distance separating fiducial marks in the images on the negative of targets that are located at 0° and 5° from the lens axis in the object space. These values of the focal length have been selected to give best average definition across the entire negative and do not necessarily correspond to those values of the focal length which give best definition on the axis. The probable errors of these determinations do not exceed ±0.10 mm.

B. Distortion of Pleon Lens and Rectifier

The values of the distortion listed in Table II are measured in millimeters and indicate the

TABLE II. Distortion of the Pleon lens, rectifier, and final print from rectifier.

Angular separation from the axis (degrees)	Distance from center of the Pleon lens negative mm	Distortion in Pleon lens negative mm	Contributions to distortion in final print		Net distortion mm
			Pleon lens (adjusted) mm	Projection lens mm	
0	0.00	0.00	0.00	0.00	0.00
5	6.30	.00	.00	+.02	.02
10	12.64	− .08	− .06	.12	.06
15	19.02	− .30	− .24	.29	.05
20	25.47	− .78	− .64	.67	.03
25	32.00	− 1.62	− 1.32	1.41	.09
30	38.64	− 3.00	− 2.45	2.47	.02
35	45.38	− 5.12	− 4.19	4.19	.00
40	52.20	− 8.32	− 6.80	6.88	.08
45	59.08	−13.04	−10.66	10.60	− .06
50	65.91	−19.98	−16.34	15.51	− .83
55	72.68	−30.16	−24.66	23.96	− .70
60	79.22	−45.44	−37.15	35.34	−1.81
65	85.39	−68.80	−56.26	51.92	−4.34

displacement of the image from its distortion-free position. A positive value indicates a displacement from the center of the plate. The probable errors for the Pleon lens data do not exceed ±0.02 mm for the range 0° to 45°; beyond this range the probable error increases rapidly and may be as high as ±0.20 mm at 65°. The probable errors for the projector lens do not exceed ±0.03 mm for the range 0° to 45°; beyond this range the probable error increases rapidly and may be as high as ±1.00 mm at 65°.

The distortion of the Pleon lens was determined in the usual manner with the aid of the precision lens testing camera,[6] with the exception that a second setting of the camera bench was necessary to get the region from 45° to 70°. In the case of the projector lens, a half-tone screen with accurately measured spacings was used as target, a deep blue filter (tricolor *C*) was placed over the target and exposure made with a moving lamp instead of the illuminator supplied with the projector. (This method was necessary because the special bulb required for the projector was not available.) The print was made on a Panatomic-X plate. Correspondence of the angular values reported for both lenses was accomplished by a series of interpolations

[6] I. C. Gardner and F. A. Case, "Precision camera for testing lenses," RP984, J. Research Nat. Bur. Stand. **18**, 449 (1937).

TABLE III. Resolving power in lines per millimeter.

	Pleon lens (measured)		Projection lens (computed)	
	Tangential	Radial	Tangential	Radial
0°	82	82	100	100
5°	82	82	100	100
10°	86	83	102	98
15°	85	83	97	95
20°	72	83	78	90
25°	59	81	59	81
30°	54	81	50	74
35°	55	59	45	48
40°	54	47	39	34
45°	57	34	35	21
50°	39	27	20	14
55°	38	29	15	12
60°	43	30	13	9
65°	18	29	4	6
70°	—	31	—	4

with the distance from the center of the master negative made on the precision lens testing camera serving as the connecting link. The primary purpose in effecting this correspondence was to permit the distortion of the lens and the projector to be evaluated at the same point on the negative made with the Pleon lens. Thus, these values can be used in evaluating the performance of the combination as is done in the last column of Table II, designated "Net distortion in final print."

C. Measured Resolving Power of the Pleon Lens and Computed Resolving Power of the Rectifier

The values of the resolving power, shown in Table III, are given at 5° intervals from the center of the field, and, in the case of the Pleon lens, are obtained by photographing test charts comprised of patterns of parallel lines. The series of patterns of the test charts are imaged on the negative with the lines spaced 10, 15, 20, 29, 41, 58, 81, 116, and 163 lines per millimeter. The values marked "tangential" give the number of lines per millimeter in the image on the negative of the finest pattern of the test chart that is distinctly resolved into separate lines when the lines lie perpendicular to the radius drawn from the center of the field. The row marked "radial" gives similar values for the pattern of test lines lying parallel to the radius. Because of the unusual distortion characteristics of this lens, the above series of resolving power values is valid

only on the axis of the lens. Therefore, in order to avoid error, line spacings were measured in each image on the negative and the values of resolving power computed from these measurements.

The value of the resolving power of the projection lens was not measured, but the resolving power in the final print has been computed on the assumption that the projection lens reproduces all detail present in the original negative. Reference to Table II shows that the distance from the axis to the image of a point at the angular distance β from the axis is closely proportional to β. In the final image, if the distortion is eliminated, the corresponding distance is proportional to $\tan\beta$. Therefore, the instantaneous value of the magnification introduced by the projection lens, corresponding to any value β is $1/1.223\cos^2\beta$, where 1.223 is the reciprocal of the axial magnification introduced by the projection lens. It is, therefore, evident that the formula,

$$\text{Resolving power} = 1.223r\cos^2\beta,$$

where r is the resolving power of the Pleon lens corresponding to the value β, is the resolving power of the combination of lens and projector, assuming that no loss of detail is caused by the projection lens. It is, therefore, the maximum resolving power obtainable in the final projected print of a negative made with the Pleon lens neglecting reductions that may result from aperture limitations. In view of aperture limitation discussed in the description of component F in Fig. 6, it is possible that the maximum resolving power for the rectifier may not exceed 20 lines per millimeter, which is, however, still adequate for good prints.

D. Effect of Vignetting for the Pleon Lens

In Table IV the vignetting of the Pleon lens is given, together with the comparable quantities

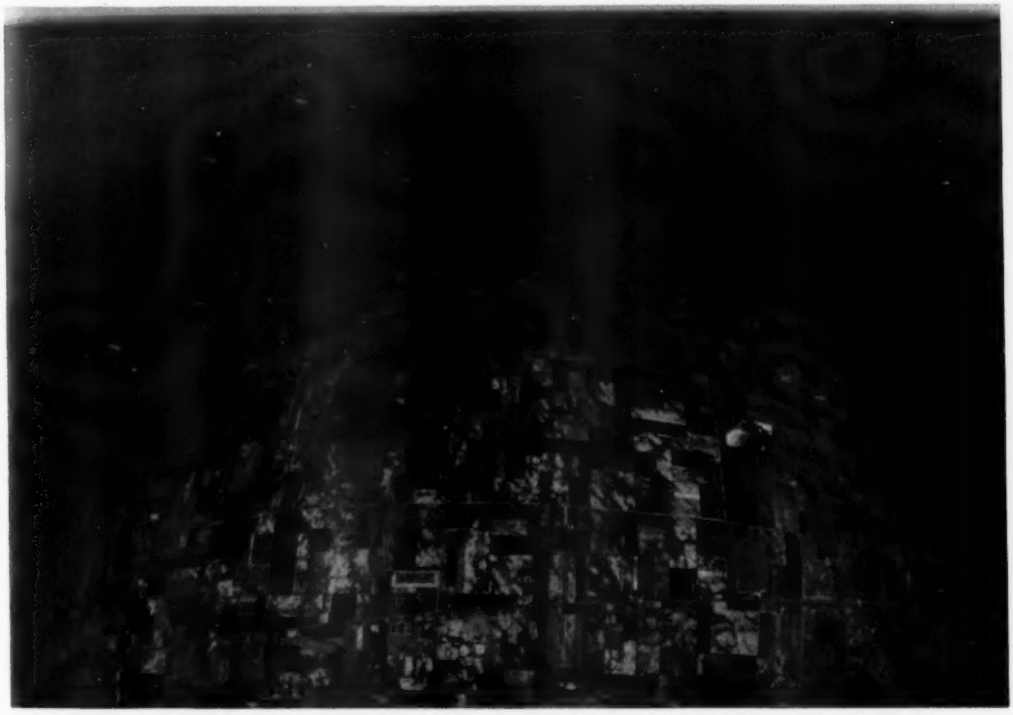

FIG. 8. Print from half of negative exposed in airplane camera with Pleon lens.

FIG. 9. Rectified copy of portion of photograph shown in Fig. 8. This probably does not represent the best obtainable results, because the rectifier, when received in this country was imperfect. The lamp was broken and the variable density filter missing. This photograph is shown as produced by the rectifier without change of scale in reproduction.

for an ideal lens and for a Topogon type lens. Let A_β be the projected area of the stop opening as viewed from the object space at the angular obliquity β; and let A_0 be the corresponding area of the stop opening as viewed from the object space along the lens axis. Then the ratio A_β/A_0, on the basis of first-order imagery, is equal to $\cos\beta$ for the case of the ideal lens having no vignetting. Appreciable vignetting exists in the Pleon lens as the measured value of A_β/A_0 is smaller for it than for the ideal lens. However, for values of $\beta \geq 30°$, the loss of light by vignetting is much less for the Pleon lens than for the Topogon type lens.

Figure 8 shows one-half of a photograph, to the original scale, as made with the Pleon lens by AAF personnel at Wright Field. At the peripheral parts of the lens the full possibilities are not realized because of haze. It is obviously desirable to have ideal atmospheric conditions and, possibly, to use infra-red plates, if the full 130° field is to be achieved.

Figure 9 shows a section of the rectified print to the final scale. This probably does not represent the best possible print, because of the haze effect in the original negative and also because, as has been mentioned, the lamp and variable density filter designed to be used with the rectifier were not available. The rectified print was made by Mr. Walter R. Darling, of the National Bureau of Standards, and he is to be commended for the resourcefulness and ingenuity which he showed in obtaining so good a print with an incomplete rectifier.

TABLE IV. Vignetting of the Pleon lens.

Angular separation from the axis	Relative area of diaphragm stop $A\beta/A_0$		
	Ideal lens (cosine)	Pleon lens	Topogon type lens
0°	1.00	1.00	1.00
10°	0.98	0.96	0.96
20°	0.94	0.87	0.87
30°	0.87	0.80	0.72
40°	0.77	0.67	0.49
45°	0.71	0.60	0.25
50°	0.64	0.52	—
60°	0.50	0.27	—
65°	0.42	0.05	—

Preparation of Aspherical Refracting Optical Surfaces by an Evaporation Technique

L. G. SCHULZ*
Department of Electrical Engineering, Ohio State University, Columbus, Ohio
(Received October 14, 1947)

By selective deposition of evaporated dielectrics it was found possible to form aspherical surfaces on plane glass plates which, when used with a lens, made the combination free from spherical aberration. A theory is given for the calculation of the correcting surfaces, and the experimental procedure for their preparation is described. The results are shown by means of ronchigrams.

INTRODUCTION

IN the past, selective deposition of evaporated aluminum has been used to correct mirror defects and to parabolize spherical mirrors.[1] It seemed reasonable, therefore, to expect that a similar procedure might be used to figure surfaces of transmission optical systems. An earlier publication reported that an evaporation technique had been used successfully to prepare correcting surfaces that would eliminate spherical aberration from a lens system.[2] At this time a more complete description can be given of the experimental work and also of the theory used to calculate the correcting surfaces.

Because of the great difficulty in grinding and polishing aspherical surfaces, applied geometric optics has been limited almost entirely to surfaces of a spherical form.[3] At an early date, however, it had been shown theoretically that by using specially figured surfaces the number of elements in an optical system might be reduced appreciably. Although parabolic mirrors are used in telescopes and more recently aspherical correction plates have been employed in the Schmidt camera, practically all optical surfaces are spherical. If aspherical surfaces are ever to be used extensively it will be necessary to find a method of producing them cheaply. Accordingly, the evaporation method was examined as a possibility.

Although the purpose of this work was to examine certain experimental procedures, it was at once evident that a direct and simplified theory for the calculation of correcting surfaces would be helpful. Very complete mathematical treatments have been given of certain types of non-spherical surfaces, in particular those used with the Schmidt camera.[4–7] These rigorous treatments, however, do not lend themselves readily to practical applications. The theory to be given here is a third-order approximation. It is concerned only with the calculation of surfaces for the elimination of spherical aberration, and is restricted to thin lenses. A plano-convex lens with an object at infinity will first be considered in detail, and following this, a general method will be developed for a lens of any shape and with the object at any distance from the lens. The result will be the same as that given by the Hamiltonian method.[8]

ELIMINATION OF SPHERICAL ABERRATION FROM A PLANO-CONVEX LENS

Figure 1A shows a ray diagram for a plano-convex lens with an object at infinity. A ray L, parallel to the axis, and at a height Y from it, is refracted first at the spherical surface and then at the plane surface, finally striking the axis at I', a distance S' from the plane surface. The course of the ray will be described in several steps. Figure 1B shows the refraction at the spherical surface. This surface separates two

* Westinghouse Research Fellow, now at The Institute for the Study of Metals, University of Chicago, Chicago, Illinois.

[1] John Strong, *Procedures in Experimental Physics* (Prentice-Hall, Inc., New York, 1945).

[2] L. G. Schulz, J. Opt. Soc. Am. **37**, 509 (1947).

[3] A. E. Conrady, *Applied Optics and Optical Design* (Oxford University Press, London, 1929), p. 3.

[4] M. Von Rohr, *Die Bilderzeugung in Optische Instrumente* (Verlag. Julius Springer, Berlin, 1904).

[5] L. Silberstein, J. Opt. Soc. Am. **11**, 479 (1925).

[6] D. S. Volosov, J. Opt. Soc. Am. **37**, 342 (1947).

[7] B. Strömgren, "Das Schmidtche Spiegelteleskop," Viert. Astro. Ges. **70**, 65 (1935).

[8] J. G. Synge, *Geometric Optics* (Cambridge University Press, Teddington, England, 1937).

regions of different media; the first region is air with an index of refraction taken equal to unity, and the second region is glass with an index of refraction n. By geometry and Snell's law,

$$\sin i = Y/R \quad \text{and} \quad \sin r = Y/Rn. \tag{1}$$

Further, by geometry,

$$\sin\theta/R = \sin r/D, \tag{2}$$

where

$$\theta = i - r.$$

These relations lead to

$$D = R(\sin r/\sin i \cos r - \sin r \cos i). \tag{3}$$

If the range of Y relative to R is restricted so that

$$(Y^2/R^2)^2 \ll Y^2/R^2, \tag{4}$$

the cosine functions of i and r can be replaced by the approximations

$$\begin{aligned} \cos i &= 1-(Y^2/2R^2), \\ \cos r &= 1-(Y^2/2R^2n^2). \end{aligned} \tag{5}$$

On substituting Eqs. (1) and (5) into Eq. (3), the expression for D given in Eq. (3) takes the form

$$D = (R/n-1)[1-(Y^2/2R^2n)]. \tag{6}$$

From Fig. 1B

$$\begin{aligned} D+R = S_0 &= (Rn/n-1) \\ &\times[1-(Y^2/2R^2n^2)] = (Rn/n-1)+\Delta S_0. \end{aligned} \tag{7}$$

The spherical aberration of the spherical surface is then defined as

$$\Delta S_0 = -(Rn/n-1)[Y^2/2R^2n^2]. \tag{8}$$

The same procedure can be followed to find the aberration introduced by refraction at the plane surface of the lens. In Fig. 1C a ray of light is shown in the medium of refractive index n, directed so as to strike the axis at the point I a distance S from the plane surface. As a result of the refraction it will strike at I' a distance S' from the surface where S' is given by

$$S' = (S/n)[1-(Y'^2/2S^2)(n^2-1)]. \tag{9}$$

The results given in Eqs. (7) and (9) can now be used to find the total aberration of the lens shown in Fig. 1A. First, changing S_0 to $S+t$ in Eq. (7) and substituting the resulting value of S into Eq. (9), gives

$$\begin{aligned} S' = &-\frac{t}{n}+\frac{R}{n-1} \\ &\times\left[1-\frac{Y^2}{2R^2}\left\{\frac{1}{n^2}+\frac{(n^2-1)(n-1)^2}{n^2}\right\}\right]. \end{aligned} \tag{10}$$

Here Y' has been taken equal to Y; a more correct value is

$$Y' = Y[1-(t/S)+(Y^2/2RS)]. \tag{11}$$

In making these substitutions the inequality expressed in Eq. (4) is assumed to be satisfied. From Eq. (10) the total spherical aberration of the complete lens is

$$\Delta S' = -\frac{Y^2}{2R(n-1)}\left[\frac{1}{n^2}+\frac{(n^2-1)(n-1)^2}{n^2}\right]. \tag{12}$$

If the procedure of Eqs. (1) to (6) is applied to a paraboloidal surface,

$$X = Y^2/2R, \tag{13}$$

then Eq. (7) has the form

$$S_0 = (Rn/n-1)[1+(Y^2/2R)(n^2-1)/n^2]. \tag{14}$$

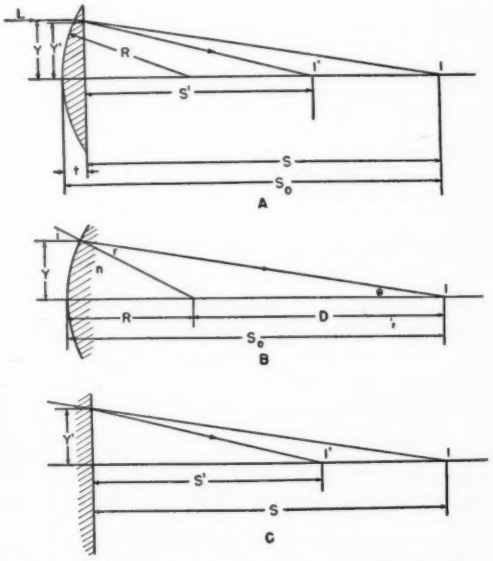

FIG. 1. Refraction of a light ray by a plano-convex lens. In A are shown the complete lens with an object at infinity and the image formed at I' a distance S' from the plane surface. B shows the refraction at the spherical surface forming an image at I. C shows the refraction at the plane surface; I is the object and I' the final image.

Equation (14) indicates that for this surface the spherical aberration is positive. This suggests that it may be possible to find some surface intermediate between a spherical and paraboloidal that would have zero aberration. Such a surface can be tentatively represented by

$$X_c=(Y^2/2R)+(AY^4/8R^3). \tag{15}$$

When A is equal to one, Eq. (15) reduces to the original spherical surface,

$$X=(Y^2/2R)+(Y^4/8R^3). \tag{16}$$

The difference ΔX between the trial surface, Eq. (15), and the original spherical one, Eq. (16), is therefore

$$\Delta X=(1-A)(Y^4/8R^3). \tag{17}$$

For the surface represented by Eq. (15)

$$S+t=S_0=(Rn/n-1)\times[1+(Y^2/2R^2)\{(1-A)-(1/n^2)\}]. \tag{18}$$

By combining Eq. (18) and Eq. (9) the new value obtained for S' is

$$S'=-\frac{t}{n}+\frac{R}{n-1}\left[1+\frac{Y^2}{2R^2}\times\left\{(1-A)-\frac{1}{n^2}-\frac{(n^2-1)(n-1)^2}{n^2}\right\}\right]. \tag{19}$$

Since for no spherical aberration

$$1-A=\frac{(n^2-1)(n-1)^2+1}{n^2}, \tag{20}$$

we conclude that a plano-convex lens having a convex surface given by Eq. (15) is free from aberration if A satisfies Eq. (20). For all practical values of n, A will be positive and less than one-half. The correction surface represented by Eq. (15) therefore lies outside the original spherical surface described by Eq. (16). Accordingly, ΔX will be the thickness of additional material that must be added on the lens surface to give the surface represented by Eq. (15).

It is also possible to eliminate aberration by modifying the plane surface of the lens. Following the method already used the correcting surface is given by

$$\Delta X=BY^4/8R^3, \tag{21}$$

where

$$B=\frac{(n^2-1)(n-1)^2+1}{n^2}. \tag{22}$$

A comparison of Eq. (20) and Eq. (22) shows that B is equal to $(1-A)$ and that the correction is therefore the same in both cases. If the correcting deposit is built up of material with an index of refraction n' different from that of the glass in the lens, the value of B is

$$B^*=\left(\frac{n-1}{n'-1}\right)\left[\frac{(n^2-1)(n-1)^2+1}{n^2}\right]. \tag{23}$$

The added material forms a weak lens, which acts along with the original lens in such a way that all rays through the combination are brought to a focus in the back focal position. This interpretation suggests that it should be possible to find a correcting surface which places the final aberration-free image at any desired position in the range ΔS_0. The hypothesis underlying the argument expressed in Eqs. (13) to (20) inclusive is that some surface intermediate between a spherical and paraboloidal would eliminate aberration. Implied in the hypothesis is the assumption that any fourth-power generative curve with suitable parameters will provide correction. If Eq. (15) is written in the generalized form

$$X_c=X_0+K_1[(Y^2/2R)+(AY^4/8R^3)], \tag{24}$$

then

$$\Delta X=[(1-A)/8R^3]\times[K_2Y_0^4+Y^2(Y^2-K_3Y_0^2)]. \tag{25}$$

K_2 is a constant determined by the origin of the coordinate system, K_3 is a parameter, and Y_0 is the radius of the lens. If both K_2 and K_3 are equal to zero, Eq. (25) reduces to Eq. (17) which is shown graphically in Fig. 2A. Two other special cases are of interest. The first is the curve shown in Fig. 2B, which results when K_2 is equal to one and K_3 equal to two. For this surface all rays are brought to a focus at the near focal position defined by rays through the periphery of the lens. The second, for which K_2 and K_3 are both equal to one, is shown in Fig. 2C. With a lens having such a surface all rays are brought to a focus at the midpoint of $\Delta S'$.

GENERAL THEORY

For the case of a plano-convex lens the aberration $\Delta S'$ given in Eq. (12) is a relatively simple function of Y, R, and n. For the more general case of a lens with two spherical surfaces, the method used to obtain Eq. (12) becomes long and tedious. It can be shown, however, that where the approximation of Eq. (4) is satisfied, $\Delta S'$ is proportional to Y^2 and, therefore, can be corrected by a fourth-power surface of the form given in Eq. (24).[9] The special case wherein K_2 and K_3 are equal to unity can be rewritten in terms of the image distance S' and a new constant B':

$$\Delta X=(B'/8S'^3)[Y_0^4+Y^2(Y^2-Y_0^2)]. \quad (26)$$

The effect of the surface represented by Eq. (26) is to bring all rays to a focus at a point $S'-\Delta S'/2$ from the lens where $\Delta S'$ is the total axial aberration. Accordingly, the center of the correcting lens must have a focal length f_c given by

$$\frac{1}{f_c}+\frac{1}{S'}=\frac{1}{S'-(\Delta S'/2)}. \quad (27)$$

The value of f_c is then

$$f_c=(2S'^2/\Delta S'). \quad (28)$$

The radius of curvature R_c at Y equal to zero is

$$R_c=(n'-1)f_c. \quad (29)$$

The radius of curvature of the surface of Eq. (26) at Y equal to zero is

$$R_c=(4S'^3/B'Y_0^2). \quad (30)$$

From Eqs. (28), (29), and (30),

$$f_c=2S'^2/\Delta S'=R_c/(n'-1)$$
$$=4S'^3/[B'Y_0^2(n'-1)]. \quad (31)$$

Solving for B',

$$B'=\frac{2S'\Delta S'}{Y_0^2(n'-1)}. \quad (32)$$

The result can be readily checked by application to the plano-convex lens already considered. Using the value of $\Delta S'$ from Eq. (12) and putting S' equal to $R/n-1$,

$$B=B'(n-1)^3=\frac{n-1}{n'-1}\left[\frac{1}{n^2}+\frac{(n^2-1)(n-1)^2}{n^2}\right], \quad (33)$$

which is the same value as obtained before.

For a given lens forming an image at S', $\Delta S'$ and S' can be measured experimentally. Using these values in Eq. (32), B' is determined and, consequently, the correcting surface given by Eq. (26) is determined. It is not necessary to know the radii of curvature of the lens surfaces or the index of refraction of the glass in it.

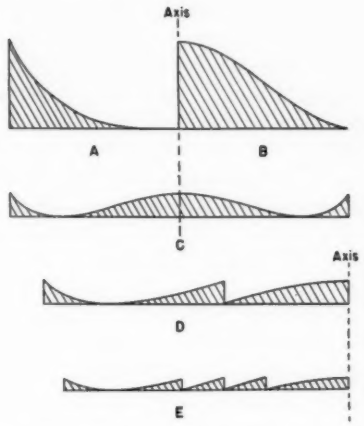

FIG. 2. Relative thicknesses for various types of correcting surfaces. In all five cases the relative scales of the vertical and horizontal axes are the same.

PRACTICAL CONSIDERATIONS

The expressions for ΔX derived in the preceding theory have all been given as deviations from a spherical surface. These expressions will be used to determine the modification of the spherical aberration. The modifications can be made by adding material to the lens surfaces through selective deposition of an evaporated dielectric, such as lithium fluoride and magnesium fluoride (these salts are chosen because of their low solubility in water). In the experiments that are described, evaporations were made on plane disks of thin glass rather than on the lens itself. It was then much easier to make the calculations and design the diaphragms. In use, these correction plates were placed in contact with the lens that was to be corrected.

[9] T. T. Smith, Bureau of Standards Paper No. 461.

Although any one of the three deposits shown in A, B, and C of Fig. 2 would have correcting action, the particular one shown in C has definite advantages. Most important, the maximum deposit at the center and the outer edges is only one-fourth of the maximum deposit of the type shown in A and B. In addition, with the form of C the region of thinnest deposit covers a large area of the lens. To reduce further the maximum thickness required, some diaphragms were cut to form a Fresnel lens of the form shown in Fig. 2D and E. A discussion of the behavior of Fresnel mirror surfaces formed by deposition of evaporated aluminum has been given earlier and will be applicable here.[10]

DESIGN OF THE DIAPHRAGMS

The method used to secure the desired deposit of dielectric followed that employed for parabolizing spherical mirrors.[1] This involved a fixed source and fixed diaphragm but with provision for rotating the surface receiving the deposit. Preliminary work showed that it would be rather difficult to arrange sources which would give a uniform deposit of a dielectric over an appreciable area. It seemed easier to use a single source placed on the axis of the system and cut the diaphragms to compensate for the slight falling off of deposit at points away from the axis. The lenses to be corrected had diameters ranging from $1\frac{1}{2}$ to $4\frac{1}{2}$ inches. Because of this small size the construction of the diaphragms was difficult. The angular opening θ as a function of the radius Y was given by

$$\theta = K\left[\frac{\Delta t(Y)}{S(Y)}\right]. \tag{34}$$

Here $\Delta t(Y)$ is the deposit desired and $S(Y)$ the radiation characteristic of the source.

A B C

FIG. 3. Shadow photographs of the diaphragms used to obtain three types of correcting surfaces The light areas are those that are cut out.

[10] L. G. Schulz, J. Opt. Soc. Am. **37**, 349 (1947).

Experience showed that diaphragms cut with multiple openings gave the best results. Typical designs are shown in Fig. 3 where A, B, and C gave the deposits C, D, and E of Fig. 2. No steps were put in the Fresnel surfaces at large values of Y because the defective area between zones becomes large relative to the total zone area. The openings were cut in twenty-mil soft copper with a file.

A Fresnel diaphragm could be used to make only one size of correction plate, whereas with the continuous surface type of Fig. 3A correction plates considerably larger than the diaphragm were possible. This was done by increasing the separation between the diaphragm and the glass receiving the deposit. Because the source was on the axis and approximately a point, it was possible to get a deposit closely approximating that for a small separation. This separation could be increased to the extent where it was approximately equal to that of the distance from the source to the diaphragm. There is some advantage in using a large diaphragm-to-glass separation in all cases since then small defects in the diaphragm tend to be eliminated.

EXPERIMENTAL ARRANGEMENT FOR MAKING CORRECTION PLATES

The general plan as well as many of the details are shown in Fig. 4. A glass disk to receive the deposit was supported at the lower end of the vertical shaft. It was possible to center this disk accurately so that deposits on both sides would be concentric. Immediately below the disk was the diaphragm supported by the blocks on the three vertical rods. Six inches below the disk was the source held in position by one-fourth inch rods. The aligning process required care, in particular for the diaphragm of the type Fig. 3B and C. First, the glass disk holder was removed and the shaft lowered until it fell to the level of the source, which was then centered to about one-eighth inch or better. Then the shaft was raised and a fine point attached to its end. This point made possible the positioning of the diaphragm to five mils or better. Lastly, the disk holder was attached to the shaft and lowered until it almost touched the diaphragm. Final adjustment usually involved securing parallelism between the glass disk and the diaphragm.

A glass bell-jar, 18 inches in diameter and 30 inches high, was lowered over the assembly and a vacuum of 5×10^{-5} mm of mercury secured with a six-inch diffusion pump. A high voltage glow discharge was very effective in cleaning out the occluded gases as well as cleaning the glass plates to be coated. During evaporation, motion was brought into the vacuum through a Wilson seal and carried to the central shaft by means of a belt and pulleys.

DEVELOPMENT OF A SOURCE

A search for a suitable arrangement for the evaporation of dielectrics resulted in the design shown in Fig. 4. A thirty-degree cone, one inch deep, was made from three-mil sheet molybdenum, and surrounded by a heating coil of ten turns of thirty-mil tungsten wire. The wire was separated from the metal cone by Alundum cement. A convenient procedure for construction was first to cover the cone with about one-thirty-second inch of Alundum paste formed by mixing Alundum cement powder and a solution of sodium silicate. After drying it was hardened by heating in a vacuum to about 1000°C. Then the cone was slipped into the heater coil, and the outside of the unit, together with the lead wires, covered with more Alundum paste. Final heating in a vacuum to about 1500°C was sufficient to evaporate all volatile material in the cement.

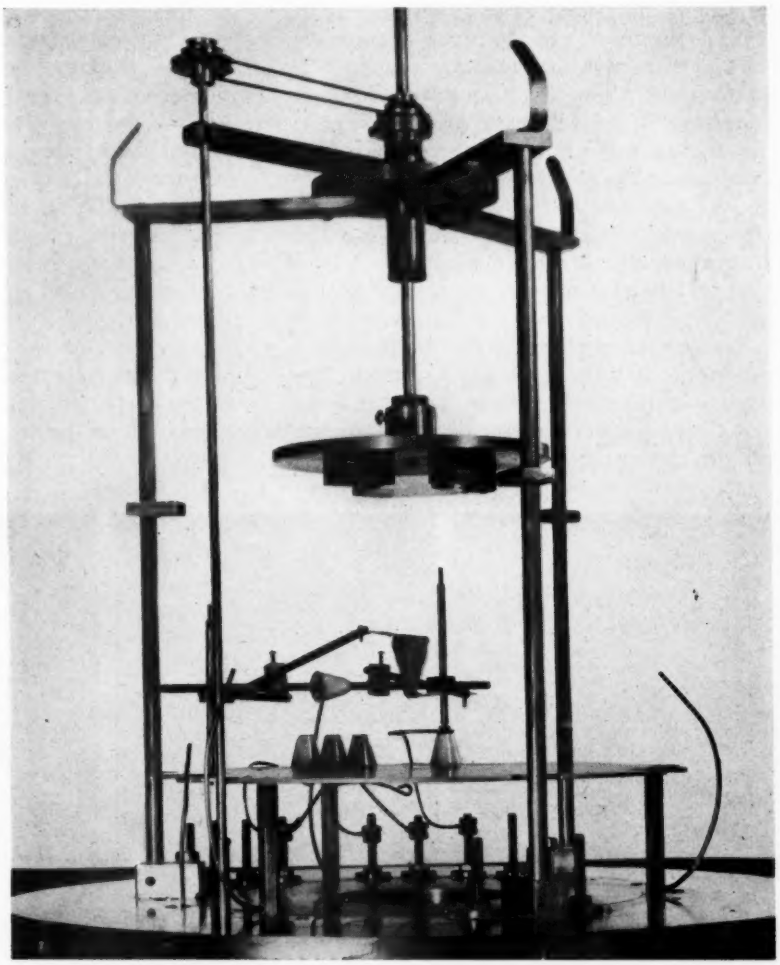

FIG. 4. The arrangement of experimental apparatus. For this photograph the diaphragm was removed.

This type of source has definite advantages over others previously described.[1] The vapor is directed upward from a source of simple geometric form; the evaporation proceeds from a clean metal surface, thus avoiding the formation of a scum which often forms in a ceramic material; the residue in the source is continuously falling to the lower tip of the cone, which is the hottest part of the source; a large charge, about 1.5 grams, can be accommodated. Furthermore, the source is relatively easy to make and is rugged (the one shown in Fig. 4 having been heated more than thirty times).

Before using these sources, their radiation characteristics were tested. A glass disk three inches in diameter when placed six inches above the source had not more than ten percent decrease in thickness from the center to the edges. The thickness was measured by counting the interference fringes in monochromatic light. There seemed to be little variation in behavior with the amount of the charge if the molten mass did not exceed about three-fourths the depth of the cone.

The correct amount of dielectric to be evaporated in preparing a correction plate for a given lens could be obtained exactly from Eqs. (32) and (26) if the radiation characteristics of the source were known completely. In practice, a more empirical procedure was satisfactory. Usually it was necessary to make several evaporations. Following the first, the disk was removed and the change in S' measured. From this it was possible to determine the number of additional evaporations required. A possible way of avoiding the trouble of getting exactly the proper amount of deposit was to over-correct slightly and then place the correction plate on the image side of the lens and adjust its position until spherical aberration was fully corrected. This involved only a small separation of lens and disk because Δt is a very sensitive function of Y. The separation would, therefore, not disturb the optics of the system. Moving the correction disk away from the lens decreased its effective Y, thereby increasing the Δt required.

TESTING METHODS AND TYPICAL RESULTS

Testing was done with both the Ronchi and the knife-edge test. Because of the difficulty in showing the quality of a lens by photographing knife-edge shadows, the results are here shown with ronchigrams. For this test a 200-mesh metal screen was mounted on a knife-edge motion, and the lens viewed through the screen when the screen was slightly in front of the focal plane of the lens. A distant vertical slit of adjustable length and width illuminated by monochromatic light was used as a source. In Fig. 5A is shown the appearance of a lens $1\frac{11}{16}$ inches in diameter and with a 7-inch focal length placed directly behind a 3-inch glass disk. The curvature of the lines indicates the presence of aberration. In B is shown the Ronchi pattern after a correcting deposit has been put on the glass disk. When the screen is moved into the focal plane of the lens a hori-

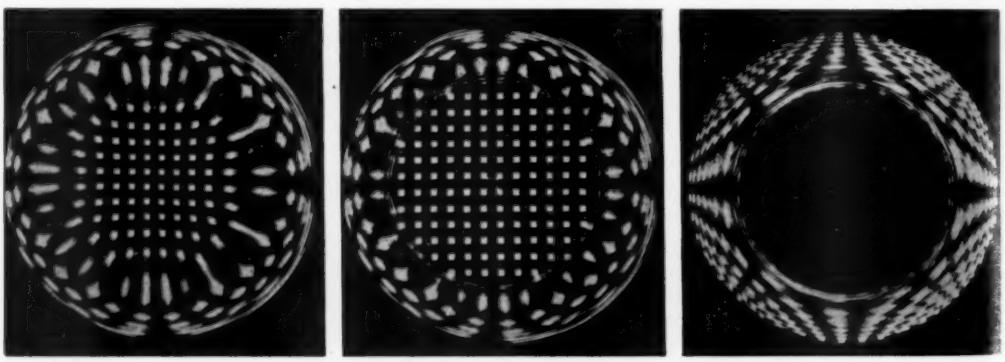

A B C

FIG. 5. Ronchigrams of a lens having a continuous correcting surface. A, before correction; B, after correction; C, with the image blocked out. The slit source length is approximately equal to its width.

zontal wire cuts out the image of the source as is shown in C.

Figure 6 shows the appearance of a Fresnel-type correcting plate. The largest diameter is the outline of a 4½-inch lens with a focal length of 16 inches. A correction deposit, E of Fig. 2, has been evaporated on a 3-inch plane glass disk which is placed concentric with the lens and in contact with it. Before the deposit had been evaporated, the ronchigram was that shown in A and after correction as in B. The additional photograph, C, shows the screen at the focal plane of the lens and with a vertical wire intercepting the image of the source.

PRODUCTION OF THICK DEPOSITS

Chief among the limitations to the application of the evaporation method is the appearance of "bloom" on thick deposits. With metals as well as dielectrics as the thickness of an evaporated film is increased the surface increases in roughness and at a certain thickness becomes sufficiently coarse to scatter light in a way that gives a characteristic white appearance to the film. Because bloom is much easier to detect on reflecting films than on refracting, a just opaque layer of aluminum was evaporated over test surfaces of dielectric to enhance the bloom. Using this test on lithium fluoride it was found that thicknesses of 50,000A free from bloom could be obtained consistently, and occasionally this could be extended to 75,000A. The procedure used to obtain the most satisfactory films was as follows: The glass was thoroughly cleaned by standard methods and then placed in the evaporation chamber with the diaphragm removed. After cleaning fifteen minutes with a glow discharge, a uniform layer of 3000A was deposited. There was appreciable improvement in the toughness of this layer as well as its adherence to the glass when the glass was heated during evaporation. Following this initial deposit the diaphragm was put in place and the chamber again evacuated. During all succeeding evaporations every effort was made to keep the glass cool. The temperature of the source was raised until the charge began to melt and settle toward the center. This temperature was never exceeded, evaporation proceeding at about 5000A per minute. After each 15,000A of deposit the glass was permitted to cool for thirty minutes. If these precautions were not observed thick deposits usually flaked off on cooling. When several charges were to be evaporated successively it was essential that the air be admitted very slowly into the bell-jar to avoid formation of a fine layer of dust over the surface receiving the deposits.

An effort was made to discover methods of increasing the useful thickness, but little progress was made by the empirical method of noting the effect of variation in evaporation conditions. In connection with other experiments a more detailed study was therefore made of the nature of thin evaporated films. Although complete details are to be given elsewhere, the relevant conclusions can be outlined here. Electron diffraction by the reflection method showed that all evaporated films have very pronounced orientation

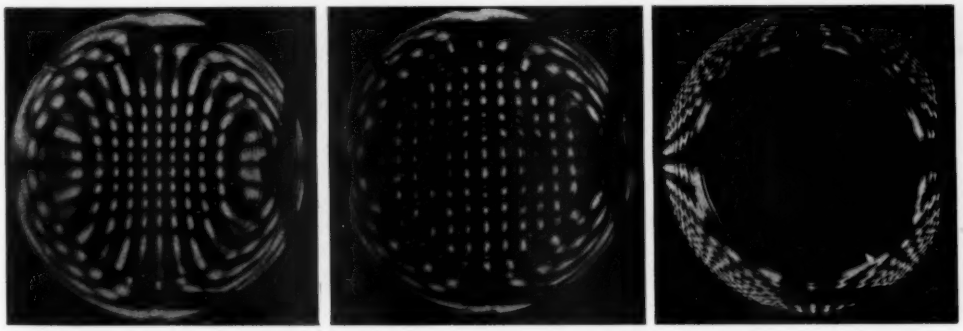

A B C

FIG. 6. Ronchigrams of a lens used with a broken surface correction plate. A, B, and C are the same as in Fig. 5. The slit length is about three times that of its width.

relative to the substrate. Representative results are shown in Fig. 7. For lithium fluroide the first few hundred angstroms were of random orientation, but after that thickness was exceeded the (111) orientation persisted up through 250,000A, which was the limit studied.[11] Following are the orientations of a few other materials: NaCl and KCl, (110); NaBr and KBr, (211); MgF_2, (302); CaF_2, (111), and Al, (100). This result for aluminum is consistent with the observation that when this metal is deposited normal to the substrate it shows less bloom than that given by the same thickness which is obliquely deposited.

The results given by diffraction and electron microscopy indicated that bloom is produced by the increase of particle size in the surface of the films. At first sight it seemed that alternate layers of different dielectrics might be expected to suppress this tendency to grow large crystals, but built-up films of this kind had very poor mechanical properties. Apparently strong ionic crystals of the alkali halide type are too brittle to withstand the strain that exists at boundaries. A more promising procedure was to separate two layers of lithium fluoride with a plastic. A mixture of amyl acetate and collodion was made to flow over a deposit that was nearing the blooming thickness. The amyl acetate evaporated, leaving an optically uniform covering of collodion a few thousand angstroms thick. Greater smoothness was obtained by adding a second coat of collodion. After the second drying a deposit of lithium fluoride would begin with a random structure and not show bloom until about 50,000A. Thus an effective thickness of

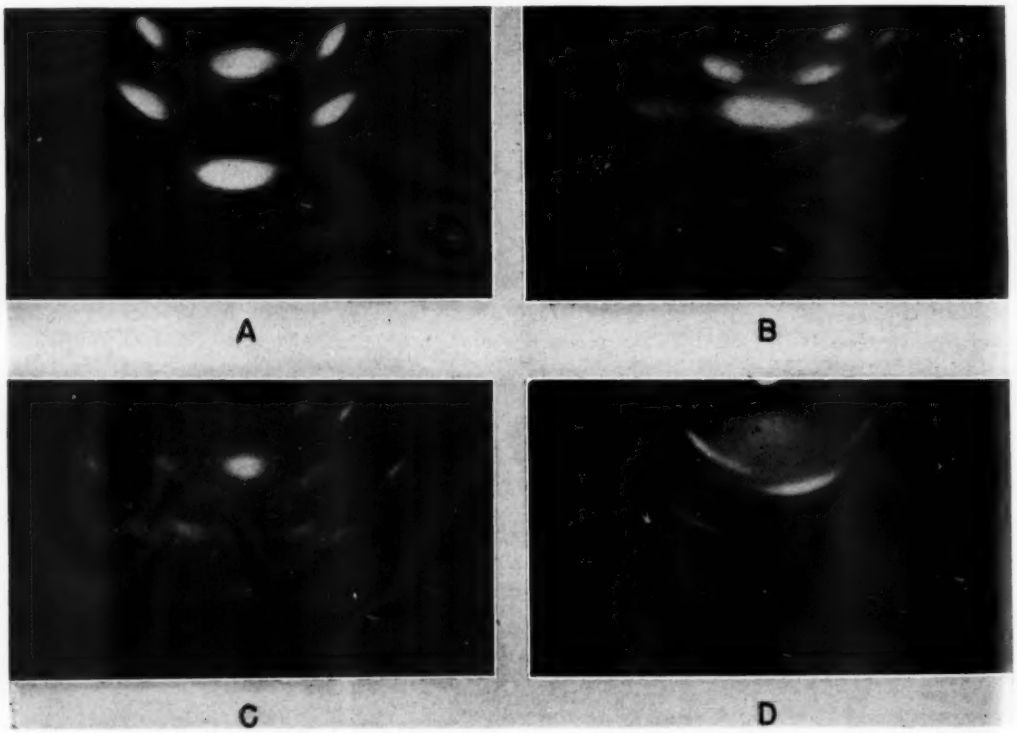

FIG. 7. Electron diffraction patterns of evaporated films showing strong preferred orientation. A, lithium fluoride, (111); B, magnesium fluoride, (302); C, sodium chloride, (110); D, aluminum, (100).

[11] For an interpretation see "fiber structure patterns" in any X-ray text, for example, G. L. Clark, *Applied X-Rays* (McGraw-Hill Book Company, Inc., New York, 1940).

100,000A was produced. Unfortunately, it was found much more difficult to put collodion over the second deposit of lithium fluoride because the amyl acetate had a tendency to penetrate through slight defects to the first layer of collodion. This tendency could be eliminated by rapid evaporation of the amyl acetate in a blast of hot, clean air. For metals, on the other hand, no such special care was necessary; collodion and aluminum, for example, could be alternated repeatedly. To form a reflecting surface the bulk of the deposit might be lithium fluoride, which could be followed by collodion and aluminum. Such a sequence would be useful in parabolizing spherical mirrors by the method of Gaviola and Strong.[12]

In these experiments lithium fluoride was used as the dielectric because of its conveniently low melting point and the success with which it had been used in the construction of interference filters. Magnesium fluoride, the only other dielectric tested, was used to give a final, thin, insoluble coating over the somewhat more soluble lithium fluoride. Collodion was used as the plastic because it was readily available. Since bloom is of surface origin, a plastic with the same index of refraction as the dielectric would be desirable. Possibly a systematic search would reveal materials better than lithium fluoride and collodion.

EVALUATION OF THE RESULTS

Figures 5 and 6 show that it is possible to eliminate spherical aberration through the use of correction plates prepared by the evaporation technique. A critical test of the lens in Fig. 5 showed that it was slightly under-corrected and the lens in Fig. 6 somewhat over-corrected. The width of the defective region between zones in Fig. 6 was about forty mils; most of this was caused by diffraction effects and the remainder by errors in aligning the diaphragm during evaporation.

The general method here demonstrated could be extended to the production of more complicated deposits than those required to correct for spherical aberration. Thus, by choosing the proper ratio of radii of curvature of the lens surfaces it would also be possible to correct for coma.[5] Even with the thicknesses now available it is possible to make lenses of very long focal length from plane disks of glass. In this exploratory work the practice of evaporating onto plane glass disks to form correcting plates was adopted because of convenience and is not a requirement of the method. The glass used for correcting plates must be optically flat and of a quality comparable to that of the lens to be corrected.

As already indicated, the chief limitation to the evaporation method is the appearance of bloom on thick deposits. The experimental limits might be summarized as follows: For a single deposit of lithium fluoride 50,000A is a conservative limit, which can be very easily doubled or tripled by separation layers of a plastic. By using the Fresnel figure of the type shown in Fig. 3C the effective thickness is increased by a factor of four, and by evaporation on both sides of the lens, or correction plate, this is again doubled. This can be extended even further by using more than one correction plate. If methods are found to produce films of unlimited thickness, then the limitation to the method will be set probably by the accuracy with which the diaphragms can be cut.

ACKNOWLEDGMENTS

The author wishes to thank the Westinghouse Electric Corporation for making this work possible. Also Professor A. F. Prebus for his suggestions and Mr. John Dankworth for preparing the photographs in this paper.

[12] E. Gaviola and John Strong, J. Opt. Soc. Am. **26**, 153 (1936).

JOURNAL OF THE OPTICAL SOCIETY OF AMERICA VOLUME 38, NUMBER 5 MAY, 1948

Non-Adaptability of the ICI System to Some Near-Whites Which Show Absorption in the Far Blue Region of the Spectrum

A. E. JACOBSEN
National Lead Company, Titanium Division, Research Laboratory, Sayreville, New Jersey

(Received December 23, 1947)

Attempts to correlate readily recognizable chromatic differences between two near-white paints, which contain the widely used rutile and anatase titanium dioxide pigments, with colorimetric data calculated from spectrophotometric curves, by the accepted procedure, have been unsuccessful. The curves for these materials are essentially identical from 430 to 700 mu but differ in selective absorption from 430 mu and below. Readings with the Hunter multipurpose reflectometer for these two paints are identical. The evidence shows that the GE recording spectrophotometer is capable of measurement of the spectral differences, but the ICI system does not correctly weight the blue region of the spectrum in accord with visual perception.

INTRODUCTION

RECENTLY Nickerson[1] expressed the need for a better understanding of color problems when setting up tolerance limits for small color differences. Further remarks mention the difficulties in complete reliance on visual grading and stressed the need for special instrumental means for the detection of small differences. These comments have prompted the reporting of an experience which has been encountered while attempting to employ small color difference formulas, to show the extent of color difference for plant control purposes between the well-known near-white anatase and rutile titanium dioxide pigments when incorporated in a paint vehicle. While these paints exhibit visual differences, and spectrophotometric curves show marked differences in selective absorption in the spectral region below 430 mu., I.C.I. x,y coordinates are essentially identical. The evidence to be presented shows that the I.C.I. standard colorimetric coordinate system apparently does not weight the far blue region of the spectrum in accordance with visual perception.

INSTRUMENTS

Two instruments have been employed for these color grading studies, namely, a General Electric recording spectrophotometer and a Hunter multipurpose reflectometer. The spectrophotometer has a spectral range of from 390 to 700 mu and has a special cam which expands the usual 80 to 100 percent reflectance range twofold.

In the case of the Hunter multipurpose reflectometer,[2] a supplementary blue filter with a spectral range somewhat lower than the blue two-component filter supplied with the instrument has been employed. This filter was also composed of two components; the blue component was the same as used with the original blue filter supplied with the instrument, while the yellow component was Corning Noviol Shade O, No. 3060 (2 mm thick).[3] The spectral distribution for the blue composite filters source-filter photo-cell combination is shown in the Fig. 1.

METHOD FOR VISUAL GRADING

The visual comparisons were made by five operators skilled in the grading of near-white products for small color differences. Viewing was done in diffused north daylight with samples held at arms length and at approximately eye level with the surface normal to the axis of view.

MATERIAL UNDER STUDY

To give a little background with respect to the material being studied, it should be mentioned that the anatase and rutile pigments are near-white powders with slight chromatic differences, which in practice are tested for this difference after incorporation in an oil to give

[1] D. Nickerson, "Interrelation of color specifications." Presented at joint meeting of Inter-Society of Color Council and TAPPI, 1947.

[2] R. S Hunter, "Photoelectric tristimulus colorimetry with three filters," Nat. Bur. Stand., circular 429 (1942).

[3] The use of this filter was suggested by D. B. Judd, who also brought to the author's attention that the spectral distribution curve for the supplementary filter-light source photo-cell combination approximates the O.S.A. "excitation" curve.

a heavy paste. The pigments are used commercially in large volume in paint, rubber, paper, and allied products. The use of the rutile variety would be preferred in many cases because of its greater opacifying property but this pigment normally possesses a yellower tone than the anatase variety, and therefore for white goods of the highest quality colorwise, the anatase variety is favored. It is the relative degree of yellowness between these two pigments that is of concern to colorists. Incidentally, in practice a blue pigment or dye is sometimes added to the rutile pigment to produce a less yellow tone, but under such circumstances reflectance is lower.

The particular rutile and anatase products employed in this work are pigments of plant production and were selected because they were of the same lightness. A third pigment which actually is a blend of 90 parts of the anatase pigment and 10 parts of the rutile pigment has been included in order to show more clearly visual perceptible steps between the anatase and rutile pigments.

The test specimens on which these studies were made were identical to those used in everyday practice, namely, that the pigment was incorporated in sufficient light colored linseed oil to give a heavy paint-like paste.

EXPERIMENTS

For instrumental studies, reflectance measurements were made on smooth surfaces of the paint-like pigment-linseed oil pastes applied to a white glass plate with the usual precautions being exercised.

The spectrophotometric curves for the paints are given in Fig. 2. It will be seen from this figure that the three curves are for all practical purposes identical in reflectance from 700 to 430 mu. Below 430 mu the curves diverge, with the anatase showing less selective absorption than the rutile. The blend shows an intermediate position. Table I gives I.C.I. x,y coordinate values calculated for illument "C," using 5-mu wave-length intervals, and also the number of perceptible steps between the pigments as calculated by the formula of Judd.[4]

TABLE I. I.C.I. chromaticity coordinate data calculated from spectrophotometric curves with correlation between calculated perceptible steps and visual perception.

Identification	I.C.I. trichromatic coefficients x	y	Y values	ΔE_J	Diff. in visual perception
Anatase	0.3142	0.3215	0.9062	—	—
Blend	0.3143	0.3217	0.9050	—	3 steps in terms of anatase
Rutile	0.3145	0.3224	0.9063	0.4	7 steps in terms of anatase

For relative visual grading the same paints as used for instrumental studies were employed. The paints were applied in juxtaposition on a white glass plate, and their surfaces made smooth by drawing a straightedge over the top of the paints.

In order to determine the number of perceptible steps between the anatase and the blend, known portions of each were mixed and judged for just perceptible steps. The same procedure was followed in the determination of the number of just perceptible steps between the blend and the rutile. The results of visual grading are given in Table I.

The data in Table I show that the x and also the y coefficients for all three samples are essentially identical. The Y values are also essentially identical. The calculated ΔE_J between anatase and rutile is two perceptible steps. Based on visual grading, three steps of perception were found between the anatase sample and the blend, and seven steps of perception between the anatase and the rutile sample.

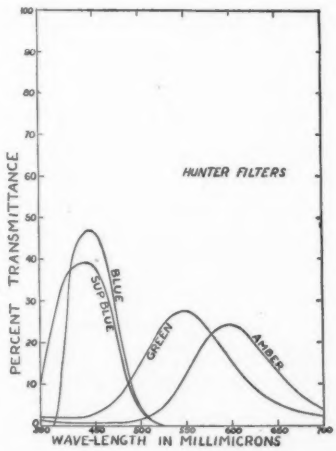

FIG. 1. Spectrophotometric transmission curves for filters supplied with Hunter multipurpose reflectometer and also for supplementary blue filter.

[4] D. B. Judd, "Specification of uniform color tolerance for textiles," Textile Research 9, 253 (1939).

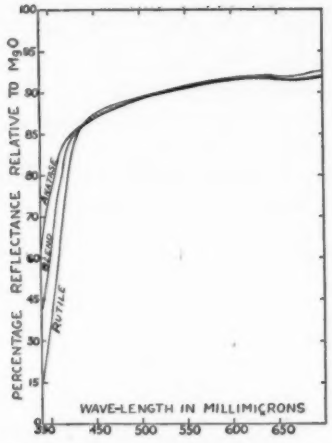

FIG. 2. Spectrophotometric reflectance curves of samples used in the study of the correlation between calculated perceptible steps and differences in visual perception.

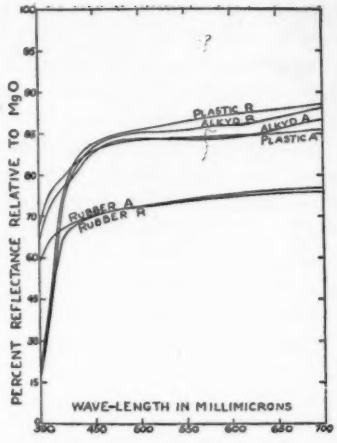

FIG. 3. Comparative spectrophotometric reflectance curves of alkyd paint vehicle, plastic and rubber pigmented with both anatase and rutile pigments. In these curves *A* designates anatase and *R* designates rutile.

Table II gives the reflectance values for the three samples using the Hunter multi-purpose reflectometer. These reflectance values are the average of two determinations.

These data show identical values for the three samples, using the amber, green, and blue filters supplied with the instrument. The readings with the supplementary blue filter show differences among the samples in the order expected from their relative spectrophotometric curves.

EXAMPLES OF PIGMENTED PRODUCTS

Figure 3 gives examples of spectrophotometric curves of paint, rubber, and plastic material in which both anatase and rutile pigments have been incorporated. No attempts have been made to estimate the relative perceptible steps between each pair of these products since the main object in giving these curves is to show spectral characteristics of commercial products containing the pigments under study. It should be mentioned, however, that all samples having selective absorption in the blue appear yellower to the eye than their respective counterparts.

TABLE II. Tristimulus colorimeter readings using filter-photo-cell-source combination closely approximately the standard-observer illuminant combination for colorimetry, and also readings with a supplementary blue filter which has spectral distribution characteristics which extend to a somewhat lower wave-length than normally accepted.

Identification	Supplementary Blue	Blue	Green	Amber
Anatase	0.872	0.873	0.912	0.922
Blend	0.861	0.873	0.912	0.922
Rutile	0.840	0.873	0.912	0.922

DISCUSSION

It is indicated from the I.C.I. x, y values and also the amber, green, and blue reflectometer values that no real difference in visual perception should be expected for the samples under study. Yet their spectrophotometric curves differ to a marked degree below 430 mu, and the samples do differ in visual perception. It is evident that the discrepancies are not due to the inability of the spectrophotometer to make sufficiently accurate curves but rather to the inability of the I.C.I. colorimetric system to weight the blue end of the visible spectrum in accordance with the spectral response of the normal eye. Insufficient work has been made to indicate the changes which are necessary in the tristimulus distribution curves to correct for the inconsistencies reported, nor has it been determined that the supplementary blue filter gives a $\bar{z}E_C$ function which precisely describes the blue tristimulus sensation of the eye. While it may be expected that the correct weighting of the blue region of the spectrum may not be as critical in the case of chromatic materials as for non-selecting materials, nevertheless it would appear that any material which exhibits an absorption in the blue region would be subject to some error.

JOURNAL OF THE OPTICAL SOCIETY OF AMERICA VOLUME 38, NUMBER 5 MAY, 1948

Coefficients of Reflection of Magnesium Oxide and Magnesium Carbonate

FRANK BENFORD, GWEN P. LLOYD, AND SALLY SCHWARZ
General Electric Research Laboratory, Schenectady, New York

(Received December 2, 1947)

Both magnesium carbonate and magnesium oxide are used in laboratories as reflectors of visible radiation and a knowledge of their spectral characteristics is desirable. The method here used to measure coefficients of reflection depends on the variation of brightness within a spherical integrator when a section of the surface is removed or added. The photometry was done with a Macbeth instrument and interference filters were used to get six zones in the spectrum. The centroids were computed for low levels of luminosity. By taking photometric readings with three part-spheres of different degrees of completeness, the coefficients can be computed for three different combinations, and comparison of results indicates the consistency of results. The average coefficient of magnesium carbonate was found to be about 0.983, while that of the oxide was about 0.991, and both have a slight selectivity in favor of the red end of the spectrum.

IN 1920 one of the writers made a determination of the coefficients of reflection of magnesium carbonate[1] using a visual spectrophotometer and employing an absolute method that freed the work from dependence on any of the photometric units. The recent appearance of interference filters suggested that the work be repeated under possibly better working conditions, and that the oxide of magnesium be also included. The latter material is important because use is made of the oxide to coat the surface of the sphere used with the recording spectrophotometer. The oxide is formed by burning magnesium ribbon in the sphere and allowing the smoke to deposit on the walls.

The theory of the integrating photometric sphere says that the amount of light involved in each reflection after the first one is proportional to the coefficient of the reflecting surface and the fraction of the sphere that takes part in the reflection. The part-sphere method here used is based on this theory and is carried out by building a sphere that can be readily taken apart and put together again so as to have any desired degree of completeness.

The construction was carried out by taking six blocks of magnesium carbonate and machining them into cubes. One face of each block was next beveled to 45 degrees on all four edges, and the center of this face was then machined out to a spherical surface. Six such blocks, when placed with their beveled surfaces in contact, will form a complete sphere. The removal of one block leaves five-sixths of a sphere, and taking away two leaves four-sixths of a sphere to take part in the reflection and integration of light. During the test, the sphere is never complete since an opening must be left for the introduction of a projected beam of light and for viewing a part of the spherical surface that is illuminated by reflected light.

A number of variations were tried, such as the use of a half-block for the final step, and in this case, the sphere was 11/12, 10/12, and 9/12 complete for the three parts of the test, as shown in Fig. 1. The view on the left shows an 11/12 sphere and the spot of original illumination shows in the upper right of the opening. The center view shows a 10/12 sphere, and the presence of room light used by the photographer is indicated by the patch of light on the face of the lower block. In the right view, the 1/12 block has been returned to place and the top block removed, giving a 9/12 sphere. It should be noted here that the blocks used in the photograph are made of a hard plaster that would take black paint on the beveled edges without staining the spherical surface. This blackening was necessary since light that escapes through the opening should not be returned. The coefficient of the plaster was low, about 0.61, and more than twenty smokings were required to completely conceal the plaster. This made the coating so thick that it chipped readily when a block was removed, and it was necessary to return to the use of the

[1] Frank Benford, "An absolute method for determining coefficients of diffuse reflection," General Elec. Rev. 23, 72 (1920).

more fragile carbonate blocks. Paint could not be used on the beveled edges and shields made of black paper were used to prevent the return of escaping light.

The mathematical part of the theory shows that given photometric readings of brightness of any part of the sphere not in the area of original illumination, the coefficient K may be computed from

$$K=\frac{P_a-P_b}{aP_a-bP_b},$$

where a and b represent the fractions of sphere active when the photometric readings P_a and P_b were obtained. The absolute values of brightnesses P_a and P_b are not necessary, but they must be in the correct ratio. The spherical areas a and b must be accurately known, and this requires accuracy in the forming of the blocks. When the assembly is made, the closeness of fit can be readily observed, and this feature should cause no trouble in the final part of the test.

The use of three different part-spheres permitted an internal check on the reliability of the results. With parts a, b, and c and photometer readings P_a, P_b, and P_c comparisons can be made between results when P_a and P_b are used, and when P_a and P_c or P_b and P_c are substituted in the equation. Data on this point will be given later.

The photometry was done with seven different interference filters fitted over the eyepiece of a Macbeth Illuminometer. The blocks were enclosed in a box that was first painted dead black and then lined with black velvet. This was a precaution against stray light, and a diaphragm was used to suppress the return of light reflected from the projecting lens, and to prevent fringe light around the beam from falling on the edges of the opening into the sphere.

The transmission band of an interference filter is wide enough to make it necessary to determine the light centroid and use this rather than the peak of transmission as defining the wave-length of the filter. A low intensity (scotopic) luminosity curve was used in the computation, since the greatest effective field brightness was less than 0.5 foot candle in the green and far less than this at the ends of the spectrum. The change of reflection with wave-length proceeds at a slow rate and any residual errors in wave-length rating can hardly have an important effect on the final results.

In Fig. 2 the lower curve gives coefficients of magnesium carbonate. Six wave-lengths from 4585A to 6250A were tested. Taylor has shown that the coefficient is quite low near 3000A, and other experimental evidence indicates the sharp change of direction given to the curve near 4500A. For full spectrum illumination, the average is about 0.983.

The oxide tests on 12 coats of smoke on carbonate gave the upper curve, where there is an additional point 5550A. The oxide is more nearly neutral, since the characteristic is less sloping, and it is a better reflector than the carbonate by about 0.008. For a full spectrum, the coefficient is about 0.991.

If perfect accuracy were attainable, then any two areas of part-sphere should lead to the same K as any other two areas. A number of checks were made using data from 11/12, 10/12, and 9/12 spheres. Typical results are represented by

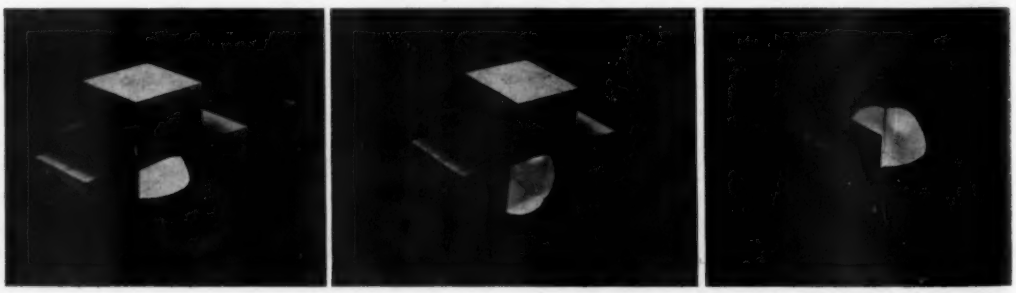

FIG. 1.

the averages 0.988, 0.987, and 0.985 for successively smaller areas *a* and *b*, *a* and *c*, and *b* and *c*. From the evidence of these comparisons, it might be concluded that the general averages might be as much as 0.001 low, but this estimate is based on the assumption that the accuracy increased with the completeness of the part-sphere. This assumption may not be correct and, therefore, the data are submitted without further suggestions as to the magnitude and direction of the errors.

It has been reported, in conversation, by several people that magnesium is variable in its reflectance, and it was thought that its hygroscopic content might have an influence. The matter was tested by placing a Petrie dish in the box with the part sphere and having alternate charges of water and a drying agent, P_2O_5, in the dish. The charges were left in repeatedly for from one to three days, with photometric tests at the end of each period. No change in coefficient was detected in any case, and any variations that occur may be due to variations in the manufacturing process.

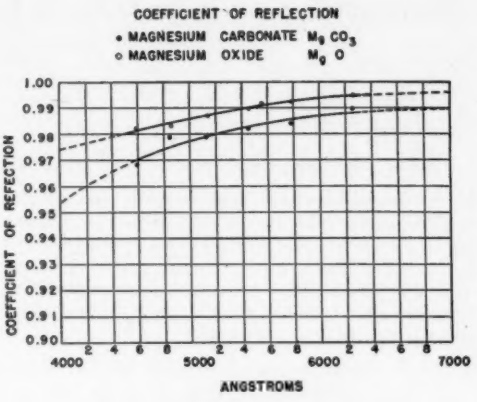

FIG. 2.

New Contributions to the Optics of Intensely Light-Scattering Materials. Part I

PAUL KUBELKA

(Received November 6, 1947)

The system of differential equations of Kubelka-Munk,

$$-di=-(S+K)idx+Sjdx, \quad dj=-(S+K)jdx+Sidx$$

(i, $j\cdots$ intensities of the light traveling inside a plane-parallel light-scattering specimen towards its unilluminated and its illuminated surface; $x\cdots$ distance from the unilluminated surface S, $K\cdots$ constants), has been derived from a simplified model of traveling of light in the material. Now, without simplifying assumptions the following exact system is derived:

$$-di=-\tfrac{1}{2}(S+K)uidx+\tfrac{1}{2}Svjdx,$$
$$dj=-\tfrac{1}{2}(S+K)vjdx+\tfrac{1}{2}Suidx,$$

($u\equiv\int_0^{\pi/2}(\partial i/i\partial\varphi)(d\varphi/\cos\varphi)$, $v\equiv\int_0^{\pi/2}(\partial j/j\partial\varphi)(d\varphi/\cos\varphi)$, $\varphi\equiv$angle from normal of the light). Both systems become identical when $u=v=2$, that is, for instance, when the material is perfectly dull and when the light, is perfectly diffused or if it is parallel and hits the specimen under an angle of 60° from normal. Consequently, the different formulas Kubelka-Munk got by integration of their differential equations are exact when these conditions are fulfilled. The Gurevic and Judd formulas, although derived in another way by their authors, may be got from the Kubelka-Munk differential equations too. Consequently, they are exact under the same conditions. The integrated equations may be adapted for practical use by introducing hyperbolic functions and the secondary constants $a=\frac{1}{2}(1/R_\infty+R_\infty)$ and $b=\frac{1}{2}(1/R_\infty-R_\infty)$, ($R_\infty\equiv$reflectivity). Reflectance R, for instance, is then represented by the formula

$$R=\frac{1-R_g(a-b\,\mathrm{ctgh}bSX)}{a+b\,\mathrm{ctgh}bSX-R_g}$$

($R_g\equiv$reflectance of the backing, $X=$thickness of the specimen) and transmittance T by the formula

$$T=\frac{b}{a\sinh bSX+b\cosh bSX}.$$

In many practical cases the exact formulas may be replaced by appropriated approximations.

INTRODUCTION

TURBID materials may be called intensely light-scattering, if the intensity of incident light is considerably diminished by passing through the considered specimen. The optics of such materials have been dealt with theoretically, especially by Stokes,[1] Channon, Renwick, and Storr,[2] Bruce,[3] Gurevic,[4] Kubelka and Munk,[5] Judd,[6] Amy,[7] and Smith.[8] The most general are the theories of Gurevic and of Kubelka and Munk. Some problems, however, were not solved by these authors:

1. Both the derivations of Gurevic and of Kubelka and Munk started from a very simplified model of the traveling of light in the material. Two directions only, contrary to each other, were considered. Zocher,[9] later in a new way deriving the main Kubelka and Munk equation, used the same model. All these authors supposed that this simplification is admissible in the special case of diffused illumination of dull materials (that is, materials reflecting diffused light only), but they did not prove it. Certainly the results of the extensive experimental work of Judd[10] and his collaborators and of experiments made by Gurevic and by Steele[11] are in very satisfactory accordance with the theoretically derived equations. However, the limits of validity of the equations remain to be determined theoretically.

2. The Gurevic as well as the Kubelka and Munk formulas are cumbersome in use. Till now practical calculating was rather impossible without graphical aids.[10,11] Therefore our second problem will be to find out other forms of the formulas, more adapted to practical use, and approximations fit for special cases.

3. Following a suggestion of Judd,[12] Ingle[13]

[1] G. G. Stokes, Proc. Roy. Soc. London **11**, 545 (1860–62).
[2] H. J. Channon, F. F. Renwick, and B. V. Storr, Proc. Roy. Soc. London **94**, 222 (1918).
[3] H. D. Bruce, Tech. Pap. 306, Nat. Bur. Stand. (1926).
[4] M. Gurevic, Physik. Zeits. **31**, 753 (1930).
[5] P. Kubelka and F. Munk, Zeits. f. tech. Physik **12**, 593 (1931); see also: F. A. Steele, reference 5; Gardner, *Handbook Paints, Varnishes, Lacquers and Colors* (H. A. Gardner Laboratory, Inc., Bethesda, Maryland, 1935) seventh edition, p. 16; Judd, see reference 6.
[6] D. B. Judd, J. Research Nat. Bur. Stand. **12**, 345 and **13**, 281 (1934).
[7] L. Amy, Rev. d'optique **16**, 81 (1937).
[8] T. Smith, Trans. Opt. Soc. (London) **33**, 150 (1931).
[9] Zocher, *Kolloidchemisches Taschenbuch*.
[10] D. B. Judd, J. Research Nat. Bur. Stand. **19**, 287 (1937) and Paper Trade J. **106**, 5 (1938).
[11] F. A. Steele, Paper Trade J. **100**, 37 (1935).
[12] D. B. Judd, Symposium on Color, 1931 (A.S.T.M.) (remark in the discussion, following the lecture of R. H. Sawyer).
[13] George W. Ingle, A.S.T.M. Bull. 32, May (1942).

made mathematical investigations in order to find out the mutual correlation between the theories of Smith and Amy, Stokes and Bruce, and Kubelka and Munk. He proved that the Smith-Amy and Stokes-Bruce equation are special cases of the Kubelka-Munk equation and may be derived from it. An analogous investigation concerning the theories of Gurevic and of Judd would be advisable.

4. The behavior of turbid materials is important not only in the case of diffuse but also of parallel primary light. The theory has to be adapted to this case.

5. The investigations of Judd and his collaborators have shown that the Kubelka-Munk formulas, under certain conditions, practically hold also if the surface of the specimen is glossy or, generally speaking, if the medium of the turbid material differs from air. Under extreme conditions, however, probably deviations will be found. Therefore this case also has to be investigated theoretically.

The first, second, and third problem will be dealt with in this paper, the remaining ones in later papers.

GENERAL REMARKS

This paper assumes, like the cited previous ones, that the turbid material forms a plane layer of constant, generally finite, thickness, being besides that infinitely extended. Practically that means that the considered specimen has to be so long and so broad that the effect of the edges may be neglected. The material is assumed to be homogeneous in this way, that the optical inhomogenities (necessarily existing when the light shall be scattered) are incomparably smaller than the thickness of the specimen and uniformly distributed in the material. On principle the medium of the material is assumed to be the same as the medium the light comes out of (generally air). One side of the specimen is illuminated. The reflected or transmitted light is not reflected again to the specimen unless we consider a backing, reflecting the transmitted light in defined manner. The change of wavelength distribution by specific absorption or by dispersion will not be taken into consideration. On principle spectrally homogeneous illumination is assumed, but generally heterogeneous light also will do provided the material is spectrally non-selective.

The derivations start from the theory of Kubelka and Munk. The reader is supposed to know either their original paper (henceforth to be cited as K&M) or the abstract given by Steele.[11]

I. RANGE OF VALIDITY OF THE GUREVIC AND KUBELKA-MUNK EQUATIONS

In order to find out if and under which conditions the Gurevic and K&M equations are exact, we shall try to derive them without using a simplifying model of light traveling. Thus, we have to respect the fact that the path of a ray passing through a layer of thickness dx is not dx but $dx/\cos\varphi$, the direction of the ray being φ from normal. The light traveling within the turbid medium consists of rays of various directions. Consequently the average path $d\xi i$ of the light passing through the layer dx towards the unilluminated side of the specimen is represented by

$$d\xi_i = dx \cdot \int_0^{\pi/2} \frac{\partial i}{i\partial\varphi} \cdot \frac{d\varphi}{\cos\varphi} \equiv u \cdot dx, \qquad (1)$$

$\partial i/\partial\varphi$ being the angular distribution of the intensity i.* Analogously, the average path $d\xi j$ of the light passing through towards the illuminated side

$$d\xi_j = dx \cdot \int_0^{\pi/2} \frac{\partial j}{j\partial\varphi} \cdot \frac{d\varphi}{\cos\varphi} \equiv v \cdot dx. \qquad (2)$$

Now, for a moment, we imagine the infinitely thin layer dx being illuminated by i only. Then the decrease of intensity caused by passing through the layer is

$$(\sigma+\epsilon) i d\xi_i = (\sigma+\epsilon) u i dx,$$

of which the part

$$\epsilon i d\xi_i = \epsilon u i dx$$

is absorbed and the part

$$\sigma i d\xi_i = \sigma u i dx$$

is reflected to the opposite side. ($\sigma \equiv$ coefficient of scatter, $\epsilon \equiv$ coefficient of absorption.) If the layer were illuminated by j only, its decrease

* Definitions of all terms we shall use are compiled in the annexed Table I.

TABLE IA. Definition of terms used in Section I.

x	distance from the unilluminated surface of the specimen (used to localize inside the specimen a plane parallel to its surfaces)
φ	direction of light in reference to the surfaces of the specimen, expressed by the angle from normal
i	intensity of light traveling inside the specimen towards its unilluminated surface
$d\xi_i$	average path of this light when passing through a layer of thickness dx
$\partial i/\partial\varphi$	angular distribution of this light
$u \equiv \int_0^{\pi/2} \frac{\partial i}{i\partial\varphi} \cdot \frac{d\varphi}{\cos\varphi}$	
j	intensity of light traveling inside the specimen towards its *illuminated* surface
$d\xi_j$	average path of this light when passing through a layer of thickness dx
$\partial_j/\partial\varphi$	angular distribution of this light
$v \equiv \int_0^{\pi/2} \frac{\partial j}{j\partial\varphi} \cdot \frac{d\varphi}{\cos\varphi}$	
$\sigma \equiv \left(\frac{dj}{d\xi_j}\right)_{j\to 0}$	coefficient of scatter defined by the average real path of light
$S \equiv (d\mathring{j}/dx)_{\mathring{j}\to 0} = 2\sigma = \left(\frac{dR_0}{dX}\right)_{X\to 0}$	coefficient of scatter defined by the corresponding thickness of layer
$\epsilon \equiv \left(\frac{di}{d\xi_i}\right)_{i\to 0} - \sigma$	coefficient of absorption defined by the average real path of light
$K \equiv \left(\frac{d\mathring{i}}{dx}\right)_{i\to 0} - S = 2\epsilon = -\left(\frac{dT}{dX}\right)_{X\to 0} - S$	coefficient of absorption defined by the corresponding thickness of layer
$\mathring{u}, \mathring{v}, \mathring{i}, \mathring{j}$	an asterisk above the letter signifies the term referring to perfectly diffused light (used only when necessary to distinguish)

Definitions of X, R_0, T, see Table IB.

would be

$$(\sigma+\epsilon)jd\xi_j=(\sigma+\epsilon)vjdx$$

and the reflected part

$$\sigma jd\xi_j=\sigma vjdx.$$

In reality, the layer dx is illuminated simultaneously from both sides so that the reflected parts of i augment j and those of j augment i. Therefore we may write:

$$-di=-(\sigma+\epsilon)uidx+\sigma vjdx, \tag{3a}$$

$$dj=-(\sigma+\epsilon)vjdx+\sigma uidx. \tag{3b}$$

(di and dj show different signs in respect of the fact that j decreases but i increases with rising x, $x=0$ corresponding to the unilluminated side of the specimen.) Comparing this system of differential equations with the fundamental one of K&M

$$-di=-(S+K)idx+Sjdx, \tag{4a}$$

$$dj=-(S+K)jdx+Sidx, \tag{4b}$$

we see both becoming identical when

$$v=u=\text{const.} \tag{5}$$

and if we write S and K instead of the terms $u\sigma$ and $u\epsilon$ which now are constant.

The condition $v=u=$const. may be accomplished in various ways. The most important example is diffused illumination of dull materials, as assumed by the authors of the previous papers. If the material is so constituted that the scattered light in all layers of the specimen has the same angular distribution and if this distribution corresponds to those of the incident light, the condition $v=u=$const. is fulfilled. Practically it will be so when the illumination is a *perfectly* diffused one and when the material forming specimens of different thickness reflects and transmits always perfectly diffused light only.

It will be shown in paragraph 2 of this paper that not only all K&M but also all Gurevic

TABLE IB. Definition of terms used in Sections II and III.

i, j, x, S, K	definitions see Table IA
$a \equiv \frac{S+K}{S} = \frac{1}{2}\left(\frac{1}{R_\infty} + R_\infty\right)$ $b \equiv (a^2-1)^{\frac{1}{2}} = \frac{1}{2}\left(\frac{1}{R_\infty} - R_\infty\right)$	constants used instead of R_∞
$r \equiv j/i$	
X	thickness of the specimen
$I \equiv (i)_{x=X}$	intensity of incident light
$J \equiv (j)_{x=X}$	intensity of light reflected by the specimen
$I_g \equiv (i)_{x=0}$	intensity of light transmitted by the specimen
$J_g \equiv (j)_{x=0}$	intensity of light reflected from the backing, entering the specimen again
$R \equiv J/I$	light reflectance of a specimen or fraction of incident light reflected from the specimen (the specimen generally being in contact with a backing)
$R_g \equiv (r)_{x=0} = J_g/I_g$	reflectance of the backing
$R_\infty \equiv (R)_{X\to\infty}$	light reflectivity of the material
$R_1 \equiv (R)_{R_g=1}$	reflectance in the ideal case of perfectly white backing
$T \equiv I_g/I$	transmittance of the specimen or fraction of incident light transmitted by the specimen
$CR_g \equiv R_0/(R)_{R_g=R_g}$	"contrast ratio"
$C_1 \equiv R_0/R_1$	"ideal contrast ratio"
$i_0, j_0, r_0, I_0, J_0, R_0$	the index 0 signifies the term referring to a perfectly black backing specimen or to a specimen without backing ($R_g=0$)
sinh, cosh, ctgh	hyberbolic functions
Ar sinh, *Ar* cosh, *Ar* ctgh	inverse hyperbolic functions (area functions)

and Judd formulas may be derived from Eqs. (4a) and (4b). Therefore, all these formulas are exact if the stipulated conditions are accomplished.

Perfectly diffused light is characterized by having the same intensity in all directions. With respect to a plane it hits this light has the angular distribution

$$\frac{\partial \overset{*}{i}}{\partial \varphi} = \overset{*}{i} \sin 2\varphi, \qquad (6)^{**}$$

and therefore

$$\overset{*}{u} = \int_0^{\pi/2} \sin 2\varphi \frac{d\varphi}{\cos\varphi} = 2. \qquad (7)$$

Consequently, parallel light, if having $u=2$ too, will realize another example of exact validity of the formulas, provided that it is illuminating a material that scatters it in perfectly diffused manner whatever its direction may be. Then i consists of perfectly diffused light formed by scattering and of the unscattered rest of the primary light conserving the original direction. For both portions $u=2$, so that for the whole i also $u=2$. Parallel light has $u=2$ if $\cos\varphi=\frac{1}{2}$, and therefore $\varphi=60°$ from normal. Consequently, such 60° light behaves like perfectly diffused light and may replace it.

Now it is convenient to insert a remark about the coefficients of scatter σ and S and the coefficients of absorption ϵ and K. σ and ϵ are defined by the average real path $d\xi = u dx$ of the light and S and K by the corresponding thickness dx of the layer.

$$S = u\sigma, \quad K = u\epsilon.$$

In order to agree with K&M we always shall define S and K by perfectly diffused light only:

$$S \equiv \overset{*}{u}\sigma = 2\sigma, \qquad (8) \qquad K \equiv \overset{*}{u}\epsilon = 2\epsilon. \qquad (9)$$

** An asterisk above the letter signifies the term referring to perfectly diffused light (used only when necessary to distinguish).

II. DEVELOPING OF NEW FORMULAS

We start from the fundamental system of differential equations of K&M (4a/4b) which, substituting

$$(S+K)/S \equiv a, \tag{10}$$

we may write also as follows:

$$-di/Sdx = -ai+j, \tag{11}$$

$$dj/Sdx = -aj+i. \tag{12}$$

From these equations we can get (see K&M) the equation

$$dr/Sdx = r^2-2ar+1 \tag{13}$$

($r \equiv j/i$), which is easy to integrate. Now we do not integrate over the whole thickness X of the specimen (as K&M do) but only between $x=0$ and $x=x$, assuming $r=0$ to correspond to $x=0$ (black backing, $r=r_0$). We get

$$x = \frac{1}{bS} Ar \operatorname{ctgh} \frac{1-ar_0}{br_0}, \tag{14}$$

and

$$b = (a^2-1)^{\frac{1}{2}}, \tag{15}$$

and from it

$$r_0 = \frac{1}{a+b \operatorname{ctgh} bSx}. \tag{16}***$$

This equation gives the ratio r_0 of the light intensities j_0 and i_0† at any place inside the specimen. Substituting

$$j = j_0 = r_0 i_0 = i_0/(a+b \operatorname{ctgh} bSx)$$

in Eq. (11) and

$$i = i_0 = j_0/r_0 = j_0(a+b \operatorname{ctgh} bSx)$$

in Eq. (12), we find them in a form suited to direct integration. Integration leads to the important formulas

$$i_0 = \text{const.}(a \sinh bSx + b \cosh bSx) = I(a \sinh bSx + b \cosh bSx)/(a \sinh bSX + b \cosh bSX) \tag{17}$$

and

$$j_0 = \text{const.} \sinh bSx = R_0 I \sinh bSx/\sinh bSX. \tag{18}$$

($X \equiv$ thickness of the specimen, $I \equiv$ intensity of illumination, $R_0 \equiv$ reflectance of the specimen.)

Substituting R_0 by the value represented by formula (27) (to be derived later), we get

$$j_0 = I \frac{\sinh bSx}{a \sinh bSX + b \cosh bSX}. \tag{18a}††$$

For most practical purposes the light J, reflected out of the specimen and the transmitted light I_0 and especially the ratios $J/I = R$ (reflectance) and $I_0/I = T$ (transmittance), are more interesting than the light intensities inside the specimen. The most simple case is that of an infinitely thick layer. Integration of Eq. (13) between the limits $x=0$ and $x=\infty$ leads, as has been shown by K&M, to a simple formula for the reflectivity

$$R_\infty \equiv \lim_{x\to\infty} \cdot r,$$

$$R_\infty = a-(a^2-1)^{\frac{1}{2}} = a-b. \tag{19}$$

By transformation we get

$$R_\infty = 1/(a+b), \tag{20}$$

and

$$a = \tfrac{1}{2}(1/R_\infty + R_\infty), \tag{21}$$

$$b = \tfrac{1}{2}(1/R_\infty - R_\infty).††† \tag{22}$$

The constants a and b are quite suited to characterize the material in practical formulas. Equations (21) and (22) represent the *practical* definitions of a and b, because R_∞ very easily may be determined directly by measurement. (The theoretically preferable definitions of a and b are based on the coefficients S and K; see Eqs. (10) and (15).) On principle it would be possible to use R_∞ itself as constant, as K&M did, but the formulas then would become more complicated.‡

*** The hyperbolic functions greatly simplify our equations. We shall use them for the future too. Especially practical calculation becomes much easier by means of hyperbolic functions. (Steele also used them when he worked out the first graphical aids based on the K&M theory.)

† The index 0 always may indicate a perfectly black backing of the specimen concerned.

†† By differentiation of Eqs. (11) and (12) (substituting then the first derivatives of i and j according to Eqs. (11) and (12) and $a^2-1=b^2$ according to Eq. (15), we get the following very simple differential equations of second order:

$$d^2i/dx^2 = b^2S^2i \quad \text{and} \quad d^2j/dx^2 = b^2S^2j.$$

The general solution of these equations can be written immediately:

$$i = c_1 \sinh bSx + c_2 \cosh bSx,$$
$$j = c_3 \sinh bSx + c_4 \cosh bSx.$$

Comparing these equations with Eqs. (17) and (18), we notice identity and that, in the special case of $j=j_0$, the constant of integration c_4 becomes $=0$.

††† Even in these relations hyperbolic functions are hidden. We also may write

$$\ln R_\infty = \operatorname{Arcosh} a = -\operatorname{Arsinh} b.$$

As to the differential equation 13, it may be expressed by the hyperbolic cosines too:

$$d \ln r/Sdx = 2(\cosh \ln r - \cosh \ln R_\infty).$$

‡ Gurevic also, instead of R_∞, uses two different functions of it, k_2 and L, which—written in our terms—correspond to Sa and Sb.

Besides, when R_∞ has to be determined indirectly it is much easier to isolate a or b from the equations and to solve them than to isolate R_∞. It must be noticed that a and b are two forms of the same constant only, mutually correlated by the relations

$$b=(a^2-1)^{\frac{1}{2}} \quad (23) \quad \text{and} \quad a=(b^2+1)^{\frac{1}{2}}. \quad (24)$$

When both a and b will occur in one formula it will be so for easier writing only.

Besides the one constant (R_∞ itself or expressed by a or b) we need a second too to characterize the scattering material. Just as Gurevic and K&M do, we choose the coefficient of scatters. It has to be determined indirectly, certainly, but generally the calculation is not very difficult. It may be noticed that in practical formulas S always occurs together with the thickness X of the specimen, that is, as the product SX, called "scattering power" of the specimen.[10]

Now we assume a finitely thick specimen in contact with a backing. (Reflectance of the backing $\equiv R_g$.) We integrate Eq. (13) over the whole thickness and get:

$$SX=\frac{1}{b}\left(Ar\ \mathrm{ctgh}\frac{a-R}{b}-Ar\ \mathrm{ctgh}\frac{a-R_g}{b}\right), \quad (25)$$

$$R=\frac{1-R_g(a-b\ \mathrm{ctgh}bSX)}{a+b\ \mathrm{ctgh}bSX-R_g}. \quad (26)$$

Because of the use of hyperbolic functions and the secondary constants a and b, formula (26) is by far less complex than the corresponding formula of K&M:

$$R=\frac{\frac{1}{R_\infty}(R_g-R_\infty)-R_\infty\left(R_g-\frac{1}{R_\infty}\right)\exp\left(SX\left(\frac{1}{R_\infty}-R_\infty\right)\right)}{(R_g-R_\infty)-\left(R_g-\frac{1}{R_\infty}\right)\exp\left(SX\left(\frac{1}{R_\infty}-R_\infty\right)\right)}$$

which has been used till now. In the case of a perfectly black backing, formula (26) becomes still more simple.

$$R_0=\frac{1}{a+b\ \mathrm{ctgh}bSX}=\frac{\sinh bSX}{a\sinh bSX+b\cosh bSX}. \quad (27)$$

In order to find an analogous formula representing transmittance $T=I_g/I$, we return to (17), and put $x=0$ and $i_0=I_g=TI$:

$$T=b/(a\sinh bSX+b\cosh bSX). \quad (28)$$

By transforming, the inverse formula may be got too:

$$SX=[Ar\sinh(b/T)-Ar\sinh b]/b. \quad (29)$$

(28) accords with the corresponding Gurevic formula

$$T=\frac{(1-R_\infty)^2e^{-bSX}}{1-R_\infty^2e^{-2bSX}},^{\ddagger\ddagger}$$

derived in quite a different way. This accordance easily may be shown:

From (28), (21), and (22) follow:

$$T=\frac{\frac{1}{2}\left(\frac{1}{R_\infty}-R_\infty\right)}{\frac{1}{2}\left(\frac{1}{R_\infty}+R_\infty\right)\sinh bSX+\frac{1}{2}\left(\frac{1}{R_\infty}-R_\infty\right)\cosh bSX}$$

$$=\frac{1-R_\infty^2}{(1+R_\infty^2)\cdot\frac{1}{2}(e^{bSX}-e^{-bSX})+(1-R_\infty^2)\cdot\frac{1}{2}(e^{bSX}+e^{-bSX})}=\frac{(1-R_\infty^2)e^{-bSX}}{1-R_\infty^2e^{-2bSX}}.$$

‡‡ For easier comparison the Gurevic formula is represented here by our own terms.

By combining (27) and (28) an equation may be developed correlating T with R_0 and R_∞ only.

$$T^2+b^2=(a-R_0)^2. \tag{30}$$

For practical calculating T or R_0 may be isolated:

$$T=((a-R_0)^2-b^2)^{\frac{1}{2}}, \tag{31}$$

$$R_0=a-(T^2+b^2)^{\frac{1}{2}}. \tag{32}$$

By transforming (30), a very simple formula may be found allowing the calculation of a and, therefore, R_∞ from one measurement of reflectance and one of transmittance without knowledge of S and X.

$$a=\frac{1+R_0^2+T^2}{2R_0}. \tag{33}$$

This formula is to be found in the Gurevic paper too. We derived it here in a new way.

A similar formula, permitting us to calculate R_∞ directly from R_0 and R may be got from (26) and (27):

$$a=\tfrac{1}{2}\left(R+\frac{R_0-R+R_g}{R_0R_g}\right). \tag{34}$$

This formula is important for determination of reflectivity by Judd's contrast ratio method. Transformed, it also may be used to calculate R from R_0 and R_∞:

$$R=\frac{R_0-R_g(2aR_0-1)}{1-R_gR_0}. \tag{35}$$

These formulas are in very close connection and full accordance with other ones, derived by Judd[6] in quite a different way. For instance, the Judd formula

$$C_1=\frac{R_gC_{Rg}(1-R_0)}{1+R_gC_{Rg}-C_{Rg}-R_gR_0} \tag{36}$$

may be reached by putting $R_g=1$ and accordingly $R=R_1$ in formula (34)

$$a=\frac{1}{2}\left(R_1+\frac{R_0-R_1+1}{R_0}\right),$$

substituting this in (35) and substituting

$$R_1=R_0/C_1 \quad \text{and} \quad R=R_0/C_{Rg}.$$

A further interesting formula which like the Judd ones and like (30) to (33) contains neither SX nor R_∞ (nor a,b) results from (26)–(28):

$$R=R_0+\frac{T^2R_g}{1-R_0R_g}. \tag{37}$$

It permits us to calculate directly any kind of contrast ratio when R_0 and T are measured. In many cases practical calculations may be very much simplified by using approximate formulas.

One way to get such approximations is to develop the hyperbolic functions to series

$$\sinh bSX=bSX/1!+b^3S^3X^3/3!+b^5S^5X^5/5!+\cdots,$$

$$\cosh bSX=1+b^2S^2X^2/2!+b^4S^4X^4/4!+\cdots,$$

$$\operatorname{ctgh} bSX=1/bSX+bSX/3-b^3S^3X^3/45+-\cdots,$$

and to neglect the higher terms. In this way formulas, suitable for light materials, thin specimens, and for poorly scattering materials have been developed. (See annexed Table III, formulas (38) to (47).) The lower the value of bSX, the better the approximations hold and the more simple ones can be used. It is not exactly the same whether this product becomes small by low values of SX (thin specimen or poorly scattering material) or by small b (bright material). A small b may be approximated itself:

$$b\to 0 \qquad a\to 1$$
$$b=(a^2-1)^{\frac{1}{2}}\approx(2(a-1))^{\frac{1}{2}}.$$

On the other hand, when only b is small we have to take into consideration that the term aSX is not necessarily small too. Consequently, there are two somewhat different series of approximamations, one for $SX\to 0$ and one for $R_\infty\to 1$, $(a\to 1)$.‡‡‡ For high values of bSX we may get approximations in a different manner. It is easy to show that then

$$\sinh bSX\to\tfrac{1}{2}e^{bSX}\leftarrow\cosh bSX,$$
$$\operatorname{ctgh} bSX\to(1-e^{-2bSX})\to 1.$$

In this way we get formulas (57)–(60), advantageous for use in the case of thick or highly scattering specimens. Dark materials permit an-

‡‡‡ When reflectivity R_∞ increases, a is approaching much faster to 1 than R_∞, and then b is approaching to 0.

TABLE II. Exact formulas for practical use.

Characteristic	nro	Formula
$R=f(SX,R_g,R_\infty)$	26	$R=\frac{1-R_g(a-b\ \mathrm{ctgh}bSX)}{a+b\ \mathrm{ctgh}bSX-R_g}$
$R_0=f(SX,R_\infty)$	27	$R_0=\frac{1}{a+b\ \mathrm{ctgh}bSX}=\frac{\sinh bSX}{a\ \sinh bSX+b\ \cosh bSX}$
$T=f(SX,R_\infty)$	28	$T=\frac{b}{a\ \sinh bSX+b\ \cosh bSX}$
$SX=f(R,R_g,R_\infty)$	25	$SX=\frac{1}{b}\left(Ar\ \mathrm{ctgh}\ \frac{a-R}{b}-Ar\ \mathrm{ctgh}\ \frac{a-R_g}{b}\right)$
$SX=f(R_0,R_\infty)$	25a	$SX=\frac{1}{b}Ar\ \mathrm{ctgh}\ \frac{1-aR_0}{bR_0}$
$SX=f(T,R_\infty)$	29	$SX=\frac{1}{b}\left(Ar\ \sinh\ \frac{b}{T}-Ar\ \sinh b\right)=\frac{1}{b}\left(Ar\ \sinh\ \frac{b}{T}+\ln\ R_\infty\right)$
$R_0=f(T,R_\infty)$	32	$R_0=a-(T^2+b^2)^{\frac{1}{2}}$
$T=f(R_0,R_\infty)$	31	$T=((a-R_0)^2-b^2)^{\frac{1}{2}}$
$R_\infty=f(R_0,T)$	33	$a=\frac{1+R_0^2-T^2}{2R_0}$ (Gurevic)
$R=f(R_0,R_g,R_\infty)$	35	$R=\frac{R_0-R_g(2aR_0-1)}{1-R_0R_g}$
$R_0=f(R,R_g,R_\infty)$	35a	$R_0=\frac{R-R_g}{1-R_g(2a-R)}$
$R_\infty=f(R,R_0,R_g)$	34	$a=\frac{1}{2}\left(R+\frac{R_0-R+R_g}{R_0R_g}\right)$
$R=f(R_0,T,R_g)$	37	$R=R_0+\frac{T^2R_g}{1-R_0R_g}$
$T=f(R,R_0,R_g)$	37a	$T=\left((R-R_0)\left(\frac{1}{R_g}-R_0\right)\right)^{\frac{1}{2}}$
$R=f(R_1,R_0,R_g)$	36b	$R=\frac{R_0(1-R_g)+R_1R_g(1-R_0)}{1-R_0R_g}$ (Judd)
$R_1=f(R,R_0,R_g)$	36a	$R_1=\frac{R-R_0+R_0R_g(1-R)}{R_g(1-R_0)}$ (Judd)

other approximation too:

$$b\rightarrow\tfrac{1}{2}R_\infty\leftarrow a$$

(formulas (48)—(56)).

It has to be noticed that the approximate formulas often fully agree with the exact ones. That means the deviations do not exceed the degree of usual experimental incertainty. The approximations are serviceable not only in very extreme cases. For instance, the ranges of useful application of the approximations both for thin and for thick specimens sometimes are so wide that a small range only remains between them where we have to use the exact formulas.

III. THE MUTUAL CORRELATION BETWEEN THE THEORIES OF GUREVIC, KUBELKA AND MUNK, AND JUDD

The theories of Gurevic, K&M, and Judd were worked out independently of each other.¶

¶ The theory of K&M has been described for the first time in a research paper of the Spolek pro chemickou a hutni vyrobu (Chemical and Metallurgical Works) at Aussig (Usti) in 1929 and then published in Zeits. f. tech. Physik in 1931. The work of Gurevic has been published in 1930, that of Judd in 1934. Judd did not know at that time of the previous papers; the abstract of the K&M paper in the English language, by Steele, was only published in 1935. K&M saw the Gurevic paper for the first time in 1931, just when they were reading their own proof sheet. They inserted quickly a citation but at that time they had not yet understood the close correlation between the two works.

The standpoints they started from were quite different. Nevertheless, those results which can be derived as well from one as from another of these theories are in full accordance, confirming such one another.

The most universal is the K&M theory. All results of Gurevic and Judd without any exception may be derived from their fundamental pair of differential equations, although really K&M at that time had found out neither the

TABLE III. Approximations (the formulas compiled in this table may be considered as examples only. When other ones are desired for special purposes they may be got by combining the quoted ones, or developed from the corresponding exact formulas in the ways indicated in Section II).

Characteristic	NFO	Formula
A. Light material: $a\to 1$; $SX<\infty$		
$R=f(SX,R_g,R_\infty)$	38*	$R\approx\frac{(1-aR_g)SX+R_gY}{(a-R_g)SX+Y}\approx\frac{(1-aR_g)SX+R_g}{(a-R_g)SX+1}\approx 1-\frac{1-R_g}{(1-R_g)SX+Y}$
$R_0=f(SX,R_\infty)$	39*	$R_0\approx\frac{SX}{aSX+Y}\approx\frac{SX}{aSX+1}\approx\frac{SX}{SX+1}$
$T=f(SX,R_\infty)$	40**	$T\approx\frac{1}{1+aSX+\frac{b^2}{2}S^2X^2\left(1-\frac{a}{3}SX\right)}\approx\frac{1}{aSX+1}\approx\frac{1}{SX+1}$
$SX=f(R_0,R_\infty)$	41	$SX\approx\frac{R_0}{1-aR_0}\approx\frac{R_0}{1-R_0}$
$SX=f(T,R_\infty)$	42	$SX\approx\frac{1-T}{aT}\approx\frac{1-T}{T}$
B. Thin specimen or poorly scattering material: $SX\to 0$; $R_\infty>0$		
$R=f(SX,R_g,R_\infty)$	43***	$R\approx\frac{(1-aR_g)SX+R_gY}{(a-R_g)SX+Y}\approx\frac{(1-aR_g)SX+R_g}{(a-R_g)SX+1}\approx R_g+[(a-R_g)^2b^2]SX$
$R_0=f(SX,R_\infty)$	44***	$R_0\approx\frac{SX}{aSX+Y}\approx\frac{SX}{aSX+1}\approx SX$
$T=f(SX,R_\infty)$	45	$T\approx\frac{1}{1+aSX+\frac{1}{2}b^2S^2X^2}\approx\frac{1}{aSX+1}\approx 1-aSX\approx 1$
$SX=f(R_0,R_\infty)$	46	$SX\approx\frac{R_0}{1-aR_0}\approx R_0$
$SX=f(T,R_\infty)$	47	$SX\approx\frac{1-T}{aT}\approx\frac{1-T}{a}$
C. Dark material: $R_\infty\to 0$; $SX>0$		
$R=f(SX,R_g,R_\infty)$	48	$R\approx R_\infty+(R_g-R_\infty)\exp\left(-\frac{SX}{R_\infty}\right)$
$R_0=f(SX,R_\infty)$	49	$R_0\approx R_\infty\left(1-\exp\left(-\frac{SX}{R_\infty}\right)\right)$
$T=f(SX,R_\infty)$	50	$T\approx\exp\left(-\frac{SX}{2R_\infty}\right)$
$SX=f(R,R_g,R_\infty)$	51	$SX\approx R_\infty\ln\frac{R_g-R_\infty}{R-R_\infty}$
$SX=f(R_0,R_\infty)$	52	$SX\approx R_\infty\ln\frac{R_\infty}{R_\infty-R_0}$
$SX=f(T,R_\infty)$	53	$SX\approx -2R_\infty\ln T$
$T=f(R_0,R_\infty)$	54	$T\approx\left(\frac{R_\infty-R_0}{R_\infty}\right)^{\frac{1}{2}}$
$R=f(T,R_\infty)$	55	$R_0\approx R_\infty(1-T^2)$
$R_\infty=f(R_0,T)$	56	$R_\infty\approx\frac{R_0}{1-T^2}$

TABLE III.—*Continued.*

D. Thick specimen or very intensely scattering material: $SX \to \infty$; $R_\infty < 1$		
$R_\infty = f(SX, R_\infty)$	57	$R_0 \approx R_\infty - 2bR_\infty^2 \exp(-2bSX)$
$T = f(SX, R_\infty)$	58	$T \approx 2bR_\infty \exp(-bSX)$
$SX = f(R_0, R_\infty)$	59	$SX \approx \frac{1}{2b} \ln \frac{2bR_\infty^2}{R_\infty - R_0}$
$SX = f(T, R_\infty)$	60	$SX \approx \frac{1}{b} \ln \frac{2bR_\infty}{T}$
$T = f(R_0, R_\infty)$	61	$T \approx (2b(R_\infty - R_0))^{\frac{1}{2}}$
$R_\infty = f(T, R_\infty)$	62	$R_0 \approx R_\infty - \frac{T^2}{2b}$
$R_\infty = f(R_0, T)$	63	$R_\infty \approx R_0 + \frac{T^2}{2b}$

* $Y \approx 1 + \frac{1}{2}b^2S^2X^2 - \frac{1}{45}b^4S^4X^4 \approx 1 + \frac{1}{2}b^2S^2X^2 \approx 1 + \frac{1}{2}(a-1)S^2X^2 \approx 1.$

** $\frac{b^2}{2} \approx (a-1) \approx 0.$

*** $Y \approx 1 + \frac{1}{2}b^2S^2X^2 - \frac{1}{45}b^4S^4X^4 \approx 1 + \frac{1}{2}b^2S^2X^2 \approx 1.$

Gurevic transmittance formulas nor the Judd formulas.

The theory of Gurevic is not so universal. His fundamental system of differential equations,

$$dR_0 = ST^2dX, \quad dT = -T(S + E - SR_0)dX,$$

does not permit one to get the K&M and the Judd formulas referring to a backed specimen. The formulas dealing with the behavior of the light inside the turbid material also cannot be got from the Gurevic equations.

The Judd theory is the most special. The formulas only mutually correlate R, R_0, and R_g at a given thickness X of the specimen. Nevertheless, these formulas are very important for practical use. Till now the Gurevic and the K&M formulas could not be used directly for practical calculating without graphical aids.

SUMMARY

1. The range of validity of the Gurevic and Kubelka-Munk theories has been theoretically determined. Perfectly diffused illumination of a perfectly dull material, as assumed by the authors of these theories, is only one example of exact validity, although the most important one. Another example is parallel light hitting perfectly dull material under an angle of 60° from normal.

2. New formulas, more adapted for practical use than the hitherto existing ones, have been developed by the Kubelka-Munk theory.

3. The theories of Gurevic, Kubelka and Munk, and Judd, starting from different standpoints, are in full accordance and confirm one another.

The Illuminant in Textile Color Matching*

DOROTHY NICKERSON**
Cotton Branch, United States Department of Agriculture, Production and Marketing Administration, Washington, D. C.
(Received February 5, 1948)

A subcommittee of the Inter-Society Color Council was established in 1944 to study two things: "What color temperature of natural daylight is used by textile color matchers?" and "What color temperature of artificial daylight is preferred by textile color matchers?" The Philadelphia Army Quartermaster Depot and three large textile companies—Forstmann, Botany, and Pacific—cooperated in the work. As a result of its study, summarized here, the subcommittee recommends that artificial daylight lamps for textile color matching be aimed at 7500°K with an illuminance of more than 75 and less than 300 footcandles. (By artificial daylighting, the subcommittee means an illuminant that has an energy distribution as similar to that of daylight of equivalent color temperature as it is possible to obtain commercially.)

THE color of daylight, both natural and artificial, has been of interest to this society since its formation in 1916, and even before that to the Illuminating Engineering Society, for in 1910 Dr. Herbert E. Ives presented to the New York Section a paper that discussed color measurement of daylight and artificial daylight. In 1914 papers were published on artificial daylight and daylight glass by Luckiesh and Cady and by Brady. Since then the names of Macbeth, Gage, Gibson, Davis, and Taylor have been closely connected with work involved in determining the color of sunlight and daylight and of its reproduction.

In 1938 results were reported to this society of work done in the United States Department of Agriculture to obtain a factual basis for setting specifications for artificial daylight for use in the grading of agricultural products. The present report is a logical extension of all such previous work. It is made by a subcommittee of the Inter-Society Color Council, of which the Optical Society of America is one of 15 national member associations.

In 1944, at the request of the American Association of Textile Chemists and Colorists, another of the Council's member associations, a subcommittee was appointed to study two things: "What color temperature of natural daylight is used by textile color matchers?" and "What color temperature of artificial daylight is preferred by textile color matchers?" The kind of natural daylight that is preferred came as a by-product of answers to these two questions.

Because of its nature, the full report of this work, including extended tables of data, has been published by the Illuminating Engineering Society, in Illuminating Engineering,[1] following presentation to their September 1947 national technical conference. However, since a report of such work holds interest for other I.S.C.C. member associations than the A.A.T.C.C. and the I.E.S., summaries are planned for prompt presentation and publication by each interested member body of the Council. Detailed data will be found in the I.E.S. report for those who wish more than the present summary.

To avoid a possible misunderstanding of the subcommittee's purpose, it should be stated that this study was not proposed to answer the question: "What illuminant is best for making accurate color matches?" Its purpose was to ascertain the color temperature of daylight used and preferred, so that a color temperature specification could be recommended for artificial daylighting. By artificial daylighting, the subcom-

* Summary of Report on I.S.C.C. Problem No. 13; (presented to the Optical Society of America, October 23–25, 1947, Cincinnati, Ohio).

** Chairman of I.S.C.C. subcommittee on Problem 13. Members of subcommittee: Constantin Monego, Julius Forstmann and Company, Inc. and Philadelphia Textile Institute; Frank J. O'Neil, Pacific Mills; P. M. Otto, Jr., Botany Worsted Mills; Frederick T. Simon, Sidney Blumenthal and Company, Inc.; Stanley Backer, Philadephia Quartermaster Depot; E. I. Stearns, Calco Chemical Division; Norman Macbeth, Macbeth Corporation; I. H. Godlove (Chairman of AATCC Color Committee during time of this study); John J. Hanlon, Mohawk Carpet Mills.

[1] D. Nickerson, "The illuminant in textile color matching, an illuminant to satisfy preferred conditions of daylight-match," Illum. Eng. **43**, 416 (1948).

mittee means an illuminant that has an energy distribution as similar to that of daylight of equivalent color temperature as it is possible to obtain commercially.

For the benefit of those not familiar with color matching requirements, perhaps it should be explained that for accurate color matching—when a match must hold under all conditions of illumination—no single illuminant is sufficient, not even daylight. To match in color under all illuminants, the spectral reflectance of two samples must be identical. An illuminant that may prove best for seeing a color difference between one pair of samples may differ completely from that which is best for another pair. The answer depends upon the spectral reflectance curve of the samples under examination, and that is why color matching units usually contain lamps of two widely different color temperatures.

The work of the subcommittee began informally in the spring of 1943 in connection with discussion of color tolerances. Representatives of several textile mills and the Philadelphia Army Quartermaster Depot agreed that before discussing standards for color tolerance specifications, illumination for inspection should be standardized.

At the first meeting in June 1943, there were laid before the group results of studies made in the United States Department of Agriculture which recommended 7500°K as a minimum color temperature and 60 to 80 footcandles as a minimum illuminance for color grading of agricultural products. The meeting also considered the A.A.T.C.C. *Tentative Specification for Standard Illuminants in Textile Color Matching* (June 26, 1942 revision), as developed by an A.A.T.C.C. Color Committee under the chairmanship of Walter M. Scott. This tentative specification recommends two standards of color matching, one a color temperature generally comparable to I.C.I. Illuminant *A*, the other to I.C.I. Illuminant *C*, a minimum illuminance of 60 to 80 footcandles for grading light colored materials, and 150 footcandles for dark colored materials. Discussion brought out the need for additional information regarding amounts and color temperatures of natural daylighting in use for textile color matching, and on artificial daylighting to give a maximum as well as minimum illuminance for preferred conditions.

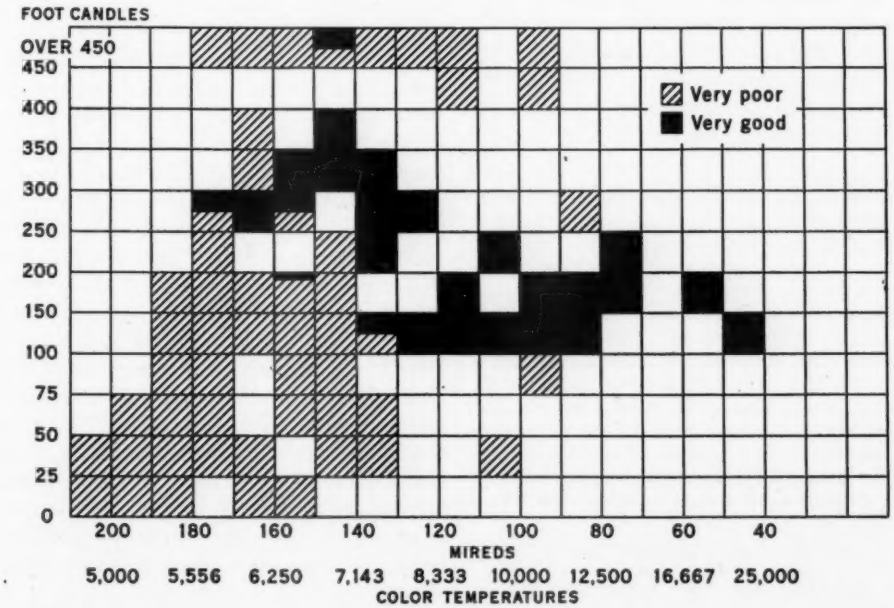

FIG. 1. Footcandle and color temperature taken at selected color matching stations in four large textile mills. Conditions for color matching called "very good" shown against those called "very poor."

FIG. 2. Portable color matching booth provided with a lamp unit in which filters and bulbs may be changed to give a series of different color temperatures, yet allow the amount and geometry of illumination to remain constant.

Representatives of Forstmann, Pacific, and Botany mills agreed to cooperate in getting such data if plans and equipment could be provided for the study. Others present agreed to provide the necessary planning and equipment.

In the several months following the June 1943 meeting, plans were developed and the following method of study agreed upon:

(1) To collect and study hourly records, for 30-day periods, on the amount and quality of natural daylight used by color matchers at color matching stations in several large textile mills, by using a Weston footcandle meter for amount, and an Ansco-Sweet densitometer, adapted to read color temperature, for quality.

(2) To have color matchers examine a series of five groups of textile samples under low to high color temperatures of controlled Macbeth illumination, and under fluorescent and daylight illumination, to record paired differences, and also to express their opinion (a) regarding the artificial illumination liked most, (b) whether preference corresponds to color of present natural daylighting, and (c) which illuminant gives results that correspond to results now obtained under natural daylight conditions.

FIG. 3. Diagrammatic representation of illuminants used.

AMOUNT AND QUALITY OF NATURAL DAYLIGHT

On the basis of over one thousand observations of illuminance and color temperature of natural daylight made at color matching stations in the cooperating mills,[2] data are recorded in the full report that bring out differences caused by the hour, season, and sky conditions. Results indicate that color temperature is high in January, decreasing until May and June; illuminance is low in January, increasing to May and June. Except where reflections interfere, there is a regularity of change in illuminance with the time of day; color temperature shows no consistent change with the time of day.

Illuminating conditions called "very good" for color matching averaged 224 footcandles at 9400°K for clear sky; 211 footcandles at 8850°K for slightly overcast sky; 332 footcandles at 6500°K for overcast sky. Conditions called "very poor" for color matching averaged 450 footcandles at 7850°K for clear sky; 500 footcandles at 6700°K for slightly overcast sky; 120 footcandles at 5800°K for overcast sky; 100 footcandles at 5800°K for very overcast sky; and 40 footcandles at 5300°K for a very dark sky.

The preference of color matchers for natural daylighting is answered in two ways. First, a nearly unanimous preference for a light or moderately overcast or "covered" sky was expressed early in the test, when each color matcher encountered on a tour of the color stations of each mill was asked what kind of a sky he preferred. Only two matchers, out of several dozen, expressed a preference for a clear sky. Second, measurements of the illuminance required to yield conditions called "very good" showed a minimum of 100 footcandles. This minimum requirement in illuminance is independent of color temperature from 25,000°K down to about 7500°K. Below this color temperature down to about 6000°K, the increase in yellowness of the incident light seemed to cause the minimum requirement in illuminance to rise to about 250 footcandles. Figure 1 is a plot of illuminance in footcandles against reciprocal color temperature in mireds, showing the distribution of conditions judged to be very good compared to those judged

[2] Two Forstmann mills are included, those at Garfield and Passaic.

to be very poor. As may be seen from Fig. 1, conditions called very poor are those which combine low color temperature and low illuminance, and those which include very high illuminance at any color temperature.

COLOR TEMPERATURE OF ARTIFICIAL DAYLIGHT PREFERRED BY TEXTILE COLOR MATCHERS

For the part of the study which concerns the determination of the color temperature of artificial daylight preferred by textile color matchers, it was necessary to give considerable thought to standardization of as many conditions as possible. This meant standardization of the illumination used and of the samples examined under those illuminants. The only important variable desired in the illuminant was color temperature. Therefore the introduction of other variables was avoided as far as possible.

Artificial daylight as it is provided by tungsten lamps filtered through Corning 590 filters is already so well established as the best practical and available source of artificial daylight for the color temperature range above that of average noon sunlight, that it was adopted without question for use in this work. It was agreed that all color matching work done under these lamps would be done also under each color matcher's selection of natural daylight, and under fluorescent daylight wherever this was available in the cooperating mills. However, since this study was aimed only at providing a series of color temperatures under which color matchers might work, most thought was given to providing a comparable series of illuminants in which color temperature was the one important variable.

This was accomplished by working out a lighting layout on a miniature scale in which background conditions and amount and geometry of illumination could be held constant. A portable booth, painted neutral gray (about Munsell N 6/) was made so that it might be set on a table.

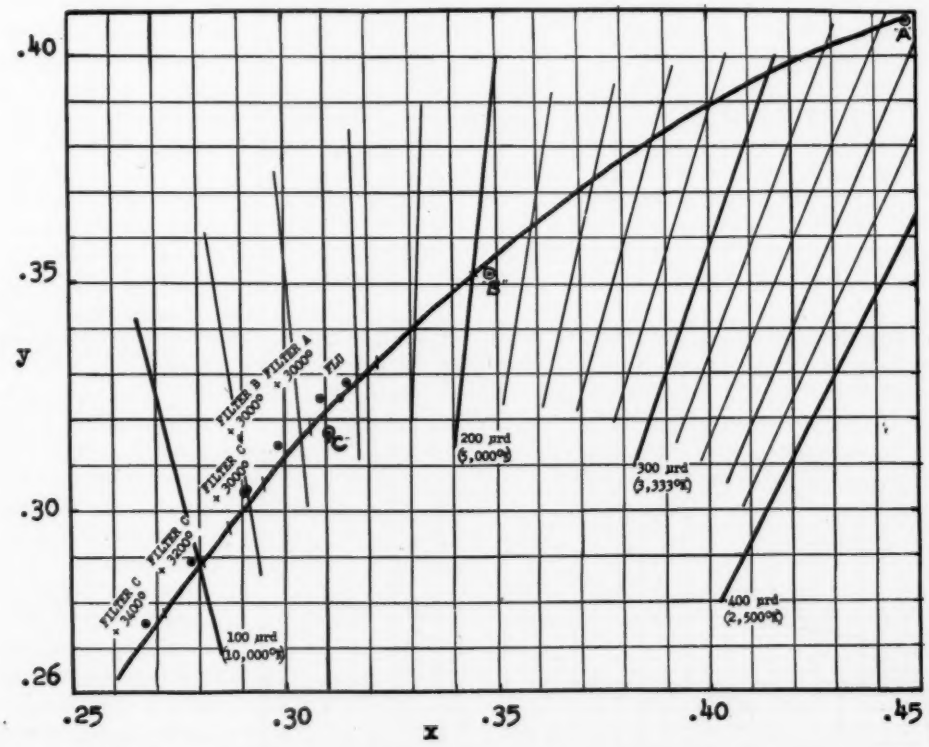

FIG. 4. Distribution of color of lamps used, plotted on an I.C.I. (x,y) diagram relative to *iso*-temperature lines.

A regular 500-watt size Macbeth lamp was hung in this booth within a specially constructed metal cylinder built to enclose the lamp, and to hold, in the bottom, a piece of sandblasted Crystalex glass to diffuse the light. The position of the cylinder housing and the diffusing glass was intended to remain constant, thus providing constant geometry for illuminating conditions throughout the test. Within the cylinder provision was made for raising and lowering the lamp so that the amount of illumination on the table surface might be held as near constant as possible. A change in color temperature was provided by a selection of filters to be used with a series of standard lamps.

A specially built portable unit, with lamps, filters, a Variac, and voltmeter, was provided for this work. It is illustrated, with the samples used in the test, in Fig. 2. This unit was moved from one mill to another for use in all tests.

Whenever fluorescent lamps were used in the mills, test work was done under them also. No control was kept of these lamps, their color or the illuminance provided by them, the units being used just as they were available at the mill.

Thus, matching tests were made under five steps of filtered daylight, one condition of natural daylighting, and fluorescent daylight whenever it was available. A diagrammatic representation of the illuminants used is shown in Fig. 3, and their colorimetric representation is shown in Fig. 4 on an I.C.I. (x, y) diagram relative to lines of constant nearest-color temperature.

The samples used in this test were to be given

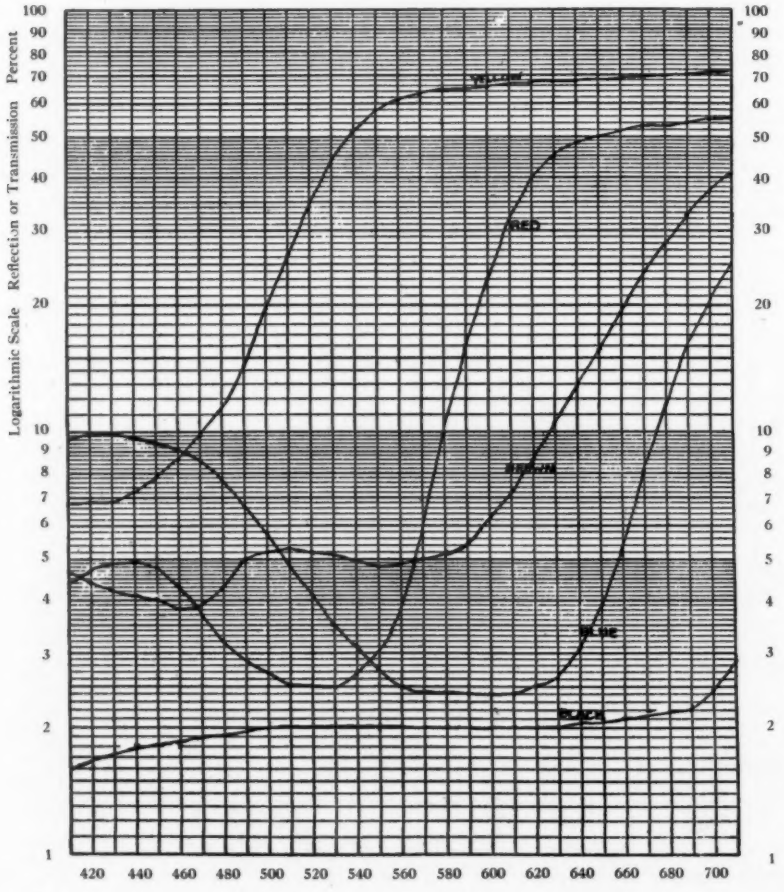

FIG. 5. Spectrophotometric curves for No. 1 samples used as standards in each color group.

to the color matchers who would examine them under this series of illuminants. Since the choice of color temperature probably would depend upon the samples examined, it was of the utmost importance that a representative set be used. Without being too numerous they had to represent all materials, all fabrics, and all colors. Three materials were selected: wool, cotton, and viscose rayon. These represent a large proportion of textile usage. Three fabrics were used: cloth, yarn, and a pile fabric. Five colors were chosen: red, yellow, blue, brown, and black.

It is practically impossible for a color matcher to decide what illumination he likes best if he is given only one sample of a particular type. A piece of red wool cloth is red under all the lamps used in this study. His normal daily task is to see differences between a sample and a standard and make a decision based on the difference.

The necessity of preparing samples with small color differences introduced additional difficulty in the choice of average samples. If all the colors consisted of one pair differing slightly in hue, a different illuminant might be found better than if each pair differed simply in depth of the dyeing. In the case of each color it was necessary to prepare all kinds of color departure from standard. Only then would the choice of lamps be based on average samples.

The method selected was to vary slightly a fundamental dye formula, usually by the addition of a small amount of toning dye. The extent of the differences chosen was intended to represent differences slightly greater than those found in commercially satisfactory matches. Nearly all would be rejected on final inspection but would require some study to decide on corrective measures.

Twenty-nine samples were used in the test. This number appeared to be ample for the colorists to make a choice of illuminants; the use of additional samples would have made the test too time consuming. Figure 5 shows spectrophotometric curves of the standards used in each series of samples.

The color examiners who took part in this study are men who earn their living by coloring or examining the color of fabrics. These men were asked to examine the 29 samples in daylight and under several conditions of artificial daylighting. Within the five sets of samples each sample was numbered. Number one of each series was used as a standard, the other samples being compared with it.

To encourage uniformity in describing the color differences, the observers were supplied with forms on which they could check the kind of difference observed. This tended to give standardized terminology for description of color differences and made it easier to analyze the results. They were, however, not limited to these terms but could use others if they preferred.

The study was set up to discover the color temperature of artificial light preferred by color matchers, yet an analysis of the results will depend upon the standard to which they are compared. The committee made three comparisons with the following results. If the preference is for artificial daylighting that provides results closest to those obtained under preferred conditions of natural daylighting, then, based on the average of these observations, the color temperature answer is 7500°K. If, however, the preference is for an illuminant that will provide results closest to those expected on a basis of the differences introduced by dye formulation, then the average results for color temperature is 8400°K. Further, if the preference is for an illuminant to provide results closest to those obtained by spectrophotometric measurement of the sample, the average color temperature result is also 8400°K (although Illuminant *C*, about 6700°K, was used in the colorimetric calculations).

Perhaps the most important fact brought out by this part of the study is that within a fairly wide range of color temperature, and with illuminance not more than 60 to 90 footcandles under the lamps, the color matching results all come very close to those obtained under natural daylight. In only one mill was there a consistently better showing for color matching results under natural as compared with artificial daylight. Even there the margin of difference was very small. Outstanding differences between results under the various color temperatures did not occur.

The mills varied in degree of agreement with expected differences from a high of 75 percent at one mill to 40 percent at another; all showed about 10 percent more agreement for compari-

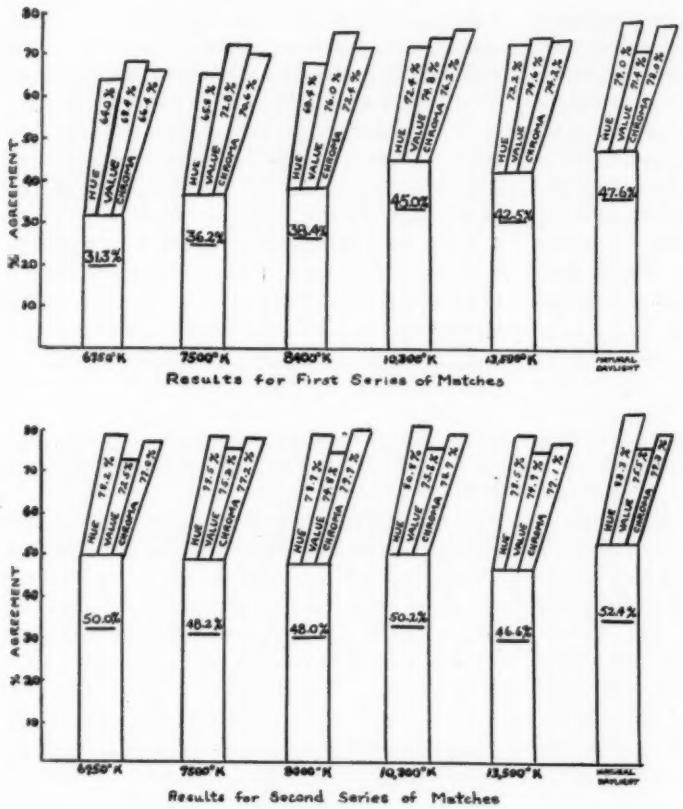

FIG. 6. Percentage of agreement among color matchers at one mill in their ability to call the matches in a common terminology.

sons with dye formulation data than with colorimetric measurements. The average agreement for all mills with dye formulation data was about 55 percent, varying only about 2 percent from this for the various illuminants. The average agreement with computed colorimetric data was about 45 percent, with about 2 percent variation for the several illuminants.

Perhaps it should be noted here that differences in results between mills may be due to one of several factors. Among these, the ability to break down the difference seen into at least three factors and for color matchers to use a common terminology in describing these differences, is probably the most important. Undoubtedly, the color matchers in one mill could see the differences as well as matchers in another mill. But seeing a color difference does not mean that one matcher can analyze this difference and record it in a terminology understood by other matchers. It takes training to do this, and while color matchers in all mills usually looked for and recorded a hue difference, they varied by mills in their ability to record other types of differences. The record sheet reminded each matcher to look for differences in lightness and saturation as well as hue. The subcommittee found, after the work was done, that the probable reasons for greater agreement in one mill than in the others was the fact that a training course in color had been given in this mill the year before during which their matchers had learned to analyze color differences and describe them in a common terminology.

Agreement among color matchers in this mill, after eliminating the practice effect found in the first series, as shown in Fig. 6, was almost 50 percent for differences called in terms of all three attributes of hue, lightness, and saturation. Agreement on single attributes was as high as 75 to 80

percent. The highest agreement on all three attributes was about 52 percent under daylight, with a variation under other illuminants of 2 to 6 percent. This mill averaged 75 percent in recognizing and agreeing with color differences due to change by dye formulation. Such a high degree of agreement sets quite a record, and shows what can be expected with training and practice.

In addition to the record of differences for samples matched under various color temperatures, color matchers also answered three questions asked at the end of the matching studies.

The distribution of answers to the first question regarding illuminant preference is shown in Fig. 7. In mills A and B the preference was clearly for 7500°K. No such definite preference appears for mill C, although in its first selection 7500°K represented the highest percentage preference, 10,300°K was its second selection. In mill D the greatest preference was for 6750°K. Answers to questions as to whether the choice corresponds to present conditions or whether it gives the same results as daylight now used showed that for a large majority of cases the preference indicated was thought to be similar, or nearest to the condition preferred for natural daylight, and that it was thought to give results similar to those obtained under natural daylight.

RECOMMENDATION

On the basis of this study in all its details, and of information available through previous studies, our subcommittee is unanimous in recommending that artificial daylight lamps for textile color matching be aimed at 7500°K, with an illuminance of more than 75 and less than 300 footcandles.

We realize that the choice of 7500°K is somewhat arbitrary since it is not outstandingly better than color temperature somewhat higher than this. The considerations which suggest 7500°K are as follows: (1) At an illuminance of 100 footcandles, 7500°K is the minimum for natural daylighting conditions called very good for matching, and at 200 footcandles it falls near the average of such conditions; (2) when colorists were asked which of several lamps they preferred, their choice on the average was near

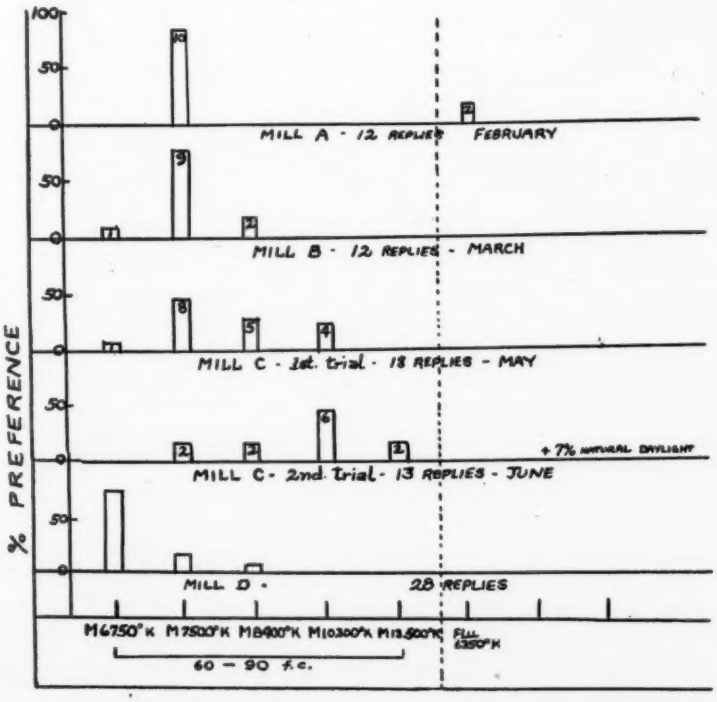
% PREFERENCE
100
50
0
MILL A - 12 REPLIES - FEBRUARY
MILL B - 12 REPLIES - MARCH
MILL C - 1st. trial - 18 REPLIES - MAY
+7% NATURAL DAYLIGHT
MILL C - 2nd. trial - 13 REPLIES - JUNE
MILL D - 28 REPLIES
M6750°K M7500°K M8400°K M10300°K M13,500°K FLU. 6350°K
60 — 90 f.c.

FIG. 7. Distribution of preferences for color temperature expressed by color matchers after they had matched under the entire series of lamps in test.

7500°K; (3) color differences observed by colorists under natural daylight chosen by them agreed best with color differences observed by them under 7500°K; (4) it is understood that manufacturers of artificial light units for color matching can produce 7500°K sources with the footcandle range indicated. While the recommendation itself makes no mention of illumination geometry, it is assumed that this should follow good lighting practice.

ACKNOWLEDGMENT

The subcommittee wishes to thank the following: Curt Forstmann and W. von Bergen of Julius Forstmann and Company; P. M. Otto, Sr. (who has since died) and Frederick R. Haigh of Botany Worsted Mills; and Harold W. Leitch and Raymond Schuster of Pacific Mills for their cooperation in encouraging, as well as permitting, this study to be made in these mills. The subcommittee also wishes to acknowledge and thank the color matchers and technical workers who participated in making the color judgments. Without their careful and time-consuming cooperation in making hundreds of check measurements, and without the wholehearted cooperation of the men in charge of each department, this study could not have been made. Of the more than 80 participants, 75 percent were actively engaged in color discrimination at the time of these studies; the other 25 percent were experienced persons although they were not actively engaged in color discrimination.

JOURNAL OF THE OPTICAL SOCIETY OF AMERICA VOLUME 38, NUMBER 5 MAY, 1948

A Method for Automatically Plotting Spectral Energy Distribution of Luminescent Materials

FRANK J. STUDER
Research Laboratory, General Electric Company, Schenectady, New York

(Received January 30, 1948)

A method is described for measuring automatically the spectral energy distribution of luminescent materials or of other light sources. A photo-multiplier operated on d.c. is used with a standard constant deviation spectrometer for measuring the energy in the spectrum. A compensator has been built in the spectrometer so that the output of the photo-cell is proportional to incident energy of any wave-length. A drive mechanism sweeps the spectrum across the exit slit at constant wave-length rate, and the photo-cell output appears on the chart of a standard photoelectric recorder. Errors, due chiefly to inaccuracies in milling the compensator, are less than 5 percent except in the extreme violet. Curves repeat within 1 or 2 percent. Spectral curves can be taken of surfaces whose brightness is as low as 1 foot lambert. The time to obtain a distribution curve may be varied from one-half to two minutes by a change of gears.

A VERY great number of different luminescent materials such as those used in fluorescent lamps and cathode-ray tubes have already been produced and new ones are continually being found. Each one of these emits light of a different characteristic color, the spectrum consisting usually of one or more broad continuous bands. On account of the wide variety of colors obtainable with luminescent sources, it has become important to have available a means for making rapid determinations of spectral energy distribution, both for determining the color characteristics of new products and for controlling the character of those being used in fluorescent lights and other standard applications. Because of the relatively low brightness of phosphors it was difficult to do this before photo-multipliers with extremely high sensitivity were developed. Such cells are now easily obtainable, however. The purpose of this paper is to describe how a photo-multiplier may be used with a modified standard spectrometer and a recorder to draw the spectral curves of phosphors automatically.

The basic scheme is essentially the same as that described earlier by the writer[1] for point by point determination of spectral energy distribution. A motor drive and compensator have been added, and the output is fed into a recorder, so that the spectral curve is drawn automatically. The range of the instrument is from 4000A to 7400A and the time to draw a spectral curve may be varied from one-half minute to two minutes. A somewhat more complex apparatus for automatic spectral recording has been described by Zworykin[2] and by A. E. Hardy.[3]

The dispersion instrument used is a conventional constant deviation spectrometer. The wave-length drum is turned by a 6-watt synchronous motor through a double cam so designed that the spectrum sweeps past the exit slit of the spectrometer at a constant wave-length rate. This means that the length of time required to turn through a given wave-length band is the same in all parts of the spectrum. The cam arrangement used may be seen in the photograph of Fig. 1.

The receiver is an electron multiplier phototube of relatively high red response (1P22). The cell is operated on d.c., the voltage for the dynodes being obtained from a regulated power supply, whose output can be varied from 400 to 1200 volts d.c. To minimize the hazard of electric shock the high voltage is produced at radio-frequency and the short-circuit output current is small. A 90-volt battery is used for the collector voltage of the multiplier.

The output of the photo-multiplier is amplified by a conventional low drift circuit and fed into a standard photoelectric recorder where the spectral energy distribution curve is drawn. The recorder chart is driven by a synchronous motor which is turned on by the same switch that con-

[1] F. J. Studer, J. Opt. Soc. Am. **37**, 288 (1947).

[2] V. K. Zworykin, J. Opt. Soc. Am. **29**, 84 (1939).

[3] A. E. Hardy, J. Electrochem. Soc. **91**, 127 (1947).

trols the wave-length motor. The chart, therefore, turns in synchronism with the wave-length drum. Thus the wave-length scale on the chart is linear since the rate (with respect to wave-length) at which the spectrum sweeps across the exit slit is constant. The spacing on the wave-length scale is determined by the speed with which the record chart is geared.

In order that the output of the photo-cell may be proportional to the energy in a constant wave-length band radiated from the source at all parts of the spectrum, compensation must be made for three things:

(1) Variation in response of the photo-cell with wave-length.

(2) Increase in the dispersion on going from red to violet in the spectrum.

(3) Absorption of the prism and lenses of the spectrometer.

This is accomplished by a disk of varying radius which rotates in front of the exit slit, being driven from the wave-length drum. This disk is designed to cover the proper amount of the exit slit to compensate for the three factors above. The data for constructing the compensator is obtained by means of a tungsten lamp of known color temperature, the light being reflected from a calibrated diffuse reflector such as a magnesium carbonate block or Vitrolite. A diffuse reflector is used rather than the direct light from the lamp since, in this way, it is assured that the aperture of the spectrometer will be uniformly filled with light. The sources to be measured must also be of such a nature as to give uniform illumination over the length of the slit. With phosphor samples and fluorescent light sources in general, this can usually be approximated without difficulty. It is likely that some other method of compensating, such as the use of a variable resistor of the proper characteristics operated from the wave-length drum, will prove to be more desirable than this one. In this case the exit slit would remain open full length through the wave-length range. However, the arrangement described above has been surprisingly satisfactory for phosphor work with the particular photo-cell which has been used.

The width of the entrance slit used for most work is 0.3 mm and the exit slit 1 mm, although these may be varied for different problems. An exit slit of 1 mm corresponds to approximately 100A at the green line of mercury and 30A at 4046A.

One matter of concern at the time the equipment was first assembled was the possibility that the spectral response of the photo-cell might change over long periods of use. However, the first instrument has now been in almost daily operation for a year, and it has not been necessary to alter the compensator. It should be pointed out that the photo-cell current is always kept at low values. For most of the work, 0.5 microamperes in the cell output gives full-scale deflection on the recorder (35 microamperes). If it

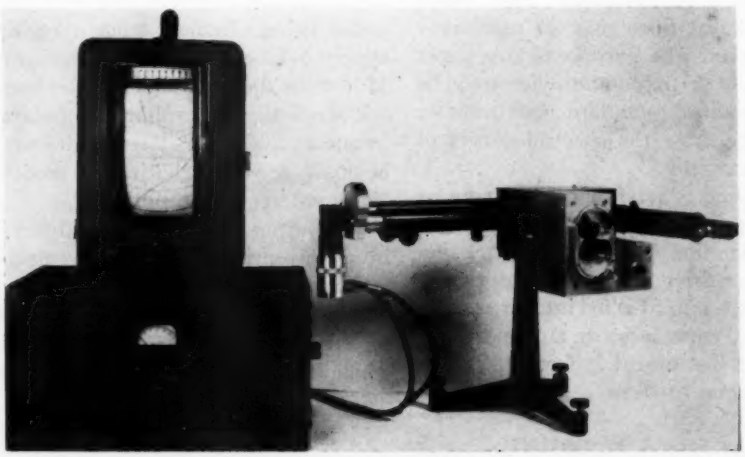

FIG. 1.

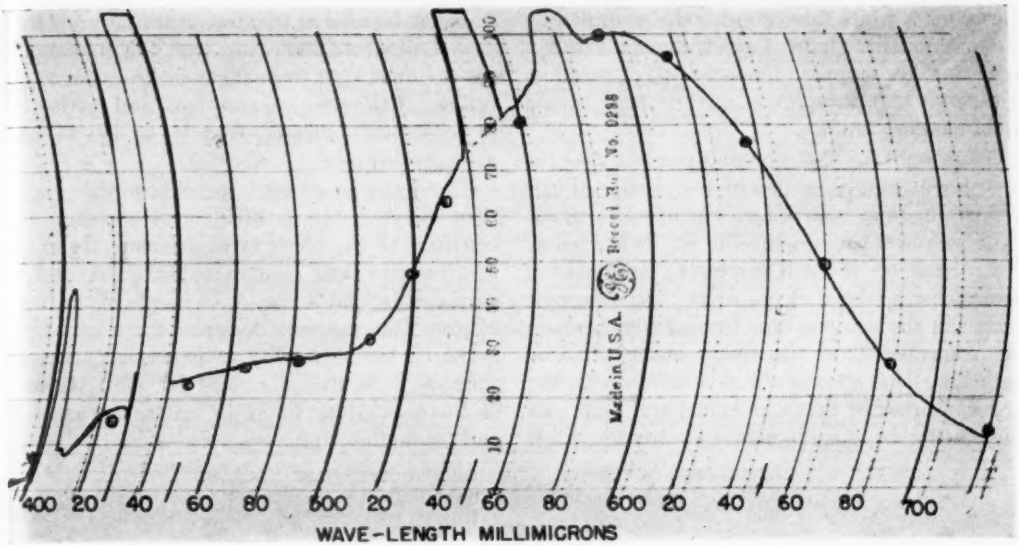

FIG. 2. Spectrum of white fluorescent lamp. Points give values for same lamp measured with double monochromator by Dr. B. T. Barnes at Nela.

should become necessary to change photomultipliers, a new compensator will of course be quired. This is not as serious a matter as it might at first seem since a skilled mechanic with precision machinery can make one in a few hours.

A photograph of the assembled equipment is given in Fig. 1. The three integral units of the equipment are easily disconnected so that it is a relatively simple matter to transport from place to place. Figure 2 gives the relative energy

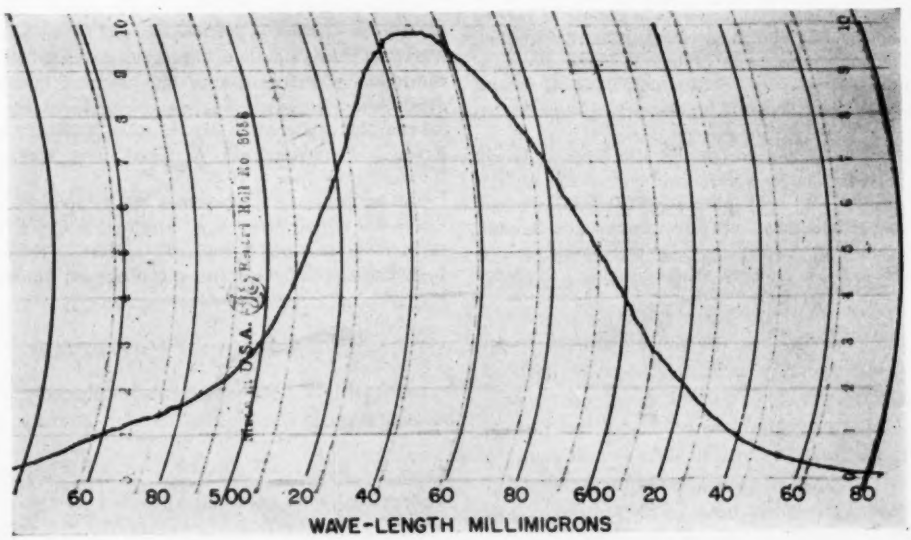

FIG. 3. Copper-activated zinc cadmium sulfide (90/10) excited by BH4 lamp.

curve for a white fluorescent lamp as drawn by the instrument. Figure 3 gives the spectral distribution for copper activated zinc cadmium sulfide (90/10) phosphor excited by light from a BH4 mercury lamp.

Tests made up to the present indicate that the instrument may be expected to repeat within 1 percent in successive measurements on a given light source. Checks with Dr. B. T. Barnes at Nela Park on several fluorescent lamps have shown discrepancies of not more than 5 percent except in the extreme blue toward 4000A where the transmission of the spectrometer prism is very low. This accuracy was achieved with the first compensator that was made, and since this was satisfactory for the measurements for which it was to be used at the time, it was not replaced. It was observed, however, that the errors arose for the most part from slight inaccuracies in the milling of the compensator disk, and further experience has indicated that these can be considerably reduced.

The writer is pleased to acknowledge his indebtedness to Mr. J. Fielding of our shop who constructed the mechanical attachments to the spectrometer and contributed a great deal to their design, and to Mr. A. L. Hardy of the Aero-Marine Division who designed the wave-length drive. He would also like to express his appreciation to Dr. S. Dushman and Dr. N. T. Gordon of this laboratory for continual encouragement and for many helpful suggestions.

Symposium on Electron and Light Microscopy

A Symposium emphasizing the supplementary relationship between electron and light microscopy, sponsored by Armour Research Foundation of Illinois Institute of Technology and the Physics Department of the Institute, is to be held at The Stevens Hotel, Chicago, Illinois, June 10, 11, and 12. The three-day session will consist of invited papers and planned discussion covering instrumentation, techniques, and applications of both electron and light microscopy. Thursday and Friday will consist of general meetings while Saturday will be devoted to panel discussions.

A number of leading microscopists in both fields will present papers on subjects which will include the applications of electron and light microscopy to metals, biology, fibers, fine particles, fats and soaps, plastics, etc. In addition, there will be papers covering techniques such as phase microscopy, microtomy, shadow casting, and replica methods. There will be ample opportunity for the interchange of ideas and problems either in large discussion groups, panel meetings, or by personal contact. In addition to these sessions there will be equipment displays by well-known manufacturers of research microscopes, vacuum equipment, high speed microtomes and film materials.

An instrument display containing equipment that is of interest to workers in microscopy will be an additional feature of the Symposium. Arrangements have been made to exhibit photomicrographs and electron micrographs near the meeting place. Anyone wishing to exhibit should submit their material to Mr. Howard T. Betz (Armour Research Foundation, 35 W. 33rd Street, Chicago 16, Illinois) before June 6, 1948.

Further information concerning the Symposium may be had by contacting either W. C. McCrone or C. F. Tufts at the Armour Research Foundation of Illinois Institute of Technology, 35 W. 33rd Street, Chicago 16, Illinois.

The $CaSiO_3$:(Pb+Mn) Phosphor

JOHN B. MERRILL AND JAMES H. SCHULMAN*
Sylvania Electric Products, Towanda, Pennsylvania
(Received October 20, 1947)

A calcium silicate phosphor, activated by lead and manganese, is described, and the conditions for its preparation are presented in detail. Under excitation by a low pressure mercury discharge, such as is employed in fluorescent lamps, this phosphor luminesces with an emission lying principally in the red end of the spectrum and with a high efficiency comparable to that of zinc beryllium silicate of the same luminescence color. Data are presented on the spectral emission of $CaSiO_3$:Pb, $CaSiO_3$:Mn, and $CaSiO_3$:(Pb+Mn), both under cathode-ray and under 2537A excitation. It is shown that $CaSiO_3$:Mn is excited to luminescence in the red end of the spectrum by cathode rays but not by ultraviolet light. The introduction of lead as an auxiliary impurity makes possible the excitation of this material by radiation in the neighborhood of the mercury resonance line. Qualitative absorption experiments indicate that the lack of response of $CaSiO_3$:Mn to 2537A excitation is due to the absence of an absorption for this radiation; and that lead acts as a sensitizer for the manganese by introducing an absorption band in the vicinity of 2537A. The presence of a sensitizer is unnecessary under cathode-ray excitation, since in this case the energy is absorbed by the host crystal itself.

CALCIUM silicate phosphors activated by lead or manganese separately have been reported in the literature.[1] $CaSiO_3$:Pb is excited by 2537A radiation and cathode rays to a broad luminescence emission lying between 2800 and 4600A, with a peak in the neighborhood of 3550A (Fig. 1). $CaSiO_3$:Mn, on the other hand, is feebly or not at all responsive to 2537A excitation but luminesces yellow or orange under cathode-ray bombardment (Fig. 2). The present paper is concerned with a study of the phosphor obtained by simultaneous incorporation of both lead and manganese in calcium silicate.[2] This phosphor responds very efficiently to mercury resonance radiation, in which respect it resembles $CaSiO_3$:Pb; but the luminescence emission that results from this excitation lies principally in the red end of the visible spectrum, wherein it is analogous to $CaSiO_3$:Mn.

PREPARATION OF $CaSiO_3$:(Pb+Mn)

The phosphor can be prepared in a number of ways, only a few of which will be mentioned here.

1. By firing, in the neighborhood of 1000–1200°C, an intimate mixture of the component metal carbonates, oxides, or hydroxides with silica.

2. By firing at this temperature an intimate mixture of preformed $CaSiO_3$:Pb and $CaSiO_3$:Mn phosphors. Each of these may be made by the first method by omission of the undesired activator.

3. By firing preformed $CaSiO_3$:Mn with a lead compound admixed, or even in the presence of only the vapors of a lead compound. The first method is, of course, the most direct and the most easily controllable.

The host material giving the brightest luminescence under 2537A excitation corresponds to the metasilicate composition. An excess of 20-mole percent of silica over the stoichiometric amount for $CaSiO_3$ was found advantageous; however, a 100-mole percent excess of silica may be used, with only ten percent loss in brightness. The manganese content of the preparations should be kept between 0.04 and 0.13 moles of manganese per mole of calcium oxide for optimum brightness under mercury resonance radiation excitation. With increase in manganese concentration within this range the luminescence color becomes subjectively redder (*q.v.*).

* Present address: Crystal Section, Naval Research Laboratory, Washington, D. C.
[1] H. W. Leverenz, R.C.A. Review IV, 161 (1940).
[2] J. B. Merrill and W. E. Stewart, British Patent 581,951, accepted Oct. 30, 1946.

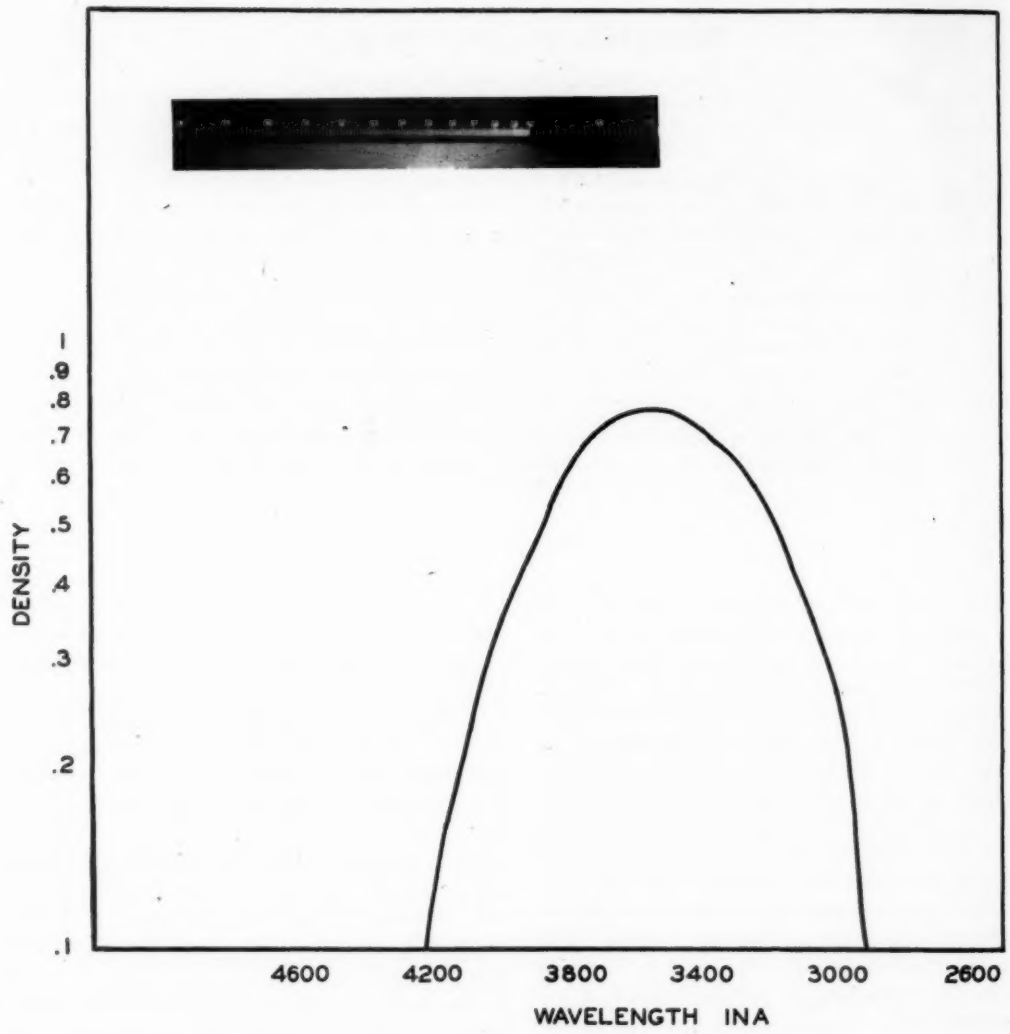

FIG. 1. Luminescence spectrum of $CaSiO_3$:Pb under cathode-ray excitation.

The successful preparation of a highly efficient phosphor of low particle size was found to require careful control of a large number of variables. The sensitivity of the phosphor to the preparative details is related to the volatility of lead compounds during firing and to the sintering and discoloration produced when they are used in excess to compensate for this volatility. Among the lead compounds used were the basic carbonate, chloride, fluoride, and the several oxides of lead. The lead concentration required for activation is very low, in the order of 0.003–0.008 mole of lead per mole of calcium oxide. This small amount may be used in the formulation if the firing is done in closed vessels allowing substantially no escape of lead vapors. With open containers a much larger amount of lead is necessary in the formulation. The amount of excess lead compound desirable may be as high as ten times the optimum concentration men-

tioned above, depending upon the rate of escape of lead-bearing vapor from the charge. This, in turn, is a function of the lead compound used, the firing temperature, the geometry of the firing vessel, the ratio of the furnace volume to size of charge, the method of blending the components before firing, and even of the air circulation characteristics of the furnace. A deficiency of lead is indicated by a low particle size and a low brightness, as well as a white color of the phosphor by reflected light. Sintering and large particle size, together with a brownish discoloration and low luminescent brightness of the powder result, on the other hand, from too much lead in the formulation. The optimum combination of charge composition, method of blending, and firing conditions gives a white powder of about 4–5-microns average particle size (air permeability method), and high luminescence efficiency. A composition giving good results when firing is done in an uncovered 7″×10″×1″ tray in a 700-cubic inch muffle furnace is as follows:

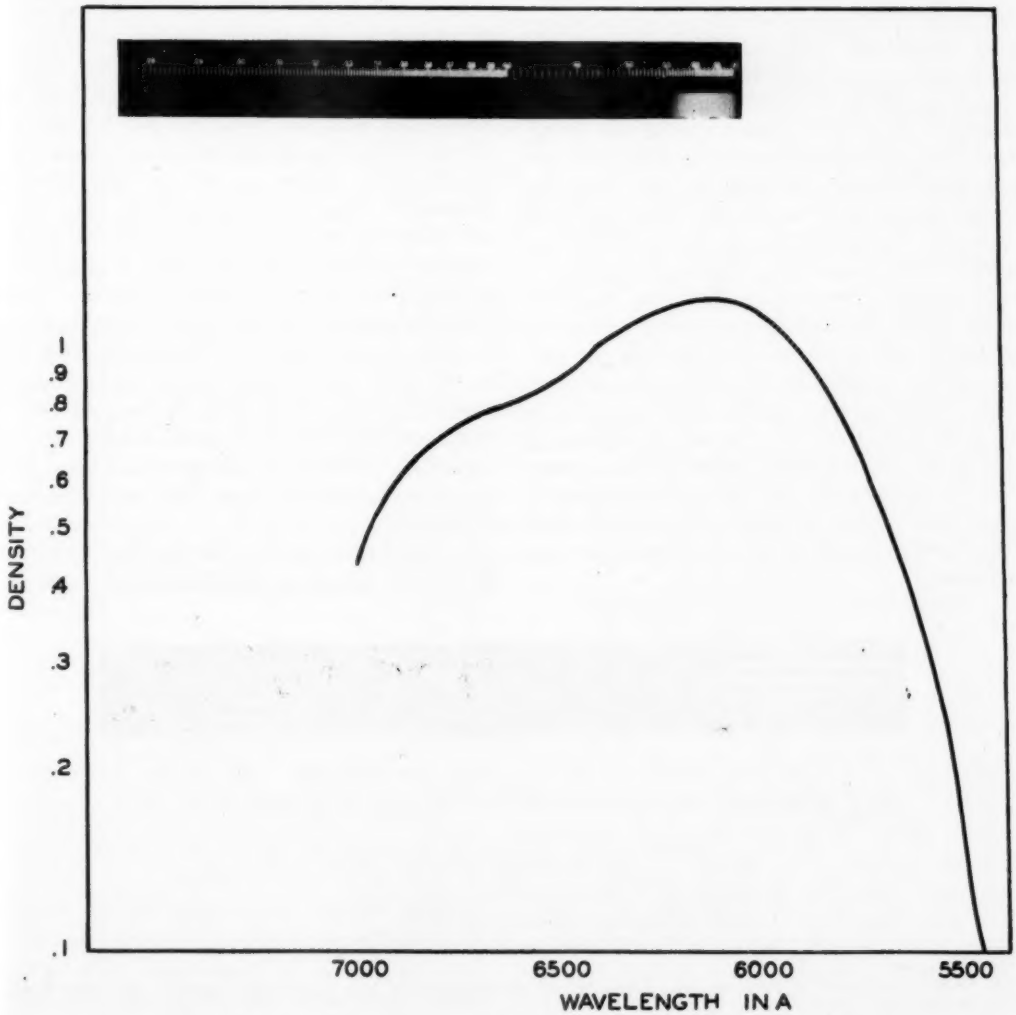

FIG. 2. Luminescence spectrum of $CaSiO_3$:Mn under cathode-ray excitation.

$CaCO_3$	1.00 mole
$SiO_2 \cdot xH_2O$	1.20 moles
PbF_2	0.008 mole
$MnCO_3$	0.066 mole.

The components, all C.P. chemicals, are pebble milled together and fired at 1150°C, for six hours. The charge is placed into the hot furnace and also removed while hot and air-cooled to room temperature. During this cooling period a tan-colored surface layer often forms, which is presumably due to oxidation of manganese by the air as the temperature drops through a certain zone favorable for this reaction. Pulverizing and refiring this material under the same conditions as the first firing removes this discoloration, the manganese being apparently more resistant to oxidation after the second firing. The surface discoloration described above is not to be confused with the brownish color produced by too much lead; the latter, when it occurs, permeates the entire charge and is not eliminated completely even after several successive firings.

Advantage may be taken of the catalytic action of fluoride on the reaction of phosphor formation and on its effect in reducing the particle size by employing a fluoride flux, such as calcium fluoride, while the lead is incorporated as the basic carbonate or as one of its oxides. In fact, from the solubility relations[3] it appears that if $CaCO_3$ and PbF_2 are pebble milled in water they should be converted to CaF_2 and $Pb(OH)_2 \cdot PbCO_3$. This was confirmed by experiment.

SPECTRAL ENERGY DISTRIBUTION AND LUMINOUS EFFICIENCY UNDER 2537A EXCITATION

The luminescence spectrum of $CaSiO_3$:(Pb+Mn) under 2537A excitation consists of two bands. The first, and by far the stronger, lies in the visible, starting at about 5000A and extending beyond 7000A, with a peak at 6100 (Figs. 3 and 4). The second band lies in the ultraviolet between 2800 and 4100A, with a peak in the vicinity of 3500A (Fig. 3).

The spectral energy distribution of the principal emission band is shown in Fig. 4 for a series of phosphors containing varying amounts of manganese. These curves were obtained by the method reported in a previous paper.[4] E_λ at 5600A has been set equal to 100 for all the curves. Combining the spectral energy data with the luminous efficiencies of standard 40-watt fluorescent lamps made with these phosphors, and using the data of Thayer[5] to correct for incomplete 2537A absorption, and for absorption of visible light by the phosphor, bulb, and lamp ends, the approximate quantum efficiencies given in Table I were calculated. The efficiencies given in the table are affected by an undetermined amount because of neglect of the near ultraviolet emission band and to the brightness loss caused by milling the phosphors, which was necessary in order to coat them on the inside of lamps.

As these figures indicate, the $CaSiO_3$:(Pb+Mn) phosphor is among the most efficient of the group

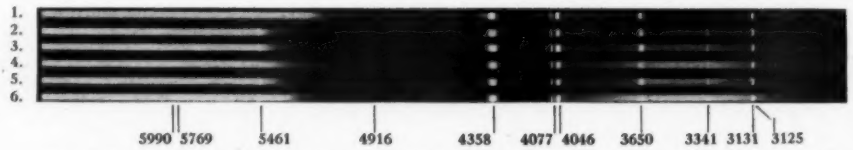

FIG. 3. Luminescence spectra of $CaSiO_3$:(Pb+Mn) phosphors in fluorescent lamps (2537A excitation).

1. $(Zn_{1.8}Be_{0.2})SiO_4$ with 3.5-weight percent Mn as activator.
2. $CaSiO_3$:(Pb+Mn) 0.055-moles Mn/mole CaO.
3. $CaSiO_3$:(Pb+Mn) 0.070-moles Mn/mole CaO.
4. $CaSiO_3$:(Pb+Mn) 0.082-moles Mn/mole CaO.
5. $CaSiO_3$:(Pb+Mn) 0.093-moles Mn/mole CaO.
6. $CaSiO_3$:(Pb+Mn) 0.044-moles Mn/mole CaO.

[3] A. Seidell, *Solubilities of Inorganic and Metal Organic Compounds* (D. Van Nostrand Company, Inc. New York, 1940), Vol. 1.
[4] J. H. Schulman, J. App. Phys. **17**, 902 (1947).
[5] R. N. Thayer, Electrochem. Soc. Preprint **87**, 25 (1945).

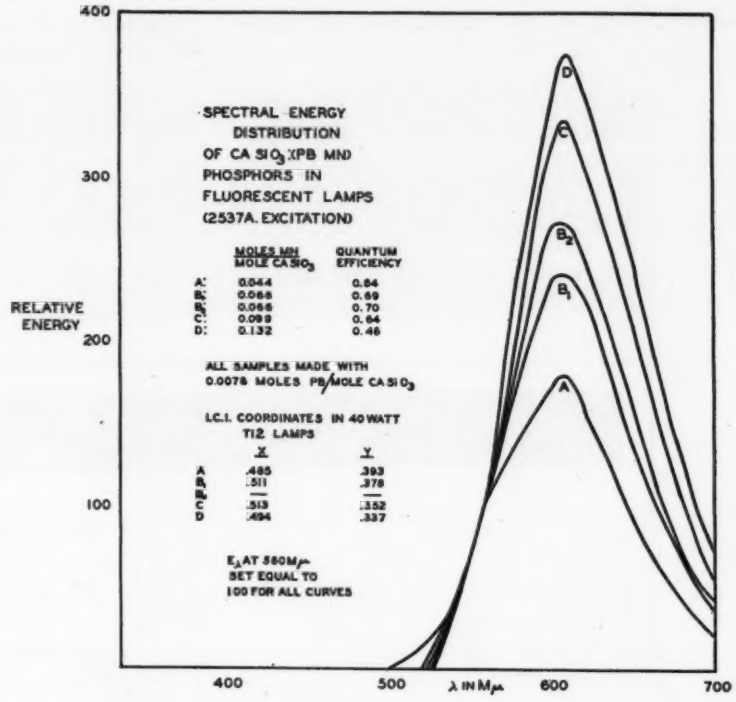

FIG. 4. Spectral energy distribution of $CaSiO_3$:(PbMn) phosphors in fluorescent lamps (2537A excitation).

of phosphors responsive to mercury resonance radiation. In addition, the phosphor exhibits very good maintenance of its efficiency when made into fluorescent lamps, 40-watt lamps made with this material averaging 90 percent of their initial luminous output after 500 hours of burning on a test cycle of 180 minutes on and 20 minutes off.

TABLE I.

Curve No. in Fig.	Moles Mn/moles CaO	Initial L.P.W. in 40-watt lamps	Quantum efficiency (percent)
A	0.044	51.0	64
B	0.066	49.7	70
C	0.099	43.4	64
D	0.132	31.2	46

Both "3500° white" and "6500° daylight" lamps can be made by blending the $CaSiO_3$:(Pb+Mn) with magnesium tungstate and zinc orthosilicate phosphors. The "3500° white" blend compares favorably with the efficiency of such a blend made from zinc beryllium silicate and magnesium tungstate and the "6500° daylight" blend made from $CaSiO_3$:(Pb+Mn) approaches very nearly the same luminous output of a blend of this color made from zinc beryllium silicate and magnesium tungstate.

LUMINESCENCE UNDER CATHODE-RAY EXCITATION

The luminescence spectra of $CaSiO_3$:Pb, $CaSiO_3$:Mn, and $CaSiO_3$:(Pb+Mn) under cathode-ray excitation are shown in Figs. 1, 2, and 5. A current density of 24 $\mu a/cm^2$ at an accelerating voltage of 4000 volts was used, the phosphors being settled onto a quartz plate enclosed in a demountable cathode-ray tube provided with a quartz window. A Bausch & Lomb medium quartz spectrograph was used with type I-F plates, exposure times for $CaSiO_3$:Mn and $CaSiO_3$:(Pb+Mn) being 1 minute, while a 10-minute exposure was required for $CaSiO_3$:Pb. Densitometer traces of the spectrograms reveal absolutely no difference in the green to red

spectral range between the cathode-ray excited emission of $CaSiO_3$:Mn and that of $CaSiO_3$:(Pb+Mn). Visual comparison and the data given above show that the cathode-ray excited emission of both the above phosphors is practically identical with the 2537A-excited luminescence of $CaSiO_3$:(Pb+Mn). The absence of the weak near ultraviolet emission band in the case of cathode-ray excitation of $CaSiO_3$:(Pb+Mn) (Fig. 5) is presumably due to the short exposure time used.

Preliminary decay rate measurements under cathode-ray excitation were made on the $CaSiO_3$:Mn and $CaSiO_3$:(Pb+Mn) phosphors using a current density of 12 $\mu a/cm^2$ and an accelerating voltage of 4000 volts. The light outputs of both phosphors were identical under constant bombardment. The decay curves of both phosphors consisted of an initial rapid exponential decay ($\alpha \cong 30$ sec.$^{-1}$) followed by a much longer decay, probably of the bimolecular type. The brightness of the $CaSiO_3$:Mn phosphor

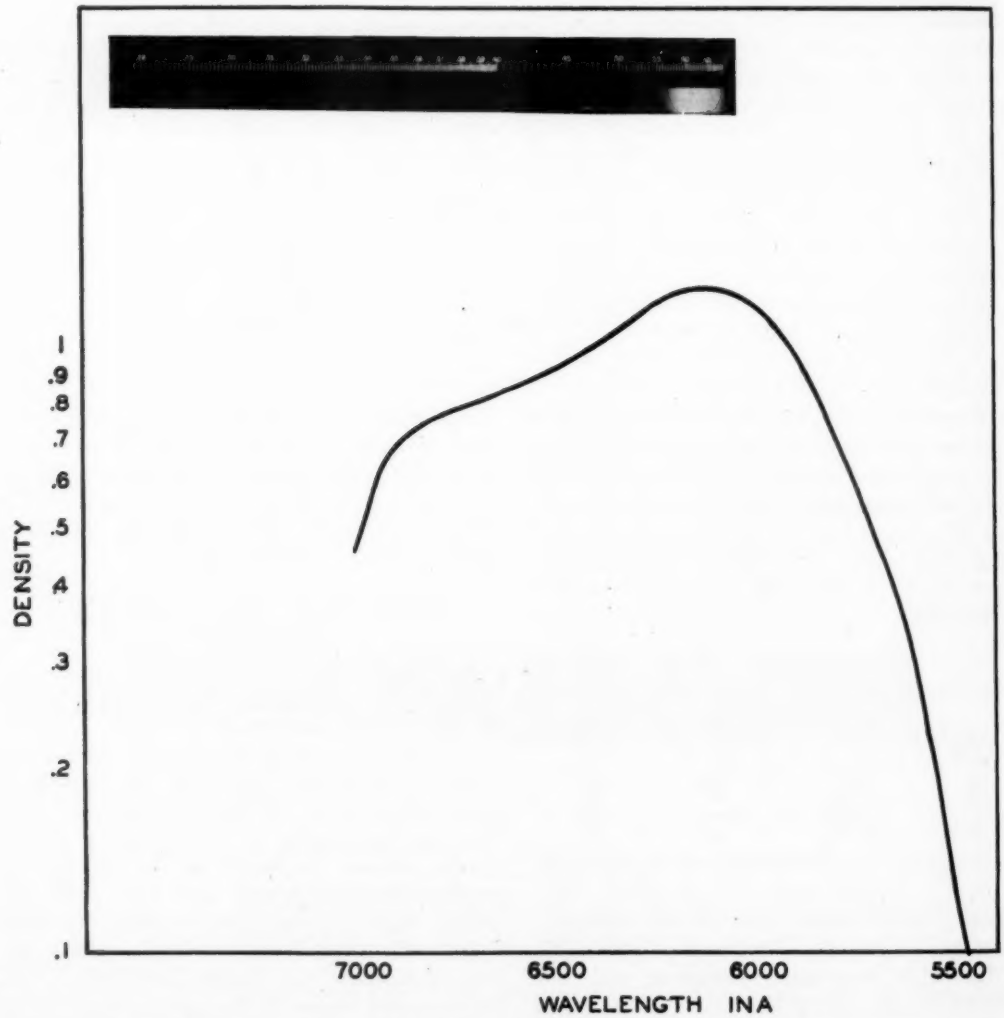

FIG. 5. Luminescence spectrum of $CaSiO_3$:(Pb+Mn) phosphor under cathode-ray excitation.

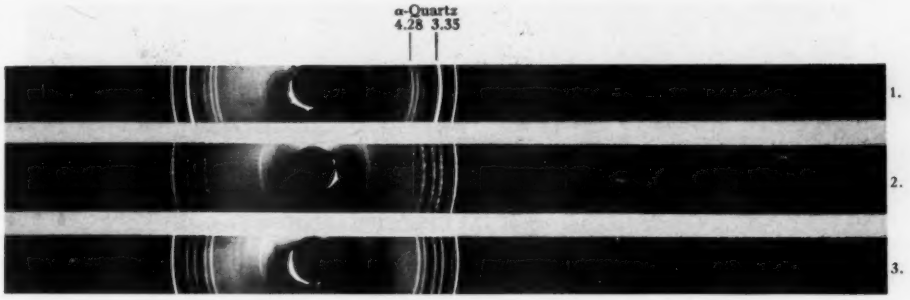

FIG. 6. X-ray diffraction patterns of $CaSiO_3$ phosphors.
1. $CaSiO_3$:(Pb+Mn) with 1.3-moles excess SiO_2.
2. Natural wollastonite.
3. $CaSiO_3$:(Pb+Mn) with 0.2-moles excess SiO_2.

dropped to about 0.013 percent of its initial value in 0.5 second, while the brightness of the $CaSiO_3$:(Pb+Mn) phosphor was thirty times as great. This ratio of phosphorescence brightness persisted up to fifteen seconds which was the longest time that the decay was followed. It therefore appears that the addition of lead to $CaSiO_3$:Mn affects the number or depth of traps in the crystal, or both.

X-RAY DIFFRACTION STUDIES

Debye-Scherrer photographs of several preparations containing lead or manganese alone, or both together (Fig. 6), showed that the material was essentially identical with the natural mineral wollastonite, a sample of which was kindly provided by Dr. Clifford Frondel, Department of Mineralogy, Harvard University. Samples containing high percentages of excess silica gave the pattern of α-quartz in addition to the wollastonite pattern.

The $SiO_2 \cdot xH_2O$ used in the preparations was amorphous to x-rays. The crystallization of the amorphous silica to α-quartz in this case differs from its behavior in the preparation of zinc orthosilicate or zinc beryllium silicate with excess silica, where it crystallizes as cristobalite.[6]

[6] G. R. Fonda, J. Phys. Chem. **43**, 561 (1939).

DISCUSSION

The observations on the $CaSiO_3$:(Pb+Mn) phosphor may be interpreted in one of three ways. First, it may be proposed that manganese alone in $CaSiO_3$ does not constitute a luminescent center, but that a lead-manganese "complex" is required. This view is contradicted by the fact that $CaSiO_3$:Mn is luminescent under cathode-ray excitation with an emission in the red end of the visible spectrum that is identical with that of $CaSiO_3$:(Pb+Mn) excited in the same way. This shows that manganese alone in calcium silicate does constitute a luminescent center under proper conditions of excitation, the formation of a lead-manganese complex being unnecessary.

Secondly, it may be assumed that a "cascade" process is operative in the $CaSiO_3$:(Pb+Mn) phosphor, 2537A radiation exciting the lead activator to an emission in the near ultraviolet, which radiation in turn excites the manganese activator to a luminescence in the visible region of the spectrum. While this interpretation appears to be the most simple and obvious one, and seems to be supported by the observed ultraviolet emission of $CaSiO_3$:Pb and $CaSiO_3$:(Pb+Mn), it is easily shown to be incorrect. $CaSiO_3$:Mn [and $CaSiO_3$:(Pb+Mn)] is only feebly excited by near ultraviolet from a "black-light" lamp or from a high pressure mercury discharge lamp, both of which emit strongly in the near ultraviolet. The high quantum efficiency

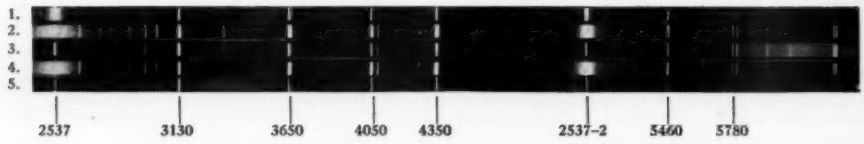

FIG. 7. Absorption of ultraviolet radiation by $CaSiO_3$ phosphors.
1. Germicidal glass coated with $CaSiO_3$ (Mn activated).
2. Germicidal glass clear.
3. Germicidal glass coated with $CaSiO_3$ (Pb and Mn activated).
4. Germicidal glass clear.
5. Germicidal glass coated with $CaSiO_3$ (Pb activated).

observed with $CaSiO_3$:(Pb+Mn) under 2537A excitation, however, requires at least an equivalent luminescence efficiency of $CaSiO_3$:Mn and $CaSiO_3$:(Pb+Mn) under near ultraviolet excitation, if the cascade mechanism is true. Secondly, from the "cascade" model, a bright luminescence response would be expected from an intimate mechanical mixture of $CaSiO_3$:Pb and $CaSiO_3$:Mn under 2537A excitation. Experiment shows that there is absolutely no response to 2537A irradiation from such a mechanical mixture; it is only after the mixture has been fired, so that lead and manganese are built into the $CaSiO_3$ structure together, that any luminescence in the red end of the visible spectral region is observed under mercury resonance radiation.

The third possibility is that the $CaSiO_3$:(Pb+Mn) phosphor is another case of sensitized luminescence, such as first described by Rothschild[7] in the group of rare-earth activated alkaline earth sulfides and more recently shown to exist by Schulman and co-workers in manganese-activated calcite[8] and manganese-activated alkali halides.[9,10] According to this interpretation, the failure of $CaSiO_3$:Mn to luminesce under 2537A excitation is merely a consequence of the absence of an absorption band in the crystal for this radiation. The role of lead is assumed to be to introduce an absorption band in the crystal in the neighborhood of mercury resonance radiation. The lead, then acts as an "absorber" or "sensitizer," the absorbed energy being transferred to near manganese neighbors by a process similar to collisions of the second kind, and the manganese then emitting this energy as its characteristic orange-red luminescence. According to this view, the near ultraviolet emission of lead in $CaSiO_3$:Pb and in $CaSiO_3$:(Pb+Mn) is incidental to its role as a sensitizer; and other impurities than lead may be possible sensitizers even though they do not activate $CaSiO_3$ themselves. (In contrast to this for the "cascade" model the emission of lead in $CaSiO_3$ is of primary importance.) The cathode-ray excited luminescence of $CaSiO_3$:Mn is readily understandable, since under this excitation a specific absorption band in the region of 2537A excitation is not required. Under cathode-ray bombardment all the atoms of the crystal absorb energy[11] which may then be transported over large distances in the crystal to the site of the manganese activator by the movement of excitons or of electrons and positive holes.[12]

The hypothesis of sensitized luminescence was indicated to be correct by making qualitative studies of the absorption of $CaSiO_3$:Pb, $CaSiO_3$:Mn, and $CaSiO_3$:(Pb+Mn) for ultraviolet radiation in the neighborhood of the mercury resonance line. This was done by coating 15-watt "germicidal" lamps along half their lengths with the various phosphor powders. Spectrograms were then taken of the discharge both through the clear portion of each lamp and through the phosphor-coated portion, and the relative attenuation of the mercury lines in the

[7] S. Rothschild, Physik. Zeits. **35**, 557 (1934), and **37**, 757 (1936).
[8] J. H. Schulman, L. W. Evans, R. J. Ginther, and K. Murata, J. App. Phys. (in press).
[9] J. H. Schulman, E. Burstein, L. W. Evans, and R. J. Ginther, (in press).
[10] K. J. Murata and R. L. Smith, Am. Mineral **31**, 527 (1946).
[11] N. F. Mott and R. W. Gurney, *Electronic Processes in Ionic Crystals* (Oxford University Press, New York, 1940), p. 102.
[12] See reference 11, p. 207 and ff.

ultraviolet, particularly of the 2537A line, was observed. As Fig. 7 shows, the mercury spectrum transmitted through $CaSiO_3$:Mn is approximately as strong as that transmitted by the germicidal glass itself, and the relative intensities of the various mercury lines are also the same in the two cases. This indicates that there is very little or no absorption of ultraviolet by $CaSiO_3$ containing the manganese activator alone. With $CaSiO_3$:Pb and $CaSiO_3$:(Pb+Mn), however, the 2537A line is very markedly reduced in intensity, indicating the presence of a strong absorption band for this region of the ultraviolet in both phosphors.

ACKNOWLEDGMENTS

The authors are indebted to S. L. Parsons, J. Berberet, and P. Donovan for the spectrograms reproduced in this paper; to G. A. Davis and V. M. Brown for the x-ray diffraction data and photographs; to L. W. Evans and W. H. Ottemiller for the decay rate data; to G. W. Keilholtz for chemical analyses of the phosphors; to A. B. Davis for his many suggestions in improving the characteristics of the phosphor; to W. E. Stewart for development of the original formula jointly with one of the authors; and to E. F. Lowry and L. Burns for their interest and support of the project.

Erratum: Spectrochemical Determination of the Major Constituents of Minerals and Rocks

[J. Opt. Soc. Am. 37, 585 (1947)]

ASLAK KVALHEIM
Government Raw Materials Laboratory, Oslo, Norway

IN Fig. 1 on page 588 the line marked Si 2516.123 should be marked Si 2524.118.

Letters to the Editor

Emission Spectra of Zinc Cadmium Sulfides

FRANK J. STUDER AND D. A. LARSON
Research Laboratory, General Electric Company, Schenectady, New York
February 4, 1948

IN the November 1947 issue of this journal, Byler has published curves giving the emission spectra of a large number of zinc sulfides and zinc cadmium sulfide phosphors. These, in general, indicate that the emission is not one broad band as has been commonly assumed, but that it is "in every case a summation of contributions from a number of individual bands whose peak positions are invariant and are characteristic of the base material rather than the activator."

These results are somewhat surprising since the spectral distribution curves recently reported by other observers for both ultraviolet and cathode-ray excitation have failed to show such an obvious multiplicity of peaks.[1-3] The writers in the last few months have taken emission curves of a number of zinc cadmium sulfide phosphors, using a recording spectro-radiometer. Under the conditions that

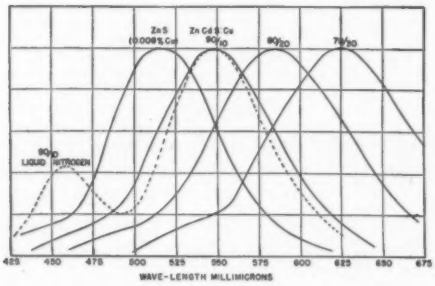

FIG. 1. Emission spectra of zinc cadmium sulfide phosphors.

these were taken, they failed to give any indication of a structure such as Byler reports. The exciting source was a BH4 lamp approximately 4 inches from the phosphor sample. A typical series for various proportions of zinc and cadmium in copper-activated phosphors is given in Fig. 1. These are replotted from the originals, since the recorder has curved coordinates, as will be noted in Fig. 2.

These do, to be sure, give an indication of a low intensity band on the short wave-length side of the main emission peak, such as has been generally ascribed to the emission of the self-activated sulfide. This was also found by Leverenz[1] for cathode-ray excitation. However, there is no suggestion of other maxima.

A number of the phosphors which we have measured were sent to us by Dr. Byler, and were the same as he had used in his investigations.

The spectro-radiometer has sufficiently high resolution so that peaks of the magnitude that Byler finds should be clearly indicated. It is a glass-prism instrument, whose exit slit remains of constant width while a curve is taken. Consequently, the wave-length band entering the photo-cell varies across the spectrum. For these curves an exit slit of 0.5 mm was used, which corresponds to 90A approximately at 6500A and 15A at 4000A. The entrance slit was such that the image of a spectrum line filled approximately one-third of the exit slit.

In Fig. 2 is given a curve taken at higher resolution for the same ZnCd S (90/10), as shown in Fig. 1. For this a diffraction grating instrument was used for which the wave-length band accepted by the photo-cell was constant and equal to 18A. No compensation was made in this instrument for variation in photo-cell response with wave-length, but maxima of any appreciable magnitude should be clearly evident. It will be noted that the lines 4046A and 4077A are easily resolved.

It is true that the color of the luminescence of the zinc cadmium sulfides is influenced to some extent by the excitation conditions, such as the intensity of the exciting light. Our recording instrument, to be sure, calls for stronger excitation than it is necessary to use with long exposures in the photographic method which Byler employed. However, observations were made over a range in which the exciting lamp (BH4) was moved from 4 inches to 18 inches from the phosphor, with no evidence of new bands.

With the thought that at liquid nitrogen temperature any individual bands which existed would be narrowed and

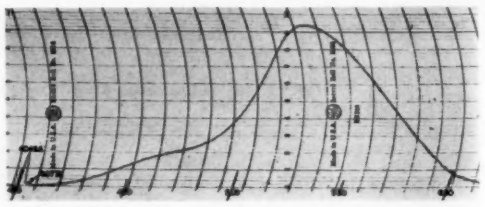

FIG. 2. Spectral response curve for ZnCdS: Cu (90/10) with grating spectrometer using 18A band width.

would therefore appear more prominently, spectra of the phosphors shown in Fig. 1 were taken when immersed in liquid nitrogen. These, in general, showed a change in distribution, the self-activated sulfide band being enhanced, but in no case was there a suggestion of more bands than were evident at room temperature. The low temperature spectrum for ZnCdS:Cu (90/10) is shown by the dashed line in Fig. 1.

The writers are fully aware that Byler's report is the outcome of a very great deal of careful and tedious work, and they hesitate to say anything to detract from it. They are, however, inclined to question the reliability of the photographic method, with its calibration several steps removed from a standard lamp.

In any case, regardless where the cause of the different results may lie, it seeems appropriate to point out, before one of our all-too-scarce theoreticians on luminescence puts a lot of effort in developing a dissertation on the multibanded spectra, that the appearance of these bands seems to be due to very special conditions.

[1] H. W. Leverenz and F. Seitz, J. App. Phys. 10, 488 (1939).
[2] Henderson, Proc. Roy. Soc. A173, 323 (1939).
[3] Fonda, Trans. Electrochem. Soc. 27, 339 (1945).

Lead Selenide Photo-Conductive Cells

J. STARKIEWICZ
Admiralty Research Laboratory, Teddington, Middlesex, England
January 12, 1948

A DESCRIPTION of the preparation and properties of lead sulfide photo-conductive cells has already been given together with a brief outline of a theory of the photo-effects.[1,2] It has been found that, for the highest photo-conductive sensitivity, both excess and defect impurity centers must be present simultaneously in the lead sulfide layer; further it has been shown that the observed photo-conductive, photo-voltaic, and rectifying effects can be explained in terms of the contacts between microcrystals of predominantly excess and defect material.

Normally, peak sensitivity in lead sulfide cells occurs at about 2.7 microns and in all cases the response at room temperature falls to less than one percent of peak response by 3.5 microns. It is known from unpublished German work that with suitably activated layers of lead selenide and lead telluride the photo-conductive effects extend to longer wave-lengths. Recently a spectral response curve for a lead selenide layer exhibiting such effects at low temperature has been published.[3] A process has been developed at this establishment for the activation in vacuum of thin layers of the latter material that results in marked photo-conductive sensitivity at room temperature. The method of preparation is analogous to that already described for lead sulfide although complicated by the tendency of selenium, formed in the course of the activation processes, to remain in the layer.

The spectral response is shown in Fig. 1—peak response is at about 3.4 microns with long wave cut-off at about 4.5 microns. The absorption of Pyrex at the longer wave-lengths necessitates the use of a cell envelope with a thin concave window of about 0.2-mm thickness (transmission 40 percent at 4.5 microns). The curve shown has been corrected for window transmission. It is of interest to note that if the layer is subjected to conditions resulting in a high degree of oxidation, the spectral response is altered with the appearance of peak response at shorter wave-lengths (1.8 microns) and with only a secondary peak at 3.4 microns. This is similar to the spectral characteristics reported by Blackwell, Simpson, and Sutherland.[3]

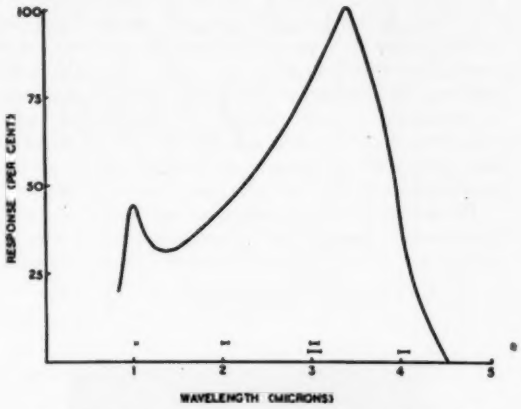

FIG. 1. Spectral response of lead selenide photo-conductive cell.

The sensitivity of a typical cell with spectral response as in Fig. 1 is such that with radiation from a 200°C source interrupted at 800 c.p.s. and with a tuned amplifier of 30 c.p.s. band width, a signal equal to noise is obtained for 10^{-7}–10^{-8} watt of energy incident upon the sensitive layer (area 10 mm×1 mm) in the wave-length range 1–4.5 microns. The response time of the cells is of the order of 10^{-5} second.

[1] L. Sosnowski, J. Starkiewicz, and O. Simpson, Nature 159, 818 (1947).
[2] L. Sosnowski, Phys. Rev. 72, 641 (1947).
[3] D. E. Blackwell, O. Simpson, and G. B. B. M. Sutherland, Nature 160, 793 (1947).

Observations of Anticoronae on Mt. Washington

DAVID L. ARENBERG
Blue Hills Meteorological Observatory, Milton, Massachusetts
(February 25, 1948)

IN a recent paper van de Hulst[1] has discussed the theory of the formation of anticoronae. In view of the lack of experimental data, it is thought advisable to present some observations made on Mt. Washington, New Hampshire some time ago. These observations were undertaken with the hope of determining the average drop size and distribution in the clouds that prevail there, but because of the press of other work during the war, the project was not completed.

"Glories" or anticoronae were produced by projecting the collimated beam of light from a G. E. mercury vapor

lamp (H-4) into the fog. An observer placed at the side of the beam and looking along it could readily count a large number of distinct colored bands, and provision was made for measuring their angular distance from the extremely bright spot at the "head" of the beam that was farthest from the source. The bands due to the green line (5461A) were most distinct and five were very common. Six and possibly seven were distinguishable under unusually stable conditions of uniform drop size. With a very high wind blowing, the diameter of these bands appeared to pulsate as the average drop size changed with the gusts. With falling rain or snow the drop size distribution broadened so that only a few bands were observable, because of the overlapping coronae, even with monochromatic light.

Polarizing screens were placed in front of the beam and in front of the observer, but the limited number of observations do not allow any qualitative conclusions to be drawn.

The brighter coronae were sometimes visible in the daytime, so it was hoped to provide a photo-multiplier pick-up and a 120-cycle audio amplifier to indicate the location of these bands at all times. With a 60-cycle voltage applied to the mercury lamp and a narrow band filter, such as the Polaroid quartz monochromator, the continuous background of sunlight could be eliminated from the readings.

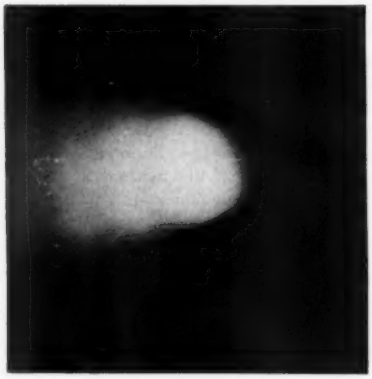

FIG. 1. Photographs of anticoronae on Mt. Washington, February, 1940.

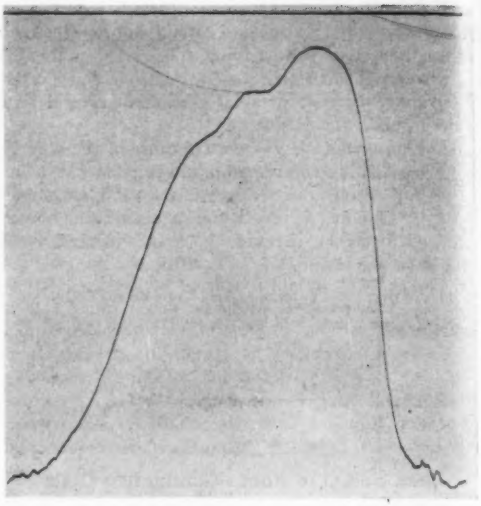

FIG. 2. Microphotometer traces photographic negative exposed to anticoronae.

A number of photographs were taken at night, and one of these, taken in February 1940 by back reflection, shows in Fig. 1 how the phenomenon appeared to an observer when the light source was placed at his left with the beam traveling horizontally in front of him. This photograph was made with an Eastman 35 camera, *f*: 3.5 aperture, Super XX film, and exposed 10 sec.

In Fig. 2 is presented a microphotometer record made from this negative by Mr. R. C. Taylor, using the Smith instrument at Brown University. The vertical scale is approximately a linear function of the light transmitted through the negative, so that the horizontal line at the top represents zero transmission and hence the maximum back reflection at zero angle by the cloud drops. The lower part of the curve gives the transmission through the unexposed part of the film. The presence of anticoronae is indicated by the dips in the left side of the curves, while the change of drop size distribution is indicated by the smoothing out of the curve on longer exposure.

[1] H. C. van de Hulst, "A theory of the anticoronae," J. Opt. Soc. Am. 37, 16 (1947).